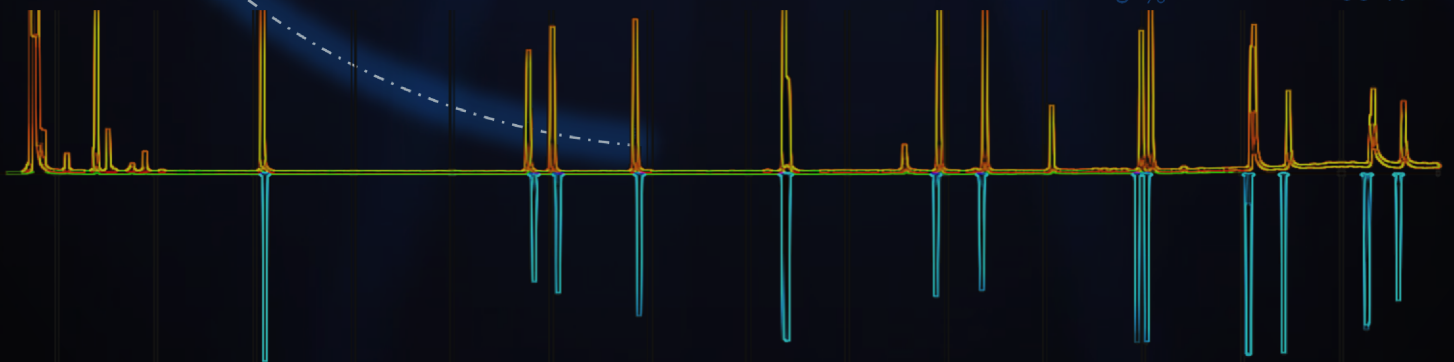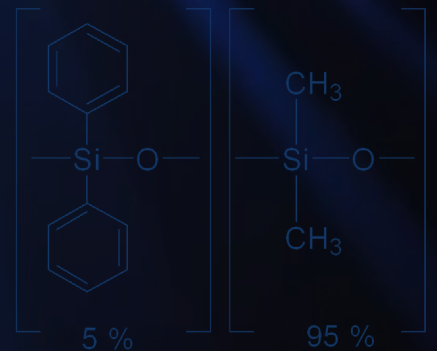Tillman Brehmer

Investigation of the interactions between analytes and stationary phases in gas chromatographic systems using simulation

CH₃

Si — O

CH₃

5 %

95 %

Investigation of the interactions between analytes and stationary phases in gas chromatographic systems using simulation

Dissertation

zur Erlangung des Doktorgrades (Dr. rer. nat.)

der Mathematisch-Naturwissenschaftlichen Fakultät

der Rheinischen Friedrich-Wilhelms-Universität Bonn

vorgelegt von

Tillman Brehmer

aus

Neuwied

Bonn

2024

The work and research towards this dissertation were carried out between February 2021 and May 2024 at the Institute of Nutritional and Food Sciences (IEL) of the Rheinische Friedrich-Wilhelms-Universität Bonn under supervision of Prof. Dr. M. Wüst and Dr. Jan Leppert.

Abstract

Volatile compounds are responsible for the odour of food, characterize their authenticity or potential health risks. One technique for investigating volatile compounds is gas chromatography. The method development is often resource-, time-, and cost-intensive but can be supported by computer simulation. Computational models are necessary, describing both the interaction of volatile compounds and the representation of the gas chromatographic system. As the models require corresponding data to describe and determine retention, the three presented investigations are concerned with determining and estimating this data.

In the first study, a database of thermodynamic retention parameters was established for a variety of volatile compounds, including FAMEs, triglycerides, PAHs, and PCBs. Retention factors from isothermal measurements were determined for 900 substance-stationary-phases-combinations, and parameters for common retention models (ABC model, K-centric model, thermodynamic model) were determined. In addition, available data from the literature was also included. A standardized approach for determining parameters was presented, and quality criteria for suitable retention parameters were established. The simulation of gas chromatographic separations using the retention parameters from the database was compared to real temperature-programmed measurements.

In the second study, the relationship between measurable elution temperature and characteristic temperature was investigated. The characteristic temperature is the most important retention parameter in the "distribution-centric retention model" (K-centric model) according to Blumberg. Influences of the temperature program due to the starting temperature and the heating rate were examined. A computational model was established using the dataset, allowing an estimation of the characteristic temperature from simple temperature-programmed measurements. This extends the prediction range, especially for volatile compounds such as benzene derivatives, aldehydes and ketones, compared to previous estimation models. The prediction of retention times based on the regression model was demonstrated using the example of alcohols and phenones.

In the third study, the 'Linear Solvation Energy Relationship' (LSER) model was used to estimate retention parameters usable for the simulation by LSER substance data. Two stationary phases were characterised. K-centric retention parameters were estimated for ca. 300 compounds, and the data were compared with parameters from isothermal measurements. Simulations of temperature-programmed GC separations using the retention parameters determined by LSER were compared with isothermal retention parameters and real measurements.

The work is an important contribution for the simulation of complex GC systems like multidimensional GC (MDGC), comprehensive GC (GC×GC) or novel techniques such as spatial thermal gradient GC and furthermore for the development of auto-optimisation GC.

Content

General Introduction

1.1 Introduction

Volatile organic compounds (VOCs) are ubiquitous in our daily lives [1]. Some of them may contribute to the recognisable odour of food (aroma)[2,3], while others play a role in the chemical communication of living organisms[4]. Of technological interest is the investigation of, for instance, odourants in the form of aroma profiles in food[5]. Other non-odourous volatile compounds are responsible to the authenticity of a food product[6,7]. Additionally, public health concerns include the identification of potential hazardous volatile compounds, such as environmental pollutants like *polychlorinated biphenyls* (PCBs) or *polyaromatic hydrocarbons* (PAHs). For these reasons, there is a growing need for investigations and examination methods of volatile compounds[8,9]. Method development is, therefore, a distinct focus of research, particularly in food chemistry. An analytical technique used for separation and determination of volatile compounds is *gas chromatography* (GC)[10]. The development of new measurement methods is often cost-, resource- and time-consuming. Suitable computer simulations can be a powerful tool optimizing the development for novel measurement methods[11–13]. For simulation computer models are necessary, describing the interaction of volatile compounds with the gas chromatographic system under various conditions[14,15]. These models need data describing the interaction of the chemical compounds (called analytes or solutes) and the gas chromatographic system with its measurement conditions and settings.

The presented thesis, was part of the DFG project "Development of a simulation for one-dimensional and multidimensional gas chromatography with temperature gradients" (Grant: 452897652). The studies and results discussed in this thesis form part of the fundamentals for the simulation of complex multidimensional GC separations such as GC×GC or spatial thermal gradient GC[16,17].

1.2 Fundamentals

In the following equations and models, temperature T and associated parameters are given in Kelvin, even if they are expressed in Celsius in examples or figures.

1.2.1 Principle of gas chromatography (GC)

Gas chromatography relies on the principles of partitioning of the sample between a stationary phase (usually a coated layer in a column) and a mobile phase (a carrier gas) to achieve separation[18]. As the sample is vaporized and injected into the column, compounds interact differently with the stationary phase based on their affinity, leading to adsorption and partition and therefore to separation as they travel through the column. The separated compounds then elute from the column at different times, allowing for their detection and quantification using a detector[10,18,19].

1.2.2 GC-ToF-MS

Figure 1.1 shows a scheme of a gas chromatograph. After injection in the GC the analyte molecules pass the separation column coated with the stationary phase, which is the surface the molecules can interact with. Depending of the composition of the stationary
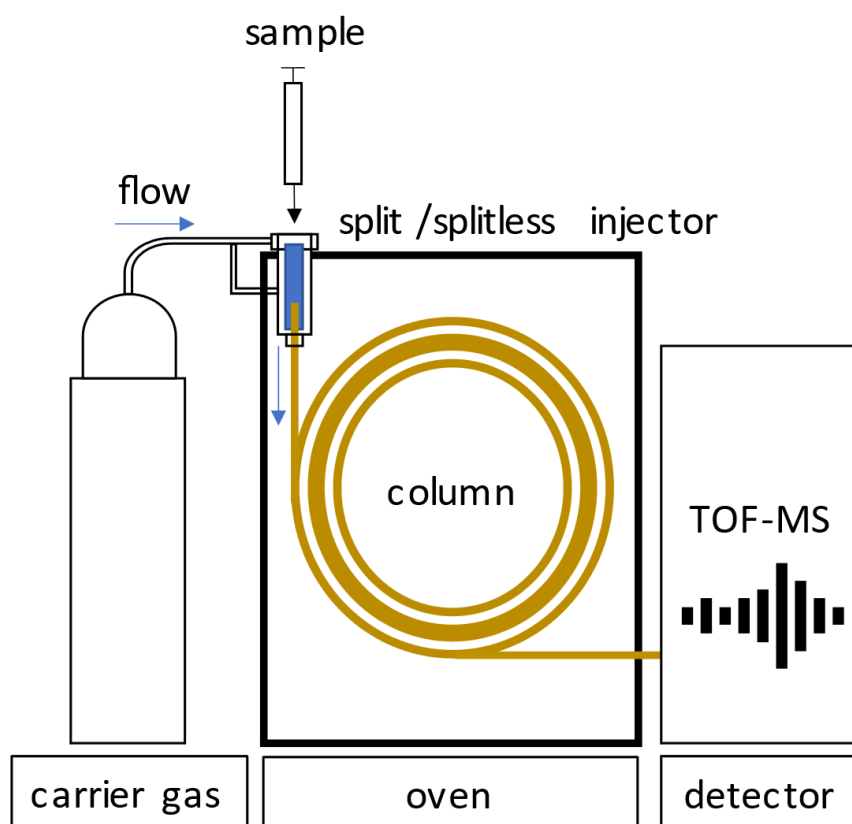

Figure 1.1 Scheme of a gas chromatograph with split/spitless injector coupled with mass spectrometer. The sample is injected in the injector, the analytes pass with the carrier gas stream through the column which is heated in the oven. After separation they finally are detected in the MS.

phase, column length or temperature the interaction with the phase is different for different analytes. The time required for the analytes to pass through the column therefore varies and can be measured as retention time t_R.

The carrier gas does not interact with the stationary phase usually. Its retention time, called void time t_M, sometimes hold up time, can be determined only by information of the column geometry, temperature and pressure. For wall coated cylindrical GC columns with length L, internal diameter d and temperature T, t_M can be determined with

$$t_M = \frac{128}{3} \cdot \frac{L^2}{d^2} \cdot \eta(T) \cdot \frac{p_i^3 - p_o^3}{\left(p_i^2 - p_o^2\right)^2} \tag{1.1}$$

where p_i is the pressure at the inlet of the column, p_o at the column outlet and the viscosity $\eta(T)$ of the carrier gas[20]. The void time t_M can be measured by detection of a non-interacting gas e.g. methane or using the oxygen signal with a mass spectrometer[21].

A ratio to evaluate the separation is given by the retention factor k and can be determined using the retention time t_R from the chromatogram at the known void time t_M

$$\ln k = \ln\left(\frac{t_R - t_M}{t_M}\right) \tag{1.2}$$

As we will see k depends on temperature itself and is related to distribution constant K. The difference between $t_R - t_M$ is also called the reduced retention time t'_R.

As detectors *flame ionisation detectors* (FID) and *mass spectrometers* (MS) are most important in GC. MS is suitable for compound identification. In this thesis all measurements are performed using a *Time-of-Flight* (ToF)-MS with electron ionisation (EI). In ToF-MS the mass of a compound ion can be determined by the time the compound need to pass a flight tube, which is proportional to the mass to charge ratio m/z. In short, heavy molecules need more time than light ones. The intensity of the signal is proportional to amount of substance in the sample, therefore MS is also suitable for quantification. Figure 1.2 shows a scheme of ToF-MS.
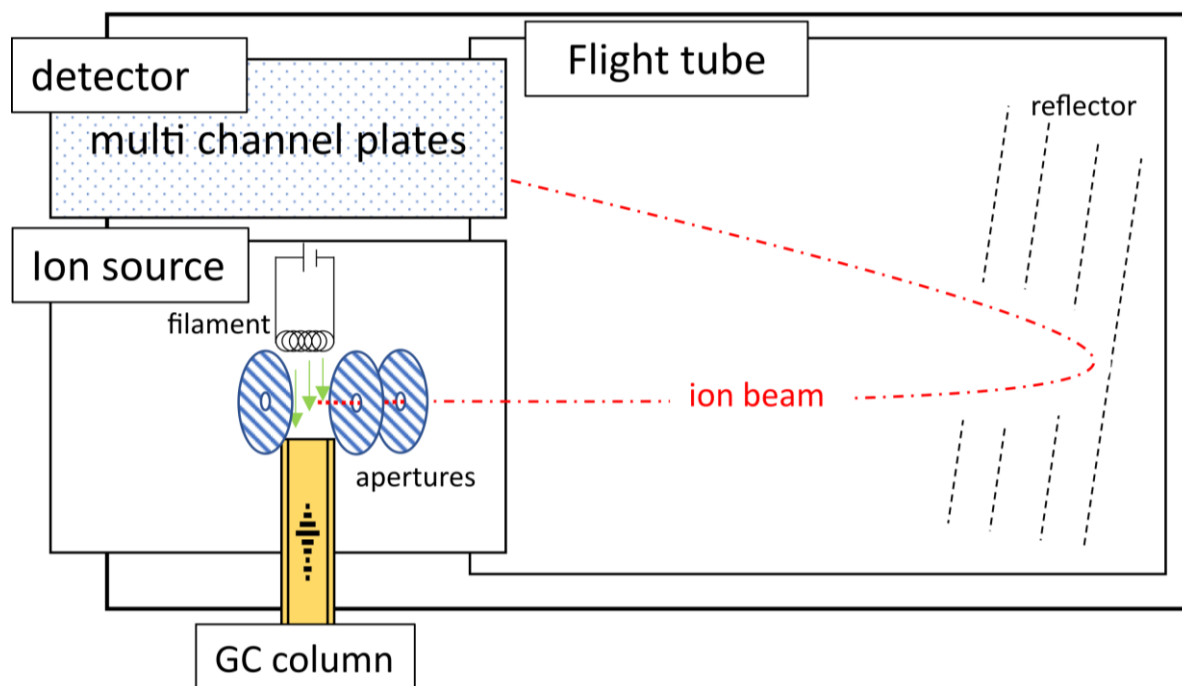
Figure 1.2 Scheme of a time-of-flight mass spectrometer (ToF-MS) with electron ionisation (EI).

1.2.3 Temperature Programmed GC

GC separations can be performed isothermal or temperature programmed, when the oven temperature is changing during the separation run. The heating rate R_T is the temporal change of the oven temperature during a temperature programmed GC separation[22]. For generalized observations and to compare GC systems with different column geometry, the heating rate can be transformed to the so-called dimensionless heating rate

$$r_T = \frac{R_T \cdot t_{M,ref}}{\theta_{ref}} \tag{1.3}$$

with the average thermal constant θ_{ref}= 30 °C and the reference void time at a defined temperature usually 150 °C[20,23], which eliminates systematic dependencies such as column diameter, length or flow[20,23]. For example, a dimensionless heating rate of $r_T = 0.4$, is equivalent to a heating rate of R_T=0.4×30 °C/t_M=12 °C per void time at 150 °C. With a reference void time of 4 min the corresponding heating rate is R_T=3 °C min^{-1}. By reducing the length of the GC column to the half value Eq. (1.1) leads to void time of ¼ of the original void time (t_M= 1 min). Under these conditions the equivalent heating rate is $R_T = 12$°C min^{-1}. This shows that a change in the system condition causes a change in the heating rates, but not the dimensionless heating rate. This is meaningful for method translation [24], an important concept in method development.

During a temperature program each analyte elutes at its retention time with a corresponding temperature[25]. The elution temperature T_{elu} of an analyte is defined as the temperature of the GC oven when the analyte is passing the outlet of the GC column and arrives at the detector of the separation system. For example, in a given single ramp temperature program that starts with the initial temperature of the GC oven T_{init} and with the heating rate R_{T} the elution temperature can be calculated via

$$T_{\mathrm{elu}} = T_{\mathrm{init}} + t_{\mathrm{R}} R_{\mathrm{T}} \tag{1.4}$$

where t_{R} is the retention time of the analyte which is passing the column outlet[23]. The prediction of the elution temperature of a solute in a temperature program can be powerful as it is always related to retention time prediction. Even if it seems logical at first glance, the elution temperature is neither equal to the boiling point nor does it depend on it[26], and therefore the order of elution is not necessarily equal to the order of the boiling points. For the separation, the vapour pressure p_{v} is important for the solvent-phase interaction[18–20].

1.2.4 Retention Index

A chromatographic and instrument-independent value that can be used to identify an unknown compound is the *retention index* (RI)[27]. It is based on the retention times of the compounds in relation to the retention times of a known, often homologous series such as alkanes. In this system, the value of the RI for each alkane is equal to one hundred times the number of carbon atoms c. Under certain chromatographic conditions, the RI makes it possible to compare data from one GC system with another. The RI was first introduced by Kovats[28] for isothermal conditions. Van den Dool and Kratz[29] modified the concept for temperature programmed GC using the adjusted retention volume. Adapted for the use of the retention times, for a compound i the retention index $RI(i)$ is defined as

$$RI(i) = 100 \cdot \left(c + \frac{t_{\mathrm{R}}(i) - t_{\mathrm{R}}(c)}{t_{\mathrm{R}}(c+1) - t_{\mathrm{R}}(c)} \right) \tag{1.5}$$

with the retention time of the ith compound $t_{\mathrm{R}}(i)$, the retention time of the alkan, with carbon number c before the ith compound $t_{\mathrm{R}}(c)$ and after $t_{\mathrm{R}}(c+1)$ [30]. Retention indices for various compounds can be found in databases such as the database of the *National Institute of Standards and Technology* (NIST)[31] or Flavornet[32].

1.2.5 Stationary phase and mobile phase

In gas chromatography first columns were columns packed with porous particles as stationary phases, e.g. granules of diatomaceous earth or silica gel coated with ethylene glycol[19,33,34]. Today usually *wall-coated-open-tubular* (WCOT) columns are used, where a liquid organic polymer is acting as liquid stationary phase, called film[35]. Therefore, this kind of GC is also called GLC (Gas-Liquid-Chromatography), whereas no liquid eluents are involved such as in real liquid chromatography (LC). Figure 1.3 gives a cross section of a WCOT column and examples for polymers used as stationary phases.
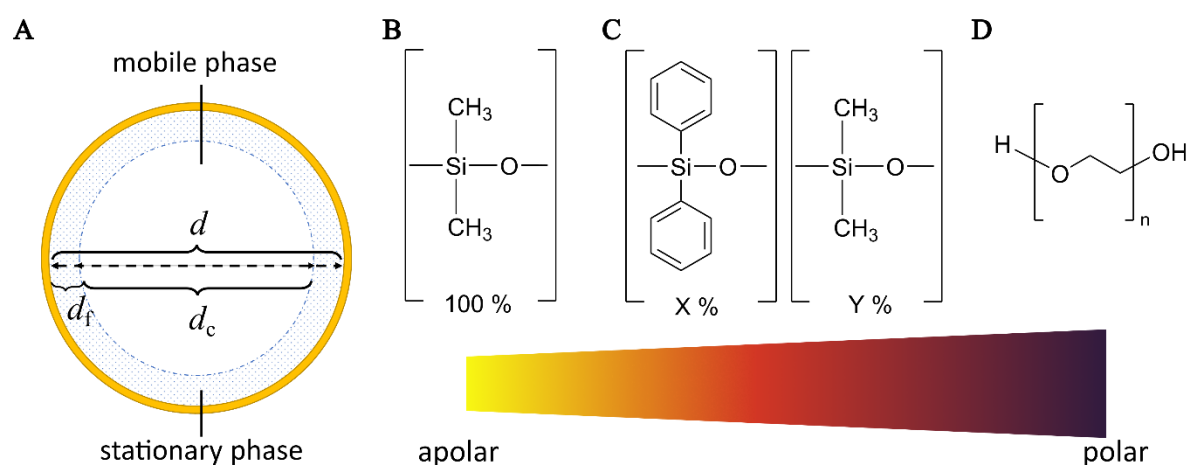

Figure 1.3: Properties of stationary phases: Cross-section of a WCOT GC column with column diameter d_c, film thickness d_f and internal diameter d (**A**). Polymer structures of stationary phases: dimethyl-polysiloxan(**B**), phenyl-dimethyl-polysiloxan (**C**), polyethylene-glycol (**D**).

Stationary phases are often differentiated by polarity, whereas wax-columns are highly polar (D) and 100 %-methyl-polysiloxan columns are highly apolar (B). An increasing amount of phenyl groups in methyl-polysiloxan phases has an influence to the polarity: for example a Rxi-5Sil MS phase has an amount of 5 % phenyl and is nearly apolar and Rxi-17Sil MS with 25 % phenyl chains is semipolar. Not all column compositions are publicly known, as they are trade secrets. This applies to phases for special applications, e.g. certain pollutants (ZB-PAH-CT for PAHs, PCBs) or pesticides.

In capillary columns the amount of the retention applies to the thickness of the film d_f, as a thick film causes more interaction than a thin film and further increases sample capacity. The ratio of the volume of the mobile phase V_m to the volume of the stationary phase V_s[36] is called the phase ratio β. Because the internal diameter d is approximately equal to the diameter of the column and $d_c >> d_f$.; therefore, β is approximately equal to the ratio of d and quadruple of the film thickness d_f[36,37].

$$\beta = \frac{V_m}{V_s} \approx \frac{d}{4d_f} \tag{1.6}$$

Usually inert gases are used as mobile phases in GC. Most common are helium, hydrogen, argon or nitrogen. As shown in Eq. (1.1) the time the mobile phase requires to pass the column applies only on the column geometry and the viscosity of the carrier gas. The viscosity itself depends on temperature [36] and is different for H_2, N_2, Ar and He and therefore the separation can be different using different carrier gas. For example changing from He to H_2 can reduce the separation run time by factor two[38,39], therefore it is highly relevant in optimization and for fast-GC applications.

1.2.6 Plate theory

Usually a compound does not elute at a sharp time point but with a variance as a peak around the time point. In the early days of gas chromatography, first concepts to describe separation mechanisms and the phenomenon of peak broadening were adopt from separation concepts known from distillation[20,40] such as the '*height equivalent to a theoretical plate*' (HETP). The idea associated the peak width of an analyte peak width a number of imaginary elementary separation stages, called the theoretical plate[20]. The height of a theoretical plate $\bar{H}$ was introduced as a quantity of the separation efficiency and depends on the column length L and the number of theoretical plates N.

$$\bar{H} = \frac{L}{N} \tag{1.7}$$

The concept was simple: the higher the number of plates, the lower the plate height and therefore the lower the peak width. It should be mentioned here, however, that neither in the separation column does anything physically comparable to a plate exist[20], nor does N correspond to the number of possible equilibrium states of the analyte between the mobile and stationary phases[40].

As van Deemter et al.[41] has shown, $\bar{H}$ depends on the average mobile phase velocity $\bar{u}$ at given temperature in packed columns via

$$\bar{H} = \bar{A} + \frac{\bar{B}}{\bar{u}} + \bar{C}\bar{u} \tag{1.8}$$

where $\bar{A}$ represents the Eddy-diffusion term, $\bar{B}$ represents the longitudinal diffusion term, and $\bar{C}$ represents the mass transfer or resistance to mass transfer term. Since capillary open-tubular columns are commonly used in GC, where no Eddy-diffusion exists, $\bar{A}$ becomes zero. The equation than is called 'Golay's equation'[35]. As shown elsewhere[40]., $\bar{B}$ depends on the diffusion coefficient of the mobile phase, whereas $\bar{C}$ depends on both the diffussions coefficient of the analyte in the stationary and the mobile phase and further retention factor k and the column geometry.

Golay's equation is a useful concept for understanding the influences that cause peak broadening qualitatively[42]. The observation of velocity $\bar{u}$ as an independed quantity is in temperature programmed GC less relevant than in isothermal GC[42]. Golay's equation is further only correct under weak gas decompression, which is not the case using a vacuum outlet e.g. in GC-MS[20]. The idea of an optimal velocity and the search for the Van-Deemter optimum, often is only the last part of an optimization and there exist even physically more meaningful concepts for method development to increase resolution and separation than Golay's equation[40]. The equation is recommended to interpret the general influences of longitudinal diffusion, Eddy-diffusion and mass transfer in a qualitative way, whereby the velocity should be interpreted as part of each term[42].

1.3 Simulation

Several approaches can be found that are suitable for retention time prediction in GC. Often simulations based on thermodynamic modelling use descriptions of the solute-phase-interactions via a prediction of partition constant K or related quantities[37,43]. Predictions based on retention indices are common[44], for multidimensional GC such as GC×GC novel approaches as machine learning (ML) and artificial intelligence (AI) becomes more important[45–47]. Most common algorithm for data processing in GC×GC are *Support Vector Machines* (SVM), *Partial Least Square Discriminant Analysis* (PLSDA)[48–50] and *Random Forest* (RF)[51–53]. Hou et al. introduced a thermodynamic approach for retention time prediction including the column properties such as L and d or instrumental condition such as temperature and pressure[15,54,55]. Leppert et al. presented a simulation[14] for prediction of retention times and peak width in temperature programmed GC[56,57] and with a spatial temperature change along the column such as it is used in *flow field thermal gradient* GC (FFTGGC)[58,59]. The simulation was released as

the package `*GasChromatographySimulator.jl*`[58] for the programming language Julia[58,60,61]. To simplify the mathematic for the simulation, approximations as linearized models are well established[62]. For example retention factor k respectively retention times can be predicted by temperature programmed measurements using a linear elution strength (LES) approximation and relative resolution maps to find efficient conditions with acceptable resolution for GC separations[63]. Such approaches are also common in retention prediction in *high performance liquid chromatography* (HPLC)[11]. There already exist commercial application such as ProEZGC[64].
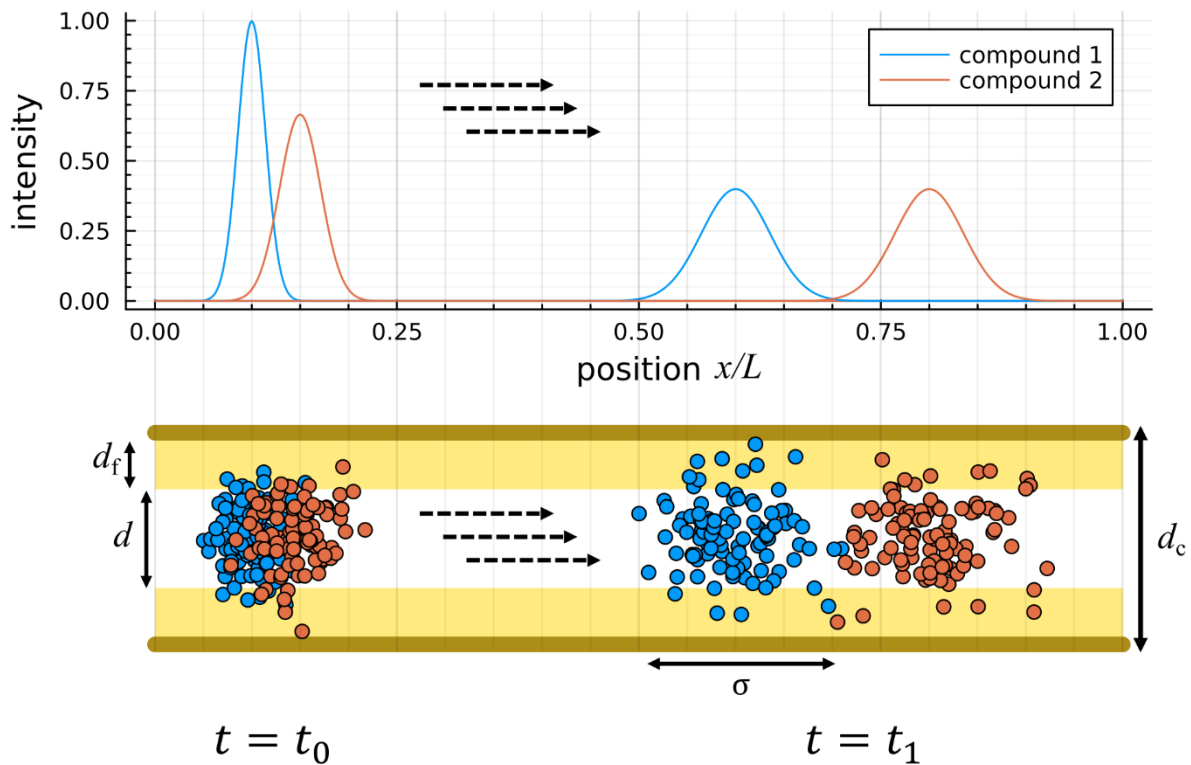
Figure 1.4: Separation of two compounds on a column with length L with film thickness d_f and internal diameter d. Position x of the compound destribution at two different times t_0 and t_1. The separation is better at t_1 but spatial band width σ also increased along the column due to diffusion.

In all thermodynamic based approaches, such as 'GasChromatographySimulator.jl', an equation of motion has to be developed using the knowledge of the presented fundamentals. For prediction of temperature programmed separations, the column is divided in discrete steps. After passing a step the analyte is located on position x in the column with length L. The time an analyte needs to pass the step is the travel time t. When x reaches L, the sum of all travel times becomes retention time t_R[65].

The migration of an analyte along the column steps as a function $t(x)$ is governed by the ordinary differential equation (ODE)

$$\frac{dt}{dx} = \frac{1}{u(x,t)} \tag{1.9}$$

and the analyte velocity $u(x,t)$. As known from Golay's equation the spatial band width σ in dimensions of length [m] increased along the column caused by diffusion processes. Measurable is the peak width τ [min] as standard deviation of an ideal gaussian peak of the compound given in the chromatogram which is related to the spatial band width σ as

$$\tau(x,t) = \frac{\sigma(x,t)}{u(x,t)} \tag{1.10}$$

The development of the peak variance $\tau^2(x)$ during the migration is governed by ODE:

$$\frac{d\tau^2}{dx} = \frac{H(x,t)}{u^2(x,t)} + 2\tau^2(x,t)\frac{\partial}{\partial x}\left(\frac{1}{u(x,t)}\right) \tag{1.11}$$

with $H(x,t)$ the local plate height. At the end of the column, $x = L$, the solutions are given as the retention time $t_R = t(L)$ and the peak width $\tau_R = \sqrt{\tau^2(L)}$ [65].

The system of ODEs, Eq. (1.9) and Eq. (1.11), can be solved numerically [14,58,66]. 'GaschromatographySimulator.jl' uses a Runga-Kutta algorithm [67] with Owren-Zennaro optimized interpolation [68] and adapted step width. [14]

The analyte velocity depends on the component of the velocity of the mobile phase u_m and the retention factor k of the analyte, Eq. (1.12).

$$u = \frac{u_m}{1+k} \tag{1.12}$$

With d the column diameter, L the column length, η the viscosity of the mobile phase gas, p_i the inlet pressure and p_o the outlet pressure, the mobile phase velocity u_m can be calculated from Eq. (1.1) as

$$u_m(x,T) = \frac{1}{64}\frac{d^2}{\eta(T)L}\frac{p_i^2 - p_o^2}{\sqrt{p_i^2 - \frac{x}{L}(p_i^2 - p_o^2)}} \tag{1.13}$$

whereby the gas decompression is considered[14,20,65,69]. As mentioned, the viscosity $\eta(T)$ of a carrier gas depends on temperature[21]. Corresponding data can be found in the literature[36,70]. In a temperature programmed measurement, the analyte speed u also changes with temperature T by retention factor k, see Eq. (1.12). Therefore, knowledge about the temperature dependence of retention factor as $k(T)$ is required to perfom simulations. The next section presents several retention models for the description of $k(T)$.

1.4 Retention models

1.4.1 Thermodynamic retention model (Van't Hoff model)

In gas chromatography the partition of a solute between the mobile phase (gas) and the stationary phase (liquid) is measured by the distribution coefficient K (or partition coefficient), defined as the ratio of the concentration of the solute in the stationary phase and in the mobile phase. It can be measured by isothermal measurements of the retention factor k and the phase ratio β of the column.

$$K = \beta k \tag{1.14}$$

The distribution coefficient K depends on the temperature T and the Gibbs free energy ΔG of the evaporation of the solute from the stationary phase[20].

$$K = \exp\left(\frac{\Delta G}{RT}\right) \tag{1.15}$$

with R the molar gas constant. The Gibbs free energy ΔG can be expressed by enthalpy ΔH and entropy ΔS change of the solute from the stationary into the mobile phase as

$$\Delta G = \Delta H - T\Delta S \tag{1.16}$$

and therefore

$$k = \frac{1}{\beta} \exp\left(\frac{\Delta H}{RT} - \frac{\Delta S}{R}\right) \tag{1.17}$$

which is an interpretation of *van't Hoff* two-parameter model describing K in relation to T.

1.4.2 *ABC* model

Enthalpy ΔH and entropy ΔS depend on the temperature T itself. To compensate for this temperature dependency a third parameter ΔC_p (change of the isobaric molar heat capacity) can be introduced and the enthalpy ΔH_{ref} and entropy ΔS_{ref} at a reference temperature T_{ref} are used. Eqs. (1.15) and (1.16) lead to

$$\ln K = \frac{\Delta S_{ref}}{R} - \frac{\Delta H_{ref} + \Delta C_p(T - T_{ref})}{RT} + \frac{\Delta C_p}{R}\ln\left(\frac{T}{T_{ref}}\right) \tag{1.18}$$

which can be converted in a three-parameter model of Clark and Glew[37,71] for curve fitting

$$\ln K = A + \frac{B}{T} + C\ln\left(\frac{T}{T_1}\right) \tag{1.19}$$

where A, B, C are curve fit parameters and $T_1 = 1$K.

It was shown [72], that using a three-parameter model results in a better fit of k over a wider temperature range than using a two-parameter model with constant ΔH and ΔS.

The parameters A, B and C can be converted to enthalpy ΔH_{ref}, entropy ΔS_{ref} for a chosen reference temperature T_{ref} and the change of the isobaric molar heat capacity ΔC_p.

$$\Delta H_{ref} = R(CT_{ref} - B) \tag{1.20}$$

$$\Delta S_{ref} = R\left(A + C + C\ln\left(\frac{T_{ref}}{T_1}\right)\right) \tag{1.21}$$

$$\Delta C_p = RC \tag{1.22}$$

T_{ref} is often chosen with 90 °C[73]. It seems reasonable to set up a model that normalises its reference variables to a certain temperature. In adsorption phenomena, especially in chromatography, the distribution of an analyte depends to a large extent on the temperature conditions, but not on the same temperature for each analyte. It is therefore criticised that the choice of a reference temperature T_{ref} for all analytes leads to physically meaningless conditions for substances with extreme retention, such as highly volatile compounds or low-volatility substances like triglycerides.

1.4.3 Distribution-centric three-parameter model (K-centric model)

For chromatography, it is more appropriate to normalise the model to the same distribution of the analyte over the stationary phases, expressed by the distribution coefficient K[37]. This approach is realised by the so called 'Distribution-centric three-parameter' model of Blumberg[37,43], also known as the 'K-centric' model. The retention factor k of a solute in a GC system is defined by the three parameters:

- T_{char} characteristic temperature
- θ_{char} characteristic thermal constant
- ΔC_{p} change of the isobaric molar heat capacity (Eq. (1.22))

and the equation

$$\ln k = \left(\frac{\Delta C_{\text{p}}}{R} + \frac{T_{\text{char}}}{\theta_{\text{char}}}\right)\left(\frac{T_{\text{char}}}{T} - 1\right) + \frac{\Delta C_{\text{p}}}{R}\ln\left(\frac{T}{T_{\text{char}}}\right) \tag{1.23}$$

These parameters, especially T_{char} and θ_{char}, have a direct chromatographic meaningful interpretation. The characteristic temperature T_{char} is the temperature, where $\ln k = 0$, respectively $k = 1$[37]. At this temperature the amount of the solute is evenly distributed between stationary and mobile phase. The characteristic thermal constant is the inverse
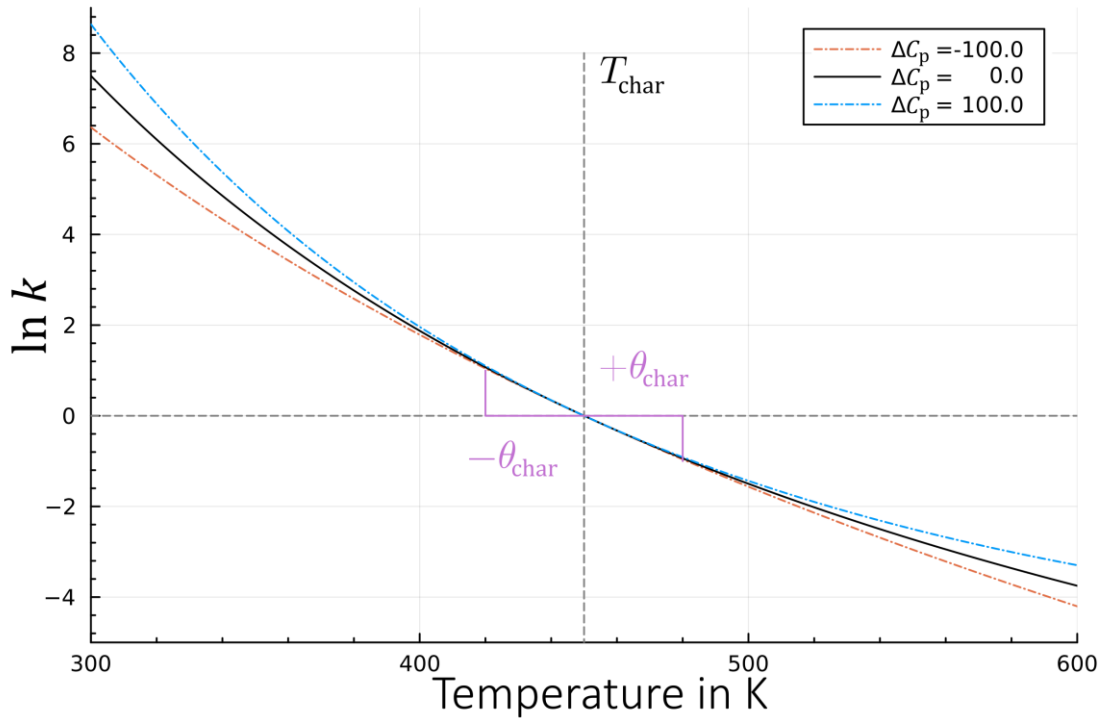

Figure 1.5: Properties of the 'Distribution-centric three-parameter model' which describes $\ln k$ in dependence of temperature T.

declining slope of the function $\ln k(T)$ at $T = T_{char}$. Therefore, an increase of the temperature around T_{char} by θ_{char} reduces $\ln k$ by an amount of 1.0. The interpretation of ΔC_p is not straightforward, but it generally defines the deviation of k from a two-parameter model for temperature significantly lower/higher than T_{char}. As Blumberg demonstrated, the K-centric parameters can be converted into ABC data and vice versa using the Lambert W-function[37].

The parameters T_{char}, θ_{char} and ΔC_p are specific for the phase ratio β_0 used to determine these parameters. Using a column with the same stationary phase but different phase ratio β_1 requires a correction factor for the retention factor calculated from Eq. (1.23).

$$k_1 = \frac{\beta_0}{\beta_1} k_0 \tag{1.24}$$

As presented in Figure 1.6, linalool and nitrobenzene change the elution order depending on the temperature respectively heating rate of the temperature program. This phenomenon can be described by the K-centric or the ABC model but not by retention index.
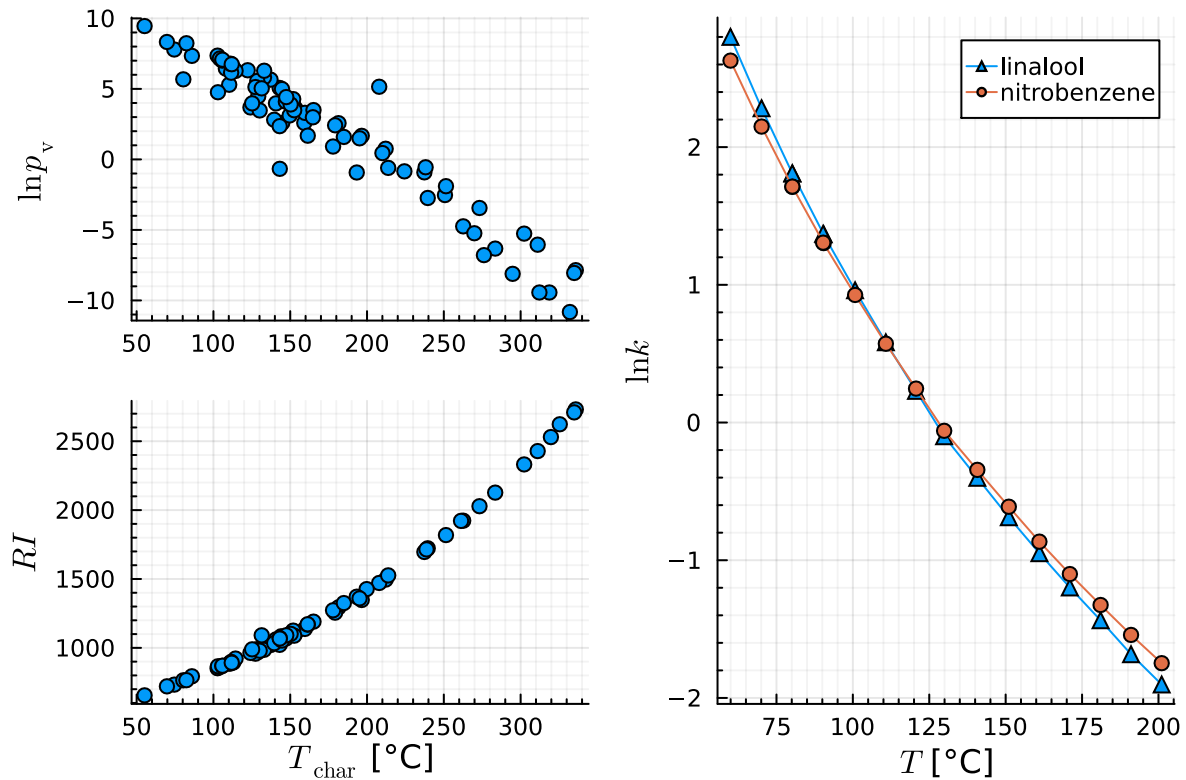

Figure 1.6: Characteristic temperature in relation to vapor pressure p_v and retention index RI[31](left), $\ln k$ vs T plot of linalool and nitrobenzene which change the elution order at different isothermal conditions (right).

The characteristic temperature is a meaningful chromatographic value. It shows strong correlations to retention index RI and vapour pressure, see Figure 1.6. Furthermore it is known that there is a relation between the characteristic temperature T_{char} of a substance and its elution temperature T_{elu} during temperature programmed GC separation with a single ramp[37]. For a GC system one heating rate $R_{\text{T,0}}$ exists where T_{elu} is equal to T_{char} [23,37]. If T_{elu} or T_{char} is much higher than the initial temperature T_{init}, the dependence can be described as a simple linear function:

$$T_{\text{elu}} = T_{\text{char}} + T_0 \tag{1.25}$$

where T_0 is the intercept which determines the shift from the heating rate $R_{\text{T,0}}$ where T_{char} is equal to T_{elu}. In the case of an initial temperature of e.g. 30 °C, the linear relationship can be assumed for an elution temperature above 90 °C[37].

1.4.4 Linear solvation energy relationship model (LSER)

The 'Linear Solvation Energy Relationship' model (LSER), also known as the 'Abraham model' or 'Solvation parameter model'[74,75] is an alternative to the above mentioned thermodynamic retention models. The approach is common e.g. in environmental chemistry to predict distribution phenomena of a target analyte with any kind of matrix[76]. Typically applications are the prediction of pollutant adsorption in soils, migration of mobile additives from or into package materials [77] or tissues.

The principle of adsorption phenomena prediction can also be used for the prediction of retention in chromatography[78,79]. In this model, the logarithm of the retention factor ln k at a defined temperature is expressed as a multiple linear regression of chemical properties of the analyte (descriptors E, S, A, B, L) and properties of the stationary phase (system constants e, s, a, b, l, c)[80].

$$\ln k = eE + sS + aA + bB + lL + c \tag{1.26}$$

In the context of LSER, the solute descriptors and system constants are experimental values whereby the individual system constants (lower case letters) represent different types of intermolecular interactions of the stationary phase and the analyte. Table 1.1 presents the definitions of the descriptors and the system constants.

Table 1.1: Parameters of the LSER model and its meaning for solute-phase-interaction by Poole [80].

solute properties		phase properties	
solute descriptor	Definition	system constant	interaction
E	the excess molar refraction	e	electron lone pair interactions (the excess dispersion interactions that result from the presence of polarizable electrons)
S	capability for interactions of a dipole type (orientation and induction)	s	interactions of a dipole-type, known as induction and orientation
A	overall resp. effective hydrogen-bond acidity	a	interactions of the hydrogen-bonding in which the stationary phase acts as a hydrogen-bond acceptor
B	overall resp. effective hydrogen-bond basicity	b	interactions in which the stationary phase acts as hydrogen-bond donor.
L	gas-liquid partition constant at 25 °C on n-hexadecane as stationary phase.	l	size dependent interactions, which are cavity formation in the stationary phase and the setup of dispersion interactions
		c	Intercept, contains deviations from the model, information about the phase ratio

The determination can be found elsewhere[81–83]. Only E for liquids can be calculated from the refractive index of the liquid I_R, at 20 °C for the sodium D-line and the characteristic volume, V[78,80]
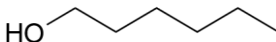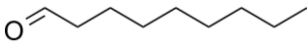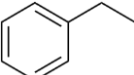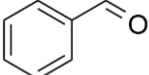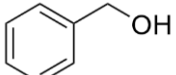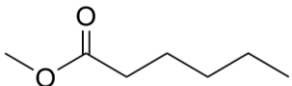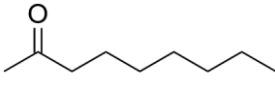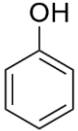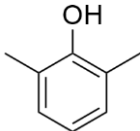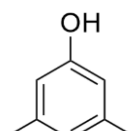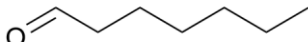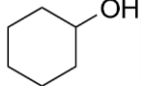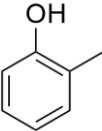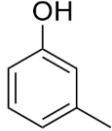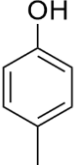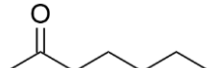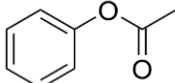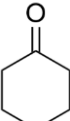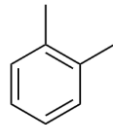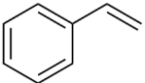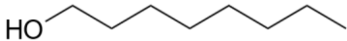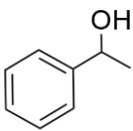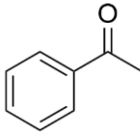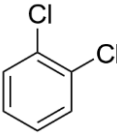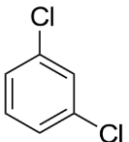
$$E = 10V\left[\left(I_R{}^2 - 1\right)/\left(I_R{}^2 + 2\right)\right] - 2.832V + 0.526 \qquad (1.27)$$
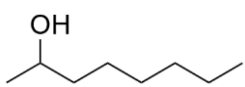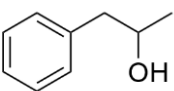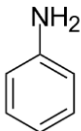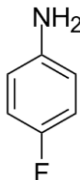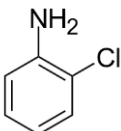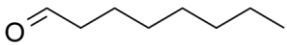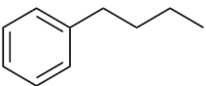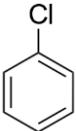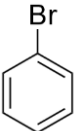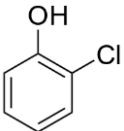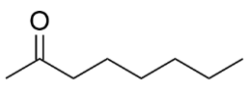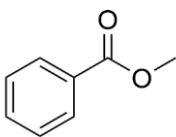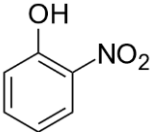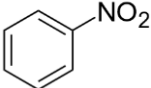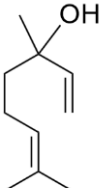
For the typical stationary phases used in GC, the value of b can be approximated as zero as there is no significant hydrogen bond activity[84]. In accordance to Poole[80] intercept c is a system property required to estimate retention factors for a specific column and temperature but is not a characteristic property of the solvation properties of the stationary phase. The system constants depend on the temperature, while the substance descriptors have fixed, specific values. For individual temperatures, the system constants can be determined by a multivariate regression using selected calibration substances whose descriptors are known.

Even a small number of 30 to 40 substances (with different functional groups and structures) is sufficient to determine the system coefficients[85] for a temperature range. 40 compounds recommended by Poole[85] and used in this thesis are given in Table 1.2.

For any analyte with known substance descriptors (capital letters), the $\ln k$ values for the defined temperature can be calculated with the systems coefficients without any other measurement on the GC column. Descriptors can be found in the literature and are collected in databases such as the LSER database (LSERD) of the Helmholtz Centre for Environmental Research (UFZ) [86] or the Wayne State University (WSU) database[78].

Table 1.2: Chemical structures of 40 compounds recommend by Poole[85] for description of the solute-phase interaction via LSER.

hexan-1-ol	n-nonanal	ethylbenzene	benzaldehyde	benzyl alcohol
methyl hexanoate	nonan-2-one	phenol	2,6-dimethyl phenol	3,5-dimethyl phenol
n-heptanal	cyclohexanol	2-methyl phenol	3-methyl phenol	4-methyl phenol
heptan-2-one	phenyl acetate	cyclohexanone	o-xylene	styrene
octan-1-ol	1-phenyl ethanol	acetophenone	1,2-dichloro benzene	1,3-dichloro benzene

octan-2-ol	1-phenyl-2-propanol	aniline	4-fluoro aniline	2-chloro aniline
n-octanal	n-butyl benzene	chloro benzene	bromo benzene	2-chloro phenol
2-octanone	methyl benzoate	2-nitro phenol	nitro benzene	linalool

1.5 Objective of the thesis

The aim of the thesis was the validation of the simulation under different GC conditions. Therefore, the main focus laid on description of the interaction between analytes and stationary phases using thermodynamic retention parameters of the K-centric model for various stationary phases and compounds in a wide volatility range:

- high volatiles: homologous alcohols, aldehydes ketones and BETXs
- medium volatiles: fatty acid methyl esters (C:4-C:24), halogen-phenols, esters, alkanes
- less volatiles: PAHs, PCBs and triglycerides.

For all columns the column geometry as L/d-ratio was determined via void time measurements. For all compounds isothermal measurements were performed in a range between $40\,°C$ and $360\,°C$ and retention factors were determined. The retention parameters were calculated via the K-centric model.

With these data a database was created. Simulations of gas chromatographic separation were performed using the retention parameters and the results were compared to real measurements. A summary of the corresponding article[87] is given in Chapter 2.

Another aim of the thesis was the search for easier determination methods or even estimates for the retention parameters since isothermal measurements for determination are laborious. In one approach the estimation of the characteristic temperature, the most important parameter of the K-centric model by temperature programmed measurements was investigated. Starting from Eq. (1.25) the dependence of elution temperature on T_{char} and vice versa was investigated. Measurements on various initial temperatures in a range of 40 to 120 °C and heating rates at 5, 10, 15, 20 °C/min were performed. A multivariate regression model was developed. Estimations of elution temperatures and retention times were performed and compared to measurements. A summary of the results[88] is given in Chapter3.

There is just a small number of available thermodynamic data for gas chromatography. But other retention data are available in databases such as RI data or LSER data. A large pool of data suitable for LSER approach can be found, e.g. in the WSU database [78,89] or LSERD from UFZ [31,86] and also can be used to describe the solute-stationary-phase interaction. Furthermore, an aim of this work was to make this data available for the simulation. For this purpose, LSER models and the K-centric model were combined. Separation columns were characterised with LSER systems constants at different temperatures. A model to describe the temperature-dependence of the system constants was developed. The data were used to estimate the K-centric retention parameters based on LSER literature data. The data then are used to perform precise temperature independent predictions of temperature programmed GC separations. The simulations based on the LSER data were compared to measurements and simulations based on isothermal parameters. Chapter 4 gives a summary of the corresponding article[90].

List of publications

Parts of this thesis have been published in peer-reviewed journals

1. T. Brehmer, B. Duong, M. Marquart, L. Friedemann, P.J. Faust, P. Boeker, M. Wüst, J. Leppert, Retention database for prediction, simulation and optimization of GC separations, ACS Omega 8 **2023**, 19708–19718.
   DOI: 10.1021/acsomega.3c01348.
   This published article is summarized in Chapter 2 of the thesis.

2. T. Brehmer, P. Boeker, M. Wüst, J. Leppert, Relation between characteristic temperature and elution temperature in temperature programmed gas chromatography – Part I: Influence of initial temperature and heating rate, J. Chromatogr. A **2023**, 1707, 464301.
   DOI:10.1016/j.chroma.2023.464301.
   This published article is summarized in Chapter 3 of the thesis.

3. T. Brehmer, B. Duong, P. Boeker, M. Wüst, J. Leppert, Simulation of gas chromatographic separations and estimation of distribution-centric retention parameters using linear solvation energy relationships, J. Chromatogr. A **2024**, 1717, 464665.
   DOI: 10.1016/j.chroma.2024.464665.
   This published article is summarized in Chapter 4 of the thesis.

Reprints of the publications 1.-3. publications are given in the appendix (Appendix A–C) of this thesis.

Further peer-reviewed articles:

4. S. Straßmann, T. Brehmer, M. Passon, A. Schieber, Methylation of Cyanidin-3-O-Glucoside with Dimethyl Carbonate, Molecules **2021**, 26(5), 1342
   DOI: 10.3390/molecules26051342

5. J. Leppert, T. Brehmer, M. Wüst, P. Boeker, Estimation of retention parameters from temperature programmed gas chromatography, J. Chromatogr. A, **2023**, 464008.
   DOI:10.1016/j.chroma.2023.464008.

6. T. Brehmer, P. Boeker, M. Wüst, J. Leppert, Relation between characteristic temperature and elution temperature in temperature programmed gas chromatography – Part II: Influence of column properties, J. Chromatogr. A **2024,** accepted

Abstracts for poster presentations and oral presentations

1. T. Brehmer, B. Duong, P. Boeker, M. Wüst, J. Leppert, Profile of Spatial Gradient of the Flow Field Thermal Gradient Gas Chromatograph (FFTGGC), 17th International Symposium on Hyphenated Technics in Chromatography and Separation Technology, Ghent, Belgium, May 18-20, **2022**

2. J. Leppert, T. Brehmer, M. Wüst, P. Boeker, Properties of spatial thermal gradient gas chromatography - The optimal gradient, 17th International Symposium on Hyphenated Technics in Chromatography and Separation Technology, Ghent, Belgium, May 18-20, **2022**

3. T. Brehmer, B. Duong, P. Boeker, M. Wüst, J. Leppert, Computersimulation von GC-Trennungen unterstützt die Methodenentwicklung zur Analyse von Polyzyklischen Aromatischen Kohlenwasserstoffen, 50. Deutscher Lebensmittelchemietag, Hamburg, September 19-21, **2022**, Lebensmittelchemie 76
DOI: 10.1002/lemi.20225910611

4. J. Leppert, T. Brehmer, M. Wüst, P. Boeker, Modular simulation of complex gas chromatographic systems, 14th GC×GC Workshop, Liège, Belgium, January 30-February 1, **2023**

5. T. Brehmer, P. Boeker, M. Wüst, J. Leppert, Estimation of retention parameters and elution temperatures in gas chromatography using different multivariate models, ANAKON 2023, Wien, Austria, April 11-14, **2023**
ISBN: 978-3-200-09056-9

6. J. Leppert, T. Brehmer, M. Wüst, P. Boeker, Simulation of gas chromatography, ANAKON 2023, Wien, Austria, April 11-14, **2023**
ISBN:978-3-200-09056-9

7. T. Brehmer, Peter Boeker, Matthias Wüst, Jan Leppert, Simulation of gas chromatography: Prediction of K-centric retention parameters and elution temperatures using different multivariate models, 20th International GC×GC Symposium, Canmore, Canada, May 28-June 1, **2023**

    J. Leppert, T. Brehmer, M. Wüst, P. Boeker, simulation toolbox for multidimensional gas chromatography, 20th International GC×GC Symposium, Canmore, Canada, May 28-June 1, **2023**

8. T. Brehmer, J. Leppert, P. Boeker, M. Wüst, Computersimulation Gaschromatographischer Trennungen: Chancen für die Lebensmittelanalytik, 51. Lebensmittelchemietage, Bonn, Germany, August 21-23, **2023,** Lebensmittelchemie 77
DOI: 10.1002/lemi.2023590 1

Retention database for prediction, simulation and optimization of GC separations

A reprint[1] of this publication is given in Appendix A of this thesis.

2.1 Author's contributions

My contribution to this research was the determination of most of the retention parameters, especially for fatty acid methyl esters (FAMEs), polychlorinated biphenyls (PCBs) and triglycerides, including data evaluation, as well as summarising the results and writing the resulting publication. I converted all data into *ABC* and thermodynamic data, validated them and created the database and did the GC simulations. The Master student Benny Duong carried out the determination of the *K*-centric parameters of polycyclic aromatic hydrocarbons (PAHs) on the Rxi-17Sil MS and ZB-PAH CT under my supervision. Master student Manuela Marquart determined the *K*-centric parameters of various allergenic fragrances on the Rxi-17Sil MS column as part of her master thesis. Luise Friedemann helped with the analysis of some chromatograms during her Bachelor thesis. Peter J. Faust was the supervisor of Luise Friedemann. Peter Boeker acquired the funding. The supervisor of my doctoral thesis, Prof. Matthias Wüst, provided guidance, important suggestions and writing assistance. Jan Leppert, helped with the simulation, provided guidance, made important suggestions, gave writing assistance, did the project administration and the funding-acquisition.

2.2 Summary

The aim of this first study was the creation of an open source database with suitable retention parameters that can be used for the simulation package GasChromatographySimulator.jl[58]. For this purpose, the retention factors k of 280 substances were determined isothermally at various temperatures. Retention parameters for the three common retention models (K-centric model[43], ABC-model[71], van't Hoff model) were calculated from the isothermal measurements. This enables the use of the data for prediction and GC simulation with other programs[15,45,47,54,55]. A standardized procedure was developed for the determination and validation of the retention parameters and the creation of the database, see Figure 2.1. Furthermore, available literature data were also inserted in the database. Using Eqs. (1.20) and (1.21), it was possible to introduce and calculate the thermodynamic parameters ΔH_{char} and ΔS_{char} at $T_{\mathrm{ref}} = T_{\mathrm{char}}$ as an interpretation of the K-centric quantities.
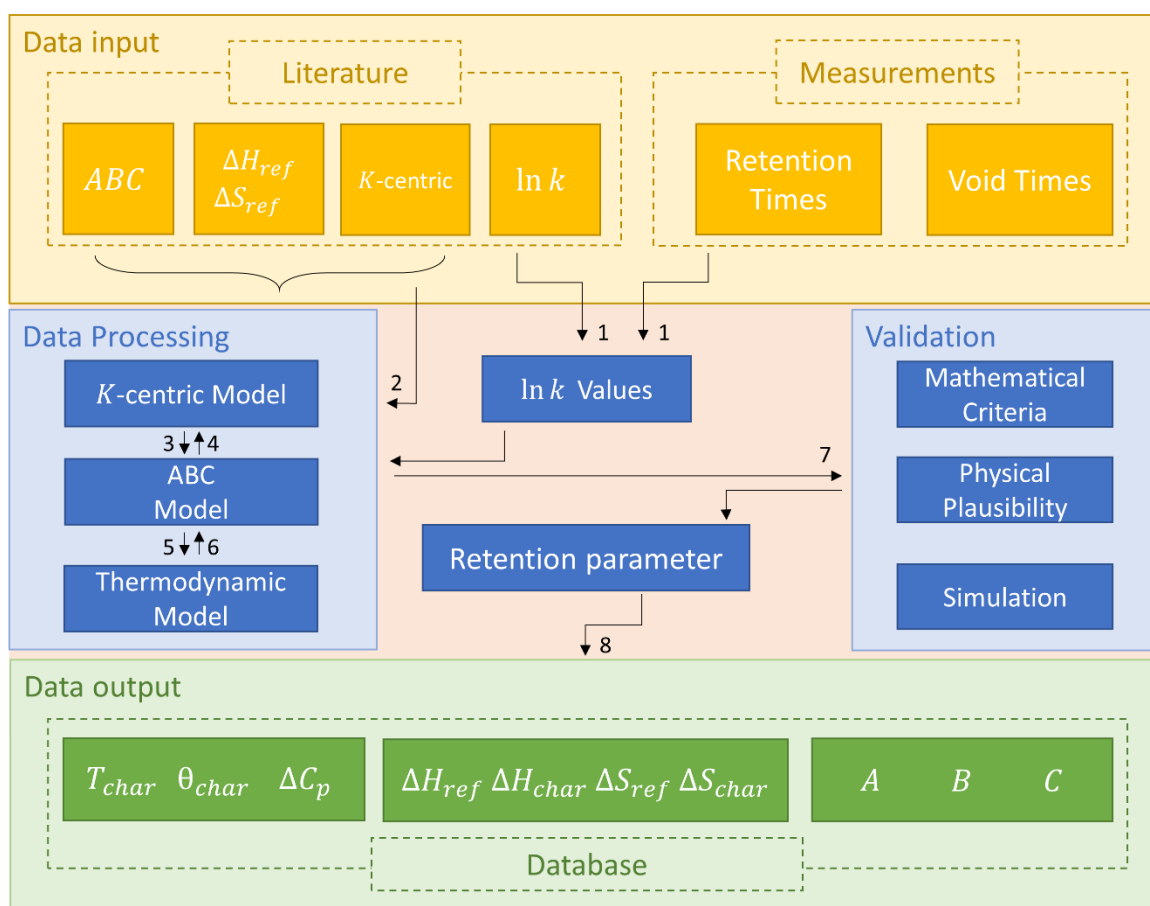
Figure 2.1: Schematic overview of the main tasks for calculation and converting of the retention parameters and creation of the database

The calculated retention parameters have to be validated to be integrated in the database (Figure 2.1 No. 7). For acceptance of the compound data we defined the following criteria:

a) The data set includes 3 data points as minimum for non-linear multivariate fit, ideally four data points or more. As a recommendation, the data should contain points around $\ln k = 0$ to achieve accurate fitting results.

b) $\ln k$ values range between -2.0 to 3.5, too high $\ln k$ values are associated with too broad peaks, increased signal-to-noise and inaccurate retention times. Since low $\ln k$ values often result in analyte peaks merging into the solvent peak, retention does not only depend on the stationary phase.

c) $0 < \theta_{char} < 100$, a negative θ_{char} cannot be accepted, because it would mean, that a temperature increase leads to higher retention times than to lower. Based on available data the parameter θ_{char} tends to be lower than 100 °C, in most cases around 30 °C[20].

d) $T_{char} > -273.15$ °C, a value of T_{char} below the absolute zero is not possible.

e) $C > 0$, negative C shows a lower bending of the fit curve, the curve becomes more linear and cause also to the wrong branch of the Lambert W function (W_0)[37].

f) $A < 0$, based on available data the parameter A tends to be negative.

g) $W(x) < -1$ respectively $-1/e < x < 0$, data are inacceptable if the value of the argument x of the Lambert W function gets lower than $-1/e$ or $W(x) > -1$. Available data shows a value of $W(x) < -1$ and is on the W_{-1} branche, therefore $-1/e < x < 0$.

As example the retention factors for allergenic fragrances, PAHs, FAMEs and triglycerides over different temperatures are presented in Figure 2.2.
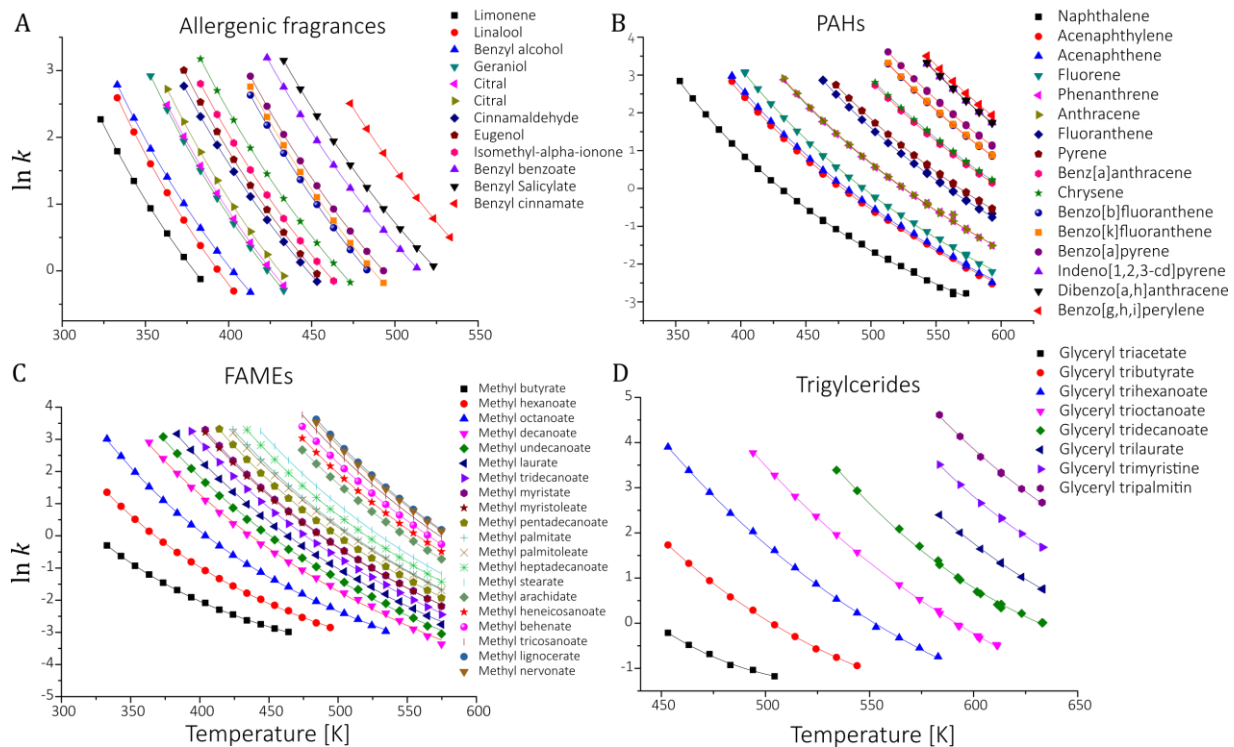
Figure 2.2: Determined $\ln k$ values over T with fits of the K-centric model (Eq. (1.23)) for each substance for a selection of allergenic fragrances (A), PAHs (B), FAMEs (C) and triglycerides (D) on Rxi-17Sil MS (β=250) as stationary phase.

The observed deviations of predicted retention times are in most cases less than 1 %. To illustrate the performance of the simulation, Figure 2.3 shows a measured and a simulated chromatogram of 16 PAHs on a Rxi-17Sil MS.
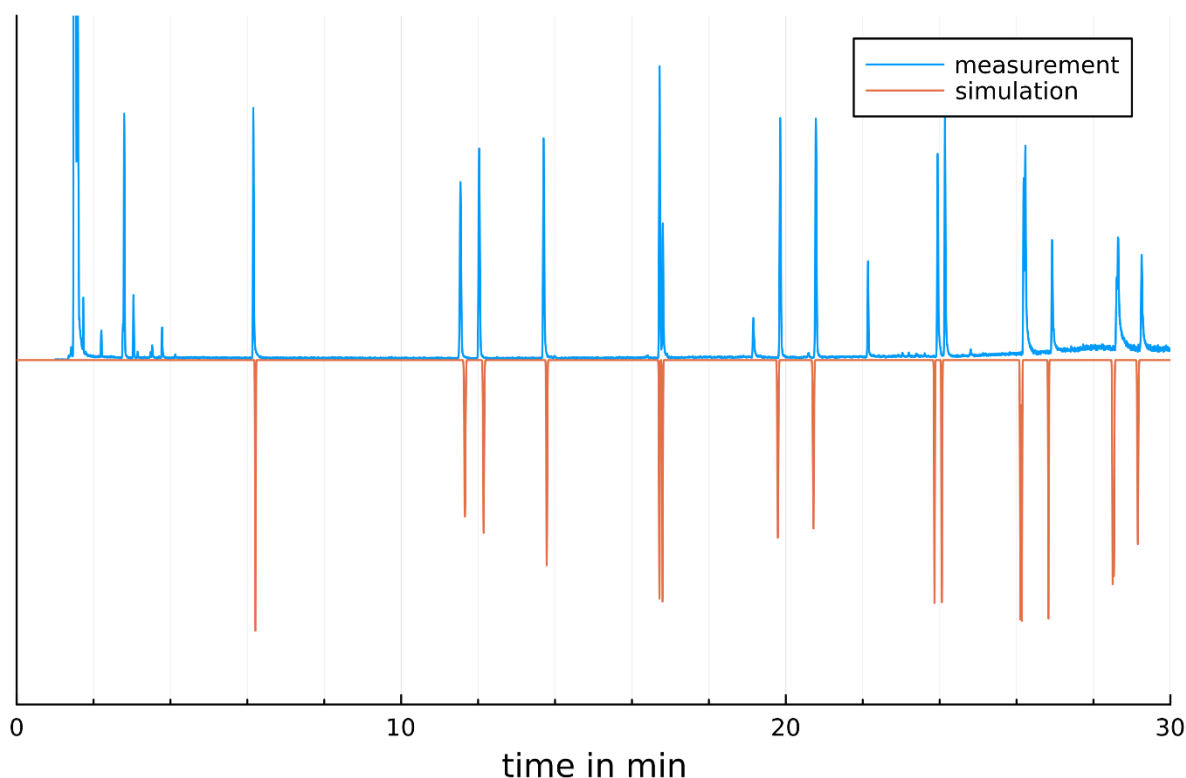
Figure 2.3: Measured and simulated chromatogram of a temperature programmed GC separation of 16 Polycyclic Aromatic Hydrocarbons (EPA PAH) on a Rxi-17Sil Ms. GC conditions: T_{init} =70 °C ; first ramp: 20 °C/min, T_1 =150 °C, hold time= 5 min; second ramp: 12 °C/min, T_2 =250 °C, hold time= 2 min ; third ramp: 15 °C/min, T_{end} =360 °C, hold time= 5 min, *rmse*=0.1425 min..

The standardized procedure of measurements and calculations, presented in the study, have a useful benefit for all chromatographers, analytical chemists and method developers, because they can be used in the own laboratories and simplify the method development.

The database includes at day of publishing[91] more than 900 entries with a large range of compounds such as VOCs, PAHs, FAMEs, PCBs or allergenic fragrances for over 20 different GC columns. The full database is available at Github[92].

Relation between characteristic temperature and elution temperature in temperature programmed gas chromatography – Part I: Influence of initial temperature and heating rate

A reprint[1] of this publication is given in Appendix B of this thesis.

3.1 Author's contributions

My contribution to this research includes all steps of retention time measurements, temperature measurements, data evaluation, Julia programming, the development of the curve fit model and writing the resulting publication. Peter Boeker acquired the funding, provided guidance, important suggestions and writing assistance. The supervisor of my doctoral thesis, Prof. Matthias Wüst, provided guidance and important suggestions. Jan Leppert supervised the experimental work, helped with programming, provided guidance, made important suggestions, gave writing assistance, did the project administration and the funding-acquisition.

3.2 Summary

Since the determination of retention parameters by isothermal measurements are laborious and time-consuming, simpler determination methods are required. The main topic of the study was to investigate the relationship between the measured elution temperature T_{elu} and the characteristic temperature T_{char}, to develop an estimation model.

As shown in the fundamentals, the elution temperature can be estimated by the characteristic temperature using a simple linear equation with intercept T_0 (Eq. (1.25))[20]:

$$T_{elu} = T_{char} + T_0 \tag{3.1}$$

Blumberg[37] demonstrated, that the relation is almost linear in temperature programmed GC for T_{char} values 60 °C higher than the initial temperature. For high volatile compounds such as aroma compounds, which elute near the initial temperature, a deviation from the simple linear relationship could be observed in first experiments, see Figure 3.1. For these compounds T_{elu} converges to an nearly constant temperature T_1.

Therefore, it was necessary to get a deeper knowledge about the relationship.
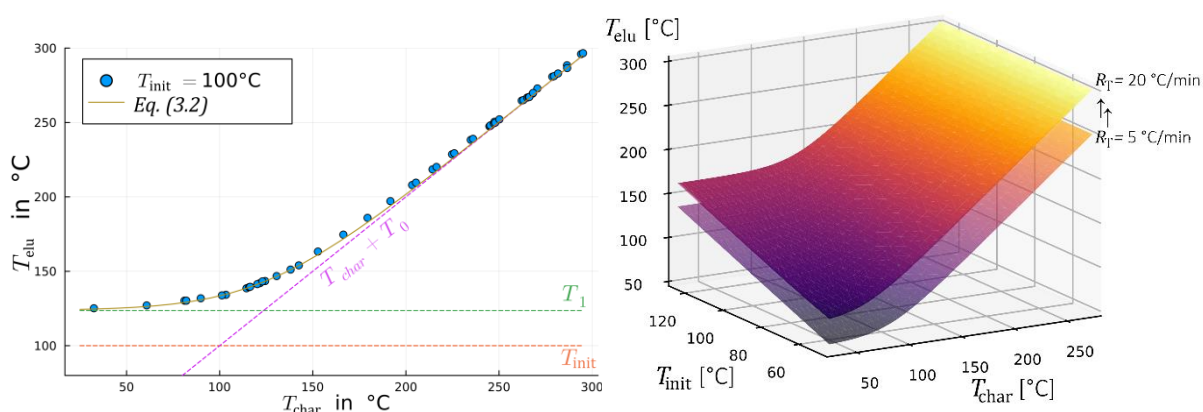
Figure 3.1: Left: Curve fit model (Eq.(3.2)) with its sub models, the constant part T_1 and the linear function $T_{char} + T_0$ and comparison to measured data., conditions: initial temperature of 100 °C, heating rate of 15 °C min^{-1} and constant flow of 1 mL min^{-1}. Right: 3D-surface of the curve fit model in the parameter space at two different heating rates.

For this purpose, the elution temperatures for 37 fatty acid methyl esters, 6 BTEXs and 40 other volatile substances are determined by measurements under 4 different heating rates, 6 initial temperatures, constant pressure mode and constant flow mode. The oven

temperature was monitored by external temperature sensors connected to a datalogger, to get exact values for the elution temperature.

Based on the data, a novel multivariate curve fit model was developed, which describes accurately the relation between the characteristic temperature T_{char} and elution temperature T_{elu} under variable heating rates R_T, respectively r_T, and initial temperature T_{init} conditions:

$$T_{elu}(T_{char}, R_T, T_{init}) = \frac{1}{\gamma}\ln\left(e^{\gamma(T_{char}+T_0)} + e^{\gamma(T_1)}\right) \tag{3.2}$$

with
$$T_0 = m_0 \cdot R_T + n_0 \tag{3.3}$$

$$T_1 = T_{init} + m_1 \cdot R_T \tag{3.4}$$

The parameters m_0, m_1 and n_0 are empirical curve fit parameters

The novel model shows good accordance to earlier estimation models[37] and expands the prediction range, especially for high volatile compounds. The model is suitable for determination of T_{char} by estimated T_{elu} and vice versa. Predictions of retention times of simple temperature programmed measurements were also possible by using the model with relative deviations <5% compared to measurements, as shown in Figure 3.2.

Table 3.1 Experimental determined parameters after multivariate fit for constant pressure and constant flow mode.

modus	γ [K^{-1}]	m_0 [min]	n_0 [K]	m_1 [min]	$R_{T,0}$ [K min^{-1}]	$r_{T,0}$	R^2	$rmse$ [K]
const. pressure ($p_{in} = 83$ kPa)	0.0548 ± 0.0015	3.365 ± 0.019	−43.12 ± 0.27	1.766 ± 0.03	12.81 ± 0.11	0.5898 ± 0.0049	0.9998	3.10
const. flow ($F = 1$mL/min)	0.03608 ± 0.0005	3.062 ± 0.016	−45.90 ± 0.23	1.57 ± 0.033	14.99 ± 0.12	0.690 ± 0.0055	0.9999	2.81

It was known, that there exists one heating rate where the elution temperature is equal to the characteristic temperature $r_{T,0}$[23]. This dimensionless heating rate could be estimated as 0.59 for constant pressure and 0.69 for constant flow by the model which is consistent to earlier estimations found in the literature[22,23,37].

Alcohols
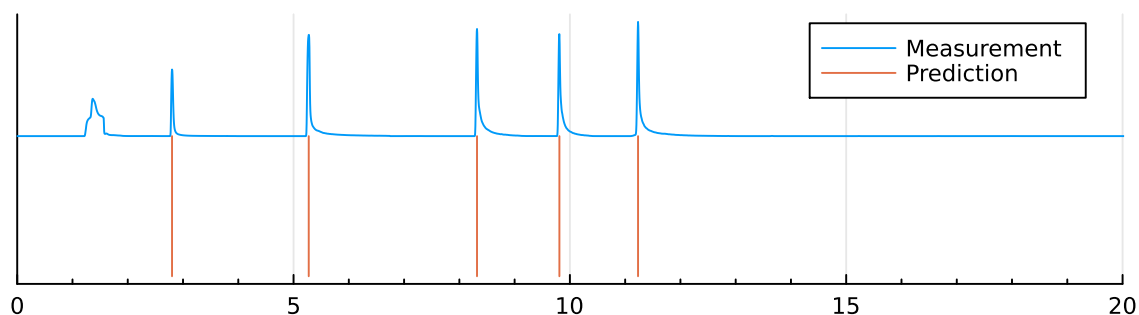
Phenones
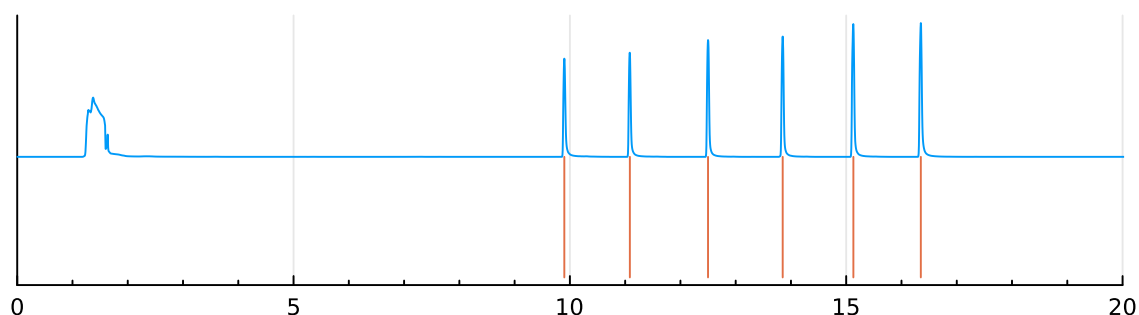
Figure 3.2 Measured chromatograms compared to predicted retention times of alcohols (pentanol, heptanol, nonanol, decanol, undecanol) and phenones (propiophenone – octanophenone). The retention times are predicted only by the T_{char} values of the substances by using the novel model; temperature program: T_{init} = 40°C, R_T = 10°C min^{-1}, p_i = 83 kPa.

The publication was the first part of the investigation. In the second part the simulation of gas chromatography was used to investigate the properties of the column, such as stationary phase, length and diameter. Using the simulation, the influence of the phase ratio β was investigated and the results compared to measurement. This publication gave the fundamentals to an estimation tool for retention parameters by temperature programmed measurements and was realised in the Julia package RetentionParameterEstimator.jl.[93]

Simulation of gas chromatographic separations and estimation of distribution-centric retention parameters using linear solvation energy relationships

The research summarized in this chapter has been published as
T. Brehmer, B. Duong, P. Boeker, M. Wüst, J. Leppert, J. Chromatogr. A 1717 (2024) 464665.
https://doi.org/10.1016/j.chroma.2024.464665.

A reprint[1] of this publication is given in Appendix C of this thesis.

4.1 Author's contributions:

My contribution to this research was the determination and evaluation of all data, including retention time measurements, calculation of the retention parameters and the LSER system constants of all investigated columns. I did the simulations and wrote the final publication. The master student Benny Duong did the determination of the K-centric parameters of PAHs on the Rxi-17Sil MS under my supervision. Peter Boeker did funding-acquisition. Matthias Wüst, the supervisor of my doctoral thesis, gave important suggestions and writing assistance. Supervisor of the experimentals Jan Leppert provided guidance, made important suggestions, gave writing and programming assistance, did the project administration and funding-acquisition.

4.2 Summary

In this work a further alternative approach to estimate K-centric retention parameters was developed. As mentioned in Chapter 1, there are different approaches to describe interactions between analytes and stationary phases, e.g. thermodynamic models like the distribution-centric 3-parameter model resp. K-centric model[43] (Eq. (1.23)) or models regarding on chemical properties such as the Linear Solvation Energy Relationships[74,94], LSER (Eq. (1.26)). For LSER, there is a high amount of compound data available in libraries. e.g. the database LSERD[86] of Helmholtz Centre for Environmental Research (UFZ) or the Wayne-State-University database (WSU)[78,79]. LSER models are valid for prediction of retention factor k[80] or retention index RI[95] under isothermal conditions. The system describing constants of the model strongly depend on temperature[85] and are not suitable for prediction of retention times in temperature programmed GC directly.
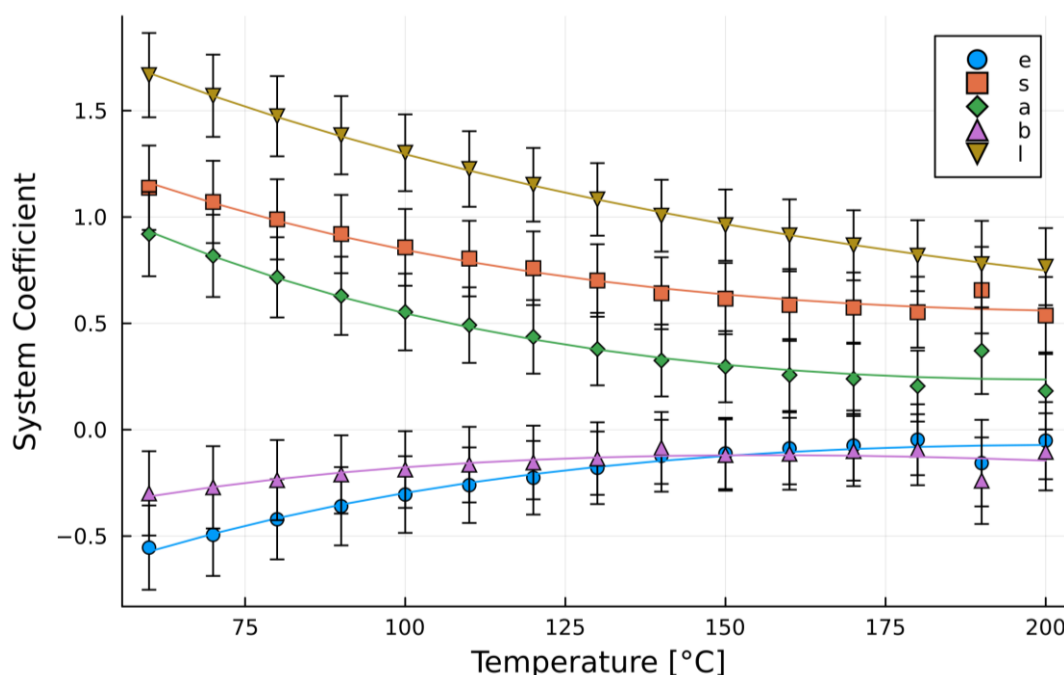
Figure 4.1: Determined system coefficients of the LSER models for a Rxi-5Sil MS phase at different temperatures (system map) and fits of the *ABC* model (Eq. (1.19)) which allows a thermodynamic interpretation of the system constants.

It was the aim of the study to combine the LSER approach and the K-centric 3-parameter model to use available LSER substance data from literature databases for the simulation software and perform precise temperature independent predictions of temperature programmed GC separations. Thus, a model to describe the temperature-dependence of the system constants was developed.

The LSER system constants of two stationary phases at different temperatures in a range from 40 °C to 200 °C were determined. For the determination a mixture recommended by

Poole[85] was used, containing 40 volatile organic compounds such as alcohols, aldehydes or phenolic compounds. Since the system constants are related to Gibbs free Energy, the classic approach was chosen for describing Gibbs related quantities and temperatures: the *ABC* model by Clark and Glew[71], Eq. (1.19). It was possible to describe the temperature impact on each system constant with the ABC-model, see Figure 4.1. For each system-constant-descriptor-interaction amounts of enthalpy and entropy could be calculated using Eqs. (1.20) and (1.21) at $T_{\text{ref}} = 90\,°C$.
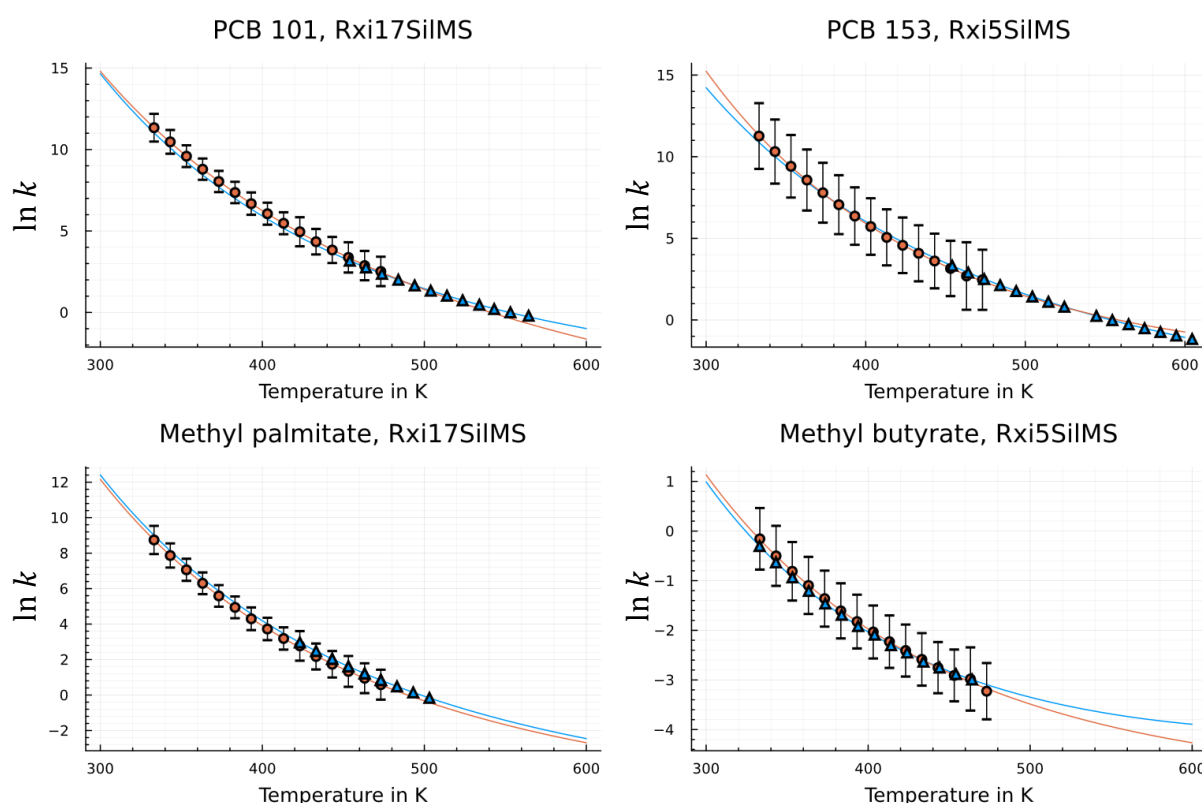
Figure 4.2: Predicted $\ln k$ values for each temperature using the LSER models (orange, circle) and isothermal determined values (blue, triangle) and curve fit of the *K*-centric model (Eq. (1.23)) for different compounds.

For any analyte with known substance descriptors, the retention factors k for the defined temperature was calculated using systems coefficients (Figure 4.2). Based on the predicted values of $\ln k$ the three parameters of the *K*-centric three-parameter retention model were calculated using the *K*-centric model. It was shown that the values of the predicted retention parameters are close to isothermal measured values. For the estimations of T_{char}, the values resulting by the LSER models are close to the values determined by isothermal measurements for both stationary phases. For the Rxi-17Sil MS the relative differences are around −3.95 to +7.81 % (median= 1.27 %), for the Rxi-5Sil MS around −7.91 to 6.31 % (median= −0.91 %). The estimated θ_{char} and ΔC_{p}

show larger deviations. It is mentioned that ΔC_p shows also large variance by data from isothermal measurements and it is the with the lowest impact of the K-centric model. Regarding the good prediction performance of the K-centric curve fits it is possible that the deviation of θ_{char} and ΔC_p compensate each other which results in an acceptable prediction of $\ln k$ values, see Figure 4.2.
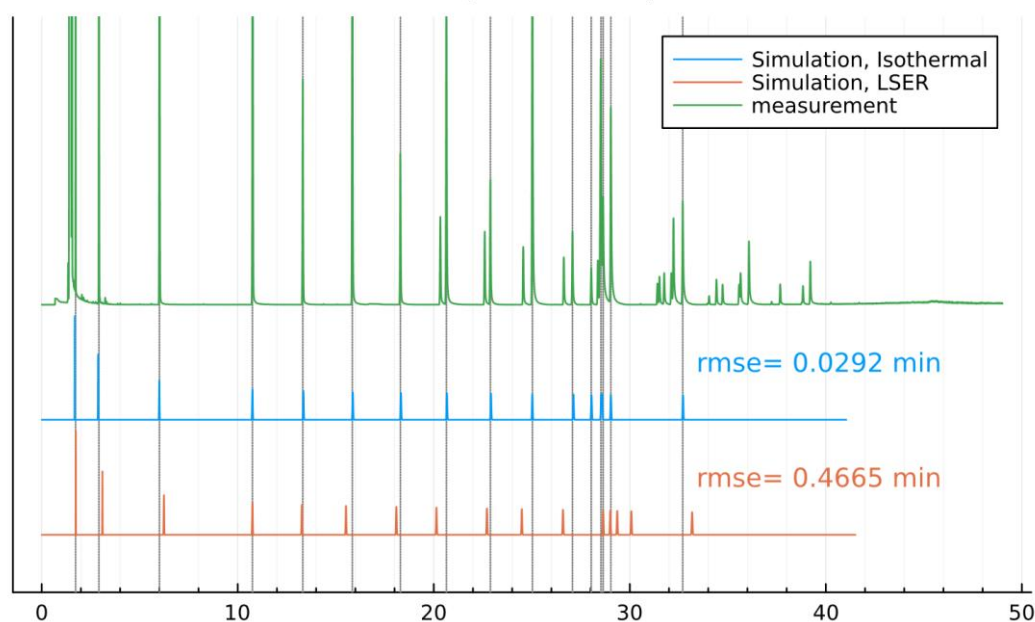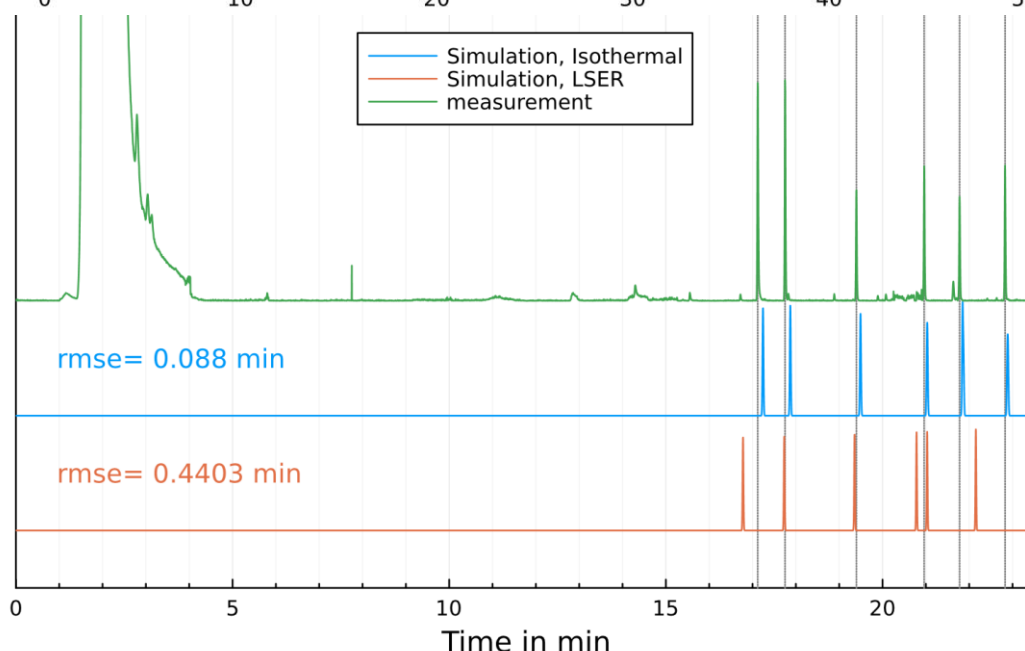
Figure 4.3: Measured chromatograms (green) compared simulation using the isothermal determined retention parameters (blue) and using the retention parameters predicted by the LSER models (orange) of FAMEs-mix on Rxi-5Sil MS(**A**) and PBC-mix on Rxi-17Sil MS(**B**). GC-conditions: **A**: T_{init}=80 °C, r_T=5 °C/min, F=1 ml/min, **B**: T_{init}=60 °C, r_T=10 °C/min, F=1 ml/min.

LSER models are suitable for the estimation of the characteristic temperature T_{char} and the elution order of the substances on the column, by literature data only. The predicted

T_{char} can also be used as start value for the determination of K-centric parameters from temperature programmed measurements[93]. For the estimation of K-centric parameters by LSER data, further approaches e.g. using graph neural networks[27] can be investigated.

Furthermore, simulations of temperature programmed GC separations using the predicted retention parameters were demonstrated and compared to simulations using isothermal determined retention parameters. Figure 4.3presents the separation of fatty acid methyl esters (FAMEs) and polychlorinated biphenyls (PCBs) compared to simulation using the different parameter sets.
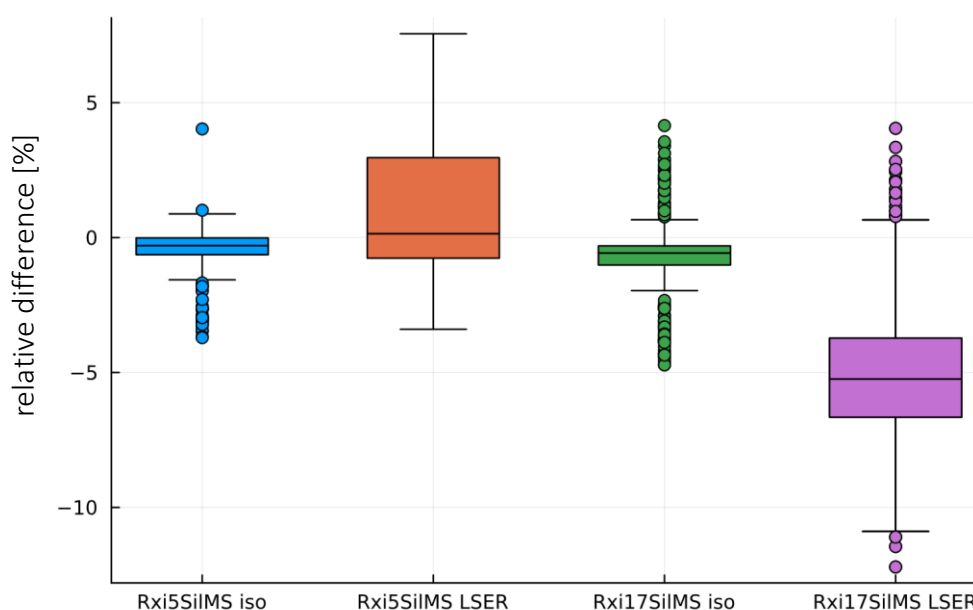
Figure 4.4: Relative differences between the measured retention times of the FAMEs and the simulated retention times using the isothermal retention parameters (iso) and the retention parameters estimated by the LSER models for both stationary phases. GC-condition:(range): T_{init}=40-120 °C, r_{T}=5-20 °C/min

Figure 4.4 shows the evaluation results of the simulations using the isothermal retention parameters (iso) and the LSER estimated parameters (LSER). In conclusion, LSER data from the literature also are suitable for recommendation of first temperature programs for a GC separation. The procedure can reduce the workload for the chromatographer during the optimization process since there is just a small number of substances, which has to be measured by isothermal measurements to calibrate the system. Regarding on benefits for other research e.g. environmental science the link between the K-centric model and the LSER model can help to determine the LSER descriptors by temperature programmed measurements using the simulation software[93]. The data then can be used to predict adsorption phenomena e.g. in soils or in food as well. There are still substances, were no LSER descriptors are available for, e.g. triglycerides, which determination is possible by simulation.

Concluding remarks and outlook

The benefits of simulating gas chromatographic separations have been sufficiently demonstrated. With the establishment of the retention database, retention data for a variety of compounds are now available for simulation. A standardized procedure was introduced for determining retention parameters, and quality criteria were defined to include these parameters in the database. This procedure can be applied by all method developers to optimize their own gas chromatographic systems based on the determined parameters. Particularly, the analysis of the distribution coefficient K respectively the retention factor k against the temperature ('ln k over T plots') and its description through the distribution-centric three-parameter model (K-centric model) provides valuable information for solving separation problems.

Relevant data for food analysis has been determined, for example, for polycyclic aromatic hydrocarbons (PAHs), polychlorinated biphenyls (PCBs), fatty acid methyl esters (FAMEs), and many other volatile compounds. In addition to public available retention data from the literature a database was created. It is publicly accessible and can be expanded successively. Currently[92], the database contains 1872 entries with 353 substances on 25 stationary phases. The retention data are documented both as K-centric data, directly readable in the Julia package 'GasChromatographySimulator.jl'[58], and as ABC model data, making them usable by other GC simulation users[15,54,55].

The simulation based on isothermal-determined retention parameters has proven to be particularly robust. For most compounds, relative deviations of under 1% were achieved in the investigated temperature programs. The database now provides enough retention data to predict multidimensional separations such as comprehensive two dimmensional GC (GC×GC) with thermal modulation. While retention times can already be predicted with machine learning[47], there are still some discrepancies. A simulation of ²D separations, which considers the instrumental properties of the GC system such as GasChromatographySimulator.jl, would be advantageous. A modular approach, allowing the simulation of numerous GC columns and separations in sequence, serves as the basis.

The results of one separation section are then used as input for the next simulation and so on. First simulations of comprehensive GC×GC separations with thermal modulation were presented at the 20th GC×GC Symposium in Canmore, Canada and the 51th Lebensmittelchemietage in Bonn, Germany. For highly precise simulation of GC×GC the modulator has to be described accurately. Typical modulation periods are about four seconds with a hot jet interval of just some hundred milliseconds. An interesting question is to know more about the intensity of the cooling effects onto the GC column during an increasing temperature program and the same for the reheating period. For this purpose, high resolution measurements of the temperature during the modulation period are recommended to be performed. Furthermore, the simulation can be expanded to other modulation technics such as flow modulation[96,97].

A more detailed examination of the elution temperature T_{elu} and the characteristic temperature T_{char} led to the development of an estimation formula incorporating temperature program parameters such as initial temperature and heating rate. The study emphasizes the significance of the characteristic temperature as a tangible chromatographic parameter directly related to elution order, elution temperature, and therefore retention time for simple temperature programs. The calculation of retention times was demonstrated using alcohols and phenones as samples. Regarding the estimation of the characteristic temperature, an extended estimation range of up to 50 °C was observed for volatile compounds (e.g. aroma compounds) compared to simple linear considerations. In a second part, the estimation model was confirmed for additional stationary phases, particularly addressing the influence of phase ratio on the model. Simultaneously, this investigation paves the way to estimate K-centric parameters from temperature-programmed measurements, potentially eliminating the need for laborious isothermal measurements. RetentionParameterEstimator.jl[93] was released, utilizing common optimization algorithms based on the Newton method for such estimation programs.

Additionally, by linking the K-centric retention model with the Linear Solvent Energy Relationships model (LSER, Abraham model), another pool of retention data for simulation purposes was created. Thus, temperature-programmed measurements can also be calculated based on substance-specific LSER descriptors. The temperature dependence of the GC system describing LSER constants was examined, leading to an empirical model describing this relationship and relating it to thermodynamic quantities.

This provides insights into the contributions of enthalpy ΔH and entropy ΔS to different types of interactions between analytes and the stationary phase.

Conversely, the simulation of gas chromatographic separation can be used to estimate LSER substance data from simulation results. This information is not only valuable for gas chromatography or analytical chemistry purposes but can also be useful for environmental science in describing other adsorption phenomena, such as the accumulation of a substance in soil, the tissue of an organism or migration from food onto package materials and vice versa[77,98].

Additional approaches to estimate K-centric parameters could lie in the connection with retention index data. Methods for retention index (RI) estimation already exist using LSER data[95] or graphical neural networks[27,99]. For RI data, there exist further databases such as the RI data base of the National Institute of Standards and Technology (NIST)[31] or Flavournet[32]. Other chemometrical data, such as structural data like Chi indices, may also be suitable for retention estimation using machine learning (ML) as shown by Minho et al. and Mazraedoost et al.[46,100]. However, such AI-based approaches often do not consider physico-chemical and instrumental relationships, making it preferable, from the author's perspective, to always include or prioritize physical computational models.

The combination of determining retention parameters from temperature-programmed measurements, substance databases, and predicting retention times can form the basis for optimizing GC measurements in an automated workflow (auto-optimization). A powerful algorithm could, for example, provide initial parameter estimates and propose a temperature program suitable for solving the separation problem after injecting a sample from a few test measurements. The simulation would then be evaluated based on additional test measurements. The new measurement would provide another data point for the parameter determination and propose another temperature program. Standardized optimization approaches could be suitable, such as Design of Experiment (DOE) [101], neural networks, and machine learning (ML)[102].

For such a system, it would be necessary to developing an

- automated peak detection
- automated optimization of the temperature program based on simulation
- interface between the software and the gas chromatographic system

Machine learning-based approaches for optimization in liquid chromatography were shown by Boelrijk et al.[103,104]. Struk et al.[105] presented a semi-automated approach for GC. *Support Vector Machines* (SVM), *Partial Least Square Discriminant Analysis* (PLSDA)[48–50] and *Random Forest* (RF)[51–53] are possible algorithms for the data processing[45–47]. A first commercial available software for method development in HPLC is ChromSword[106].

The retention data and the simulation greatly benefit the development of methods for complex samples. Complex samples include, for instance, aroma profiles or essential oils with hundreds of analytes. If the retention data are known respectively determinable, simulations are suitable to support the method development. This is evidenced by the excellent results obtained with over 80 allergenic odorants and almost 40 FAMEs and all the other compounds investigated. The ability to test various column geometries (e.g. column length) through simulation is a significant advantage, as this cannot be done non-destructively in the laboratory. The simulation reaches limitations when physico-chemical behaviour is not considered in the retention models. The thermodynamic models and thus the *K*-centric model exclusively consider ideal interactions between analytes and the stationary phase, assuming the peak width is normal-distributed around the retention time. Effects such as tailing or fronting are not considered by the simulation model. Similarly, the temperature-dependent consideration does not include phase transitions. For example, condensation effects of the analytes may occur due to cold spots or intentional thermal modulation such as cold jet in two-dimensional gas chromatography [102]. During the hot jet the analytes then regain mobility only gradually by reheating. This would not be considered by the simulation model based on the *K*-centric retention model and leading to deviations in retention time in the second dimension[102]. Experiments conducted within the project suggest that this could affect the simulation of heavy volatile compounds such as PAHs in GC×GC. Further investigation of the precise thermal conditions at the modulation site with suitably sensitive sensors should be conducted.

However, using accurate simulation as a tool to support the method development process of chemical analysis will become more import in the future not only in gas chromatography.

References

[1] A. Büttner (Ed.), Springer handbook of odor, Springer, Cham, 2017.

[2] M. Śliwińska, P. Wiśniewska, T. Dymerski, W. Wardencki, J. Namieśnik, The flavour of fruit spirits and fruit liqueurs: a review, Flavour Fragr. J. 30 (2015) 197–207. https://doi.org/10.1002/ffj.3237.

[3] S. Petronilho, R. Lopez, V. Ferreira, M.A. Coimbra, S.M. Rocha, Revealing the Usefulness of Aroma Networks to Explain Wine Aroma Properties: A Case Study of Portuguese Wines, Molecules 25 (2020). https://doi.org/10.3390/molecules25020272.

[4] S. Basu, R.E. Clark, Z. Fu, B.W. Lee, D.W. Crowder, Insect alarm pheromones in response to predators: Ecological trade-offs and molecular mechanisms, Insect Biochem. Mol. Biol. 128 (2021) 103514. https://doi.org/10.1016/j.ibmb.2020.103514.

[5] L. Culleré, A. Escudero, J. Cacho, V. Ferreira, Gas chromatography-olfactometry and chemical quantitative study of the aroma of six premium quality spanish aged red wines, Journal of Agricultural and Food Chemistry 52 (2004) 1653–1660. https://doi.org/10.1021/jf0350820.

[6] A. Wilson, J.B. Johnson, R. Batley, P. Lal, L. Wakeling, M. Naiker, Authentication Using Volatile Composition: A Proof-of-Concept Study on the Volatile Profiles of Fourteen Queensland Ciders, Beverages 7 (2021) 28. https://doi.org/10.3390/beverages7020028.

[7] R.I. Aylott, W.M. MacKenzie, Analytical Strategies to Confirm the Generic Authenticity of Scotch Whisky, J. Inst. Brew. 116 (2010) 215–229. https://doi.org/10.1002/j.2050-0416.2010.tb00424.x.

[8] K. Jurica, I. Brčić Karačonji, D. Lasić, D. Bursać Kovačević, P. Putnik, Unauthorized Food Manipulation as a Criminal Offense: Food Authenticity, Legal Frameworks, Analytical Tools and Cases, Foods 10 (2021). https://doi.org/10.3390/foods10112570.

References

[9] Y. Nolvachai, C. Kulsing, P.J. Marriott, Multidimensional gas chromatography in food analysis, TrAC Trends in Analytical Chemistry 96 (2017) 124–137. https://doi.org/10.1016/j.trac.2017.05.001.

[10] R.L. Grob, E.F. Barry (Eds.), Modern practice of gas chromatography, 4th ed., Wiley-Interscience, Hoboken, NJ, 2004.

[11] D.E. Bautz, J.W. Dolan, L.R. Snyder, Computer simulation as an aid in method development for gas chromatography: I. The accurate prediction of separation as a function of experimental conditions, J. Chromatogr. A 541 (1991) 1–19. https://doi.org/10.1016/S0021-9673(01)95980-1.

[12] L.R. Snyder, D.E. Bautz, J.W. Dolan, Computer simulation as an aid in method development for gas chromatography: III. Examples of its application, J. Chromatogr. A 541 (1991) 35–58. https://doi.org/10.1016/S0021-9673(01)95982-5.

[13] J.W. Dolan, D.E. Bautz, Computer-aided optimization of gas chromatographic separation, American Chemical Society, United States, 1990.

[14] J. Leppert, L.M. Blumberg, M. Wüst, P. Boeker, Simulation of the effects of negative thermal gradients on separation performance of gas chromatography, J. Chromatogr. A (2021) 461943. https://doi.org/10.1016/j.chroma.2021.461943.

[15] S. Hou, K.A.J.M. Stevenson, J.J. Harynuk, A simple, fast, and accurate thermodynamic-based approach for transfer and prediction of gas chromatography retention times between columns and instruments Part III: Retention time prediction on target column, J. Sep. Sci. 41 (2018) 2559–2564. https://doi.org/10.1002/jssc.201701345.

[16] J. Leppert, M. Härtel, T.M. Klapötke, P. Boeker, Hyperfast Flow-Field Thermal Gradient GC/MS of Explosives with Reduced Elution Temperatures, Anal. Chem. 90 (2018) 8404–8411. https://doi.org/10.1021/acs.analchem.8b00900.

[17] M.D. Chopra, P.J. Müller, J. Leppert, M. Wüst, P. Boeker, Residual solvent analysis with hyper-fast gas chromatography-mass spectrometry and a liquid carbon dioxide cryofocusing in less than 90 s, J. Chromatogr. A 1648 (2021) 462179. https://doi.org/10.1016/j.chroma.2021.462179.

[18] J.G. Speight, Molecular Interactions, Partitioning, and Thermodynamics, in: J.G. Speight (Ed.), Reaction mechanisms in environmental engineering: Analysis and prediction, Butterworth-Heinemann an imprint of Elsevier, Kidlington, Oxford, United Kingdom, 2018, pp. 307–336.

[19] C.F. Poole (Ed.), Gas chromatography, 1st ed., Elsevier, Amsterdam, 2012.

[20] L.M. Blumberg, Temperature-programmed gas chromatography, Wiley-VCH, Weinheim, 2010.

[21] P. Boeker, J. Leppert, B. Mysliwietz, P.S. Lammers, Comprehensive theory of the Deans' switch as a variable flow splitter: fluid mechanics, mass balance, and system behavior, Anal. Chem. 85 (2013) 9021–9030. https://doi.org/10.1021/ac401419j.

[22] L.M. Blumberg, M.S. Klee, Optimal heating rate in gas chromatography, J. Micro. Sep. 12 (2000) 508–514. https://doi.org/10.1002/1520-667X(2000)12:9<508:AID-MCS5>3.0.CO;2-Y.

[23] K.A.J.M. Stevenson, L.M. Blumberg, J.J. Harynuk, Thermodynamics-based retention maps to guide column choices for comprehensive multi-dimensional gas chromatography, Anal. Chim. Acta 1086 (2019) 133–141. https://doi.org/10.1016/j.aca.2019.08.011.

[24] L.M. Blumberg, M.S. Klee, Method Translation and Retention Time Locking in Partition GC, Anal. Chem. 70 (1998) 3828–3839. https://doi.org/10.1021/ac971141v.

[25] M. Mehran, W.J. Cooper, N. Golkar, M.G. Nickelsen, E.R. Mittlefehldt, E. Guthrie, W. Jennings, Elution order in gas chromatography, J. High Resol. Chromatogr. 14 (1991) 745–750. https://doi.org/10.1002/jhrc.1240141109.

[26] K. Cammann (Ed.), Instrumentelle analytische Chemie: Verfahren, Anwendungen und Qualitätssicherung, Spektrum Akad. Verl., Heidelberg, Berlin, 2001.

[27] C. Qu, B.I. Schneider, A.J. Kearsley, W. Keyrouz, T.C. Allison, Predicting Kováts Retention Indices Using Graph Neural Networks, J. Chromatogr. A 1646 (2021) 462100. https://doi.org/10.1016/j.chroma.2021.462100.

[28] E. Kováts, Gas-chromatographische Charakterisierung organischer Verbindungen. Teil 1: Retentionsindices aliphatischer Halogenide, Alkohole, Aldehyde und Ketone, Helvetica Chimica Acta 41 (1958) 1915–1932. https://doi.org/10.1002/hlca.19580410703.

[29] H. van den Dool, P. Dec. Kratz, A generalization of the retention index system including linear temperature programmed gas—liquid partition chromatography, J. Chromatogr. A 11 (1963) 463–471. https://doi.org/10.1016/S0021-9673(01)80947-X.

[30] V. Gold, The IUPAC Compendium of Chemical Terminology, International Union of Pure and Applied Chemistry (IUPAC), Research Triangle Park, NC, 2019.

References

[31] V.I. Babushok, P.J. Linstrom, J.J. Reed, I.G. Zenkevich, R.L. Brown, W.G. Mallard, S.E. Stein, Development of a database of gas chromatographic retention properties of organic compounds, J. Chromatogr. A 1157 (2007) 414–421. https://doi.org/10.1016/j.chroma.2007.05.044.

[32] T. Acree, H. Arn, Flavornet. https://www.flavornet.org/flavornet.html, 2004 (accessed 20 September 2023).

[33] E. Cremer, E. Prior, Application of the Chromatographic Method to the Separation of Gases and to the Determination of Adsorption Energies, Zeitschrift für Elektrochemie 55 (1951) 217–220.

[34] A.T. JAMES, A.J.P. MARTIN, Gas-liquid partition chromatography; the separation and micro-estimation of volatile fatty acids from formic acid to dodecanoic acid, Biochem. J. 50 (1952) 679–690. https://doi.org/10.1042/bj0500679.

[35] M.J.E. Golay, Theory of chromatography in open and coated tubular columns with round and rectangular cross-sections, in: D.H. Desty (Ed.), Gas Chromatography, Butteerworths, London, 1958, pp. 36–53.

[36] L.S. Ettre, Nomenclature for chromatography (IUPAC Recommendations 1993), Pure and Applied Chemistry 65 (1993) 819–872. https://doi.org/10.1351/pac199365040819.

[37] L.M. Blumberg, Distribution-centric 3-parameter thermodynamic models of partition gas chromatography, J. Chromatogr. A 1491 (2017) 159–170. https://doi.org/10.1016/j.chroma.2017.02.047.

[38] James Heseltine, Hydrogen as a Carrier Gas for GC and GC–MS, LCGC North America 28 (2010) 16–27.

[39] S.P. McCann, H. Rana, B.A. Handzo, N.H. Snow, Go With the Flow: Thinking About Carrier Gas Flow in GC, LCGC North America 38 (2020).

[40] S. Kromidas, H.-J. Kuss (Eds.), Chromatogramme richtig integrieren und bewerten: Ein Praxishandbuch für die HPLC und GC, Wiley-VCH, Weinheim, 2008.

[41] J.J. van Deemter, F.J. Zuiderweg, A. Klinkenberg, Longitudinal diffusion and resistance to mass transfer as causes of nonideality in chromatography, Chemical Engineering Science 5 (1956) 271–289. https://doi.org/10.1016/0009-2509(56)80003-1.

[42] N.H. Snow, Is Golay's Famous Equation for HETP Still Relevant in Capillary Gas Chromatography? Part 2: Assumptions and Consequences, LCGC N. Am. 40 (2022) 68–71. https://doi.org/10.56530/lcgc.na.mm7085y7.

[43] L.M. Blumberg, Chromatographic parameters: Characteristic parameters of solute retention - an insightful description of column properties, J. Chromatogr. A 1685 (2022) 463594. https://doi.org/10.1016/j.chroma.2022.463594.

[44] H. Snijders, H.-G. Janssen, C. Cramers, Optimization of temperature-programmed gas chromatographic separations I. Prediction of retention times and peak widths from retention indices, J. Chromatogr. A 718 (1995) 339–355. https://doi.org/10.1016/0021-9673(95)00692-3.

[45] M. Gaida, F.A. Franchina, P.-H. Stefanuto, J.-F. Focant, Modeling approaches for temperature-programmed gas chromatographic retention times under vacuum outlet conditions, J. Chromatogr. A 1651 (2021) 462300. https://doi.org/10.1016/j.chroma.2021.462300.

[46] L.A.C. Minho, Z.d.L. Cardeal, H.C. Menezes, A deep learning-based simulator for comprehensive two-dimensional GC applications, J. Sep. Sci. 46 (2023) e2300187. https://doi.org/10.1002/jssc.202300187.

[47] M. Gaida, F.A. Franchina, P.-H. Stefanuto, J.-F. Focant, Top-Down Approach to Retention Time Prediction in Comprehensive Two-Dimensional Gas Chromatography-Mass Spectrometry, Anal. Chem. 94 (2022) 17081–17089. https://doi.org/10.1021/acs.analchem.2c03107.

[48] G.L. Alexandrino, P.S. Prata, F. Augusto, Discriminating Lacustrine and Marine Organic Matter Depositional Paleoenvironments of Brazilian Crude Oils Using Comprehensive Two-Dimensional Gas Chromatography–Quadrupole Mass Spectrometry and Supervised Classification Chemometric Approaches, Energy Fuels 31 (2017) 170–178. https://doi.org/10.1021/acs.energyfuels.6b01925.

[49] R.A.M. Lima, S.M.M. Ferraz, V.G.K. Cardoso, C.A. Teixeira, L.W. Hantao, Authentication of fish oil (omega-3) supplements using class-oriented chemometrics and comprehensive two-dimensional gas chromatography coupled to mass spectrometry, Fresenius J Anal Chem 415 (2023) 2601–2611. https://doi.org/10.1007/ S00216-022-04428-2.

[50] L.C. Lee, C.-Y. Liong, A.A. Jemain, Partial least squares-discriminant analysis (PLS-DA) for classification of high-dimensional (HD) data: a review of contemporary practice strategies and knowledge gaps, Analyst 143 (2018) 3526–3539. https://doi.org/10.1039/C8AN00599K.

References

[51] C. Zou, D. Yu, H. Geng, X. Lan, W. Sun, A patient with 47, XYY mosaic karyotype and congenital absence of bilateral vas deferens: a case report and literature review, BMC Urol. 22 (2022) 16. https://doi.org/10.1186/s12894-022-00965-1.

[52] G. Purcaro, C.A. Rees, J.A. Melvin, J.M. Bomberger, J.E. Hill, Volatile fingerprinting of Pseudomonas aeruginosa and respiratory syncytial virus infection in an in vitro cystic fibrosis co-infection model, J. Breath Res. 12 (2018) 46001. https://doi.org/10.1088/1752-7163/aac2f1.

[53] M. Beccaria, T.R. Mellors, J.S. Petion, C.A. Rees, M. Nasir, H.K. Systrom, J.W. Sairistil, M.-A. Jean-Juste, V. Rivera, K. Lavoile, P. Severe, J.W. Pape, P.F. Wright, J.E. Hill, Preliminary investigation of human exhaled breath for tuberculosis diagnosis by multidimensional gas chromatography - Time of flight mass spectrometry and machine learning, J. Chromatogr. B Analyt. Technol. Biomed. Life Sci. 1074-1075 (2018) 46–50. https://doi.org/10.1016/j.jchromb.2018.01.004.

[54] S. Hou, K.A.J.M. Stevenson, J.J. Harynuk, A simple, fast, and accurate thermodynamic-based approach for transfer and prediction of gas chromatography retention times between columns and instruments Part I: Estimation of reference column geometry and thermodynamic parameters, J. Sep. Sci. 41 (2018) 2544–2552. https://doi.org/10.1002/jssc.201701343.

[55] S. Hou, K.A.J.M. Stevenson, J.J. Harynuk, A simple, fast, and accurate thermodynamic-based approach for transfer and prediction of GC retention times between columns and instruments Part II: Estimation of target column geometry, J. Sep. Sci. 41 (2018) 2553–2558. https://doi.org/10.1002/jssc.201701344.

[56] M. Beccaria, C. Bobak, B. Maitshotlo, T.R. Mellors, G. Purcaro, F.A. Franchina, C.A. Rees, M. Nasir, W.S. Stevens, L.E. Scott, A. Black, J.E. Hill, Exhaled human breath analysis in active pulmonary tuberculosis diagnostics by comprehensive gas chromatography-mass spectrometry and chemometric techniques, J. Breath Res. 13 (2018) 16005. https://doi.org/10.1088/1752-7163/aae80e.

[57] S.E. Reichenbach, C.A. Zini, K.P. Nicolli, J.E. Welke, C. Cordero, Q. Tao, Benchmarking machine learning methods for comprehensive chemical fingerprinting and pattern recognition, J. Chromatogr. A 1595 (2019) 158–167. https://doi.org/10.1016/J.CHROMA.2019.02.027.

[58] J. Leppert, GasChromatographySimulator.jl, Journal of Open Source Software 7 (2022) 4565. https://doi.org/10.21105/joss.04565.

[59] P. Boeker, J. Leppert, Flow field thermal gradient gas chromatography, Anal. Chem. 87 (2015) 9033–9041. https://doi.org/10.1021/acs.analchem.5b02227.

[60] J.M. White, P.K. Mogensen, B. Johnson, J. Li, C. McBride, M. Lubin, J. Weidner, Y. Yu, B. Arthur, A. Arslan, M. Zaffalon, I. Dunning, R. Arutjunjan, T. Holy, A. Noack, G. Datseris, A. Sakai, B. Legat, T. Sampson, A. Singhvi, T. Lienart, C. Rackauckas, Q. Zhang, Affan, Jérémy, K. Thelate, T. Kelman, J. Omotani, J. Assländer, F. Zierler, N. Ignatiadis, V. Martinek, A. Sengupta, I. Butterworth, LsqFit.jl, 2012. https://github.com/JuliaNLSolvers/LsqFit.jl (accessed 22 January 2024).

[61] P.K. Mogensen, A. N Riseth, Optim: A mathematical optimization package for Julia, Journal of Open Source Software 3 (2018) 615. https://doi.org/10.21105/joss.00615.

[62] Blumberg, Klee, Characteristic thermal constant and dimensionless heating rate. The links to optimum heating rate in GC, Anal. Chem. 72 (2000) 4080–4089. https://doi.org/10.1021/ac000378f.

[63] D.E. Bautz, J.W. Dolan, W.D. Raddatz, L.R. Snyder, Computer simulation (based on a linear-elution-strength approximation) as an aid for optimizing separations by programmed-temperature gas chromatography, Anal. Chem. 62 (1990) 1560–1567. https://doi.org/10.1021/ac00214a004.

[64] Pro EZGC: Chromatogram Modeler, 2023. https://ez.restek.com/proezgc (accessed 5 May 2023).

[65] J. Leppert, P.J. Müller, M.D. Chopra, L.M. Blumberg, P. Boeker, Simulation of spatial thermal gradient gas chromatography, J. Chromatogr. A 1620 (2020) 460985. https://doi.org/10.1016/j.chroma.2020.460985.

[66] C. Rackauckas, Q. Nie, DifferentialEquations.jl – A Performant and Feature-Rich Ecosystem for Solving Differential Equations in Julia, JORS 5 (2017) 15. https://doi.org/10.5334/jors.151.

[67] E. Fehlberg, Klassische Runge-Kutta-Formeln vierter und niedrigerer Ordnung mit Schrittweiten-Kontrolle und ihre Anwendung auf Wärmeleitungsprobleme, Computing 6 (1970) 61–71. https://doi.org/10.1007/BF02241732.

[68] B. Owren, M. Zennaro, Derivation of Efficient, Continuous, Explicit Runge–Kutta Methods, SIAM J. Sci. and Stat. Comput. 13 (1992) 1488–1501. https://doi.org/10.1137/0913084.

[69] Z. Wu, Retention simulation in gas chromatography, J. Chromatogr. A 840 (1999) 137–143. https://doi.org/10.1016/S0021-9673(99)00124-7.

References

[70] P. Bouchilloux, P. Darriet, R. Henry, V. Lavigne-Cruège, D. Dubourdieu, Identification of Volatile and Powerful Odorous Thiols in Bordeaux Red Wine Varieties, Journal of Agricultural and Food Chemistry 46 (1998) 3095–3099. https://doi.org/10.1021/jf971027d.

[71] E.C.W. Clarke, D.N. Glew, Evaluation of thermodynamic functions from equilibrium constants, Transactions of the Faraday Society 62 (1966) 539. https://doi.org/10.1039/tf9666200539.

[72] B. Karolat, J. Harynuk, Prediction of gas chromatographic retention time via an additive thermodynamic model, J. Chromatogr. A 1217 (2010) 4862–4867. https://doi.org/10.1016/j.chroma.2010.05.037.

[73] T.M. McGinitie, B.R. Karolat, C. Whale, J.J. Harynuk, Influence of carrier gas on the prediction of gas chromatographic retention times based on thermodynamic parameters, J. Chromatogr. A 1218 (2011) 3241–3246. https://doi.org/10.1016/j.chroma.2010.09.068.

[74] M.H. Abraham, C.F. Poole, S.K. Poole, Classification of stationary phases and other materials by gas chromatography, J. Chromatogr. A 842 (1999) 79–114. https://doi.org/10.1016/S0021-9673(98)00930-3.

[75] C.F. Poole, T.O. Kollie, Interpretation of the influence of temperature on the solvation properties of gas chromatographic stationary phases using Abraham's solvation parameter model, Anal. Chim. Acta 282 (1993) 1–17. https://doi.org/10.1016/0003-2670(93)80347-N.

[76] H.C. Tülp, K.-U. Goss, R.P. Schwarzenbach, K. Fenner, Experimental determination of LSER parameters for a set of 76 diverse pesticides and pharmaceuticals, Environ. Sci. Technol. 42 (2008) 2034–2040. https://doi.org/10.1021/es702473f.

[77] A.B. Strobel, T. Egert, P. Langguth, Predicting Leachables Solubilization in Polysorbate 80 Solutions by a Linear Solvation Energy Relationship (LSER), Pharm. Res. 38 (2021) 1549–1561. https://doi.org/10.1007/s11095-021-03096-8.

[78] C.F. Poole, Wayne State University experimental descriptor database for use with the solvation parameter model, J. Chromatogr. A 1617 (2020) 460841. https://doi.org/10.1016/j.chroma.2019.460841.

[79] C.F. Poole, Gas chromatography system constant database over an extended temperature range for nine open-tubular columns, J. Chromatogr. A 1590 (2019) 130–145. https://doi.org/10.1016/j.chroma.2019.01.028.

[80] C.F. Poole, Solvation parameter model: Tutorial on its application to separation systems for neutral compounds, J. Chromatogr. A 1645 (2021) 462108. https://doi.org/10.1016/j.chroma.2021.462108.

[81] C.F. Poole, S.N. Atapattu, S.K. Poole, A.K. Bell, Determination of solute descriptors by chromatographic methods, Anal. Chim. Acta 652 (2009) 32–53. https://doi.org/10.1016/j.aca.2009.04.038.

[82] M.H. Abraham, A. Ibrahim, A.M. Zissimos, Determination of sets of solute descriptors from chromatographic measurements, J. Chromatogr. A 1037 (2004) 29–47. https://doi.org/10.1016/j.chroma.2003.12.004.

[83] C.F. Poole, T.C. Ariyasena, N. Lenca, Estimation of the environmental properties of compounds from chromatographic measurements and the solvation parameter model, J. Chromatogr. A 1317 (2013) 85–104. https://doi.org/10.1016/j.chroma.2013.05.045.

[84] S.D. Martin, C.F. Poole, M.H. Abraham, Synthesis and gas chromatographic evaluation of a high-temperature hydrogen-bond acid stationary phase, J. Chromatogr. A 805 (1998) 217–235. https://doi.org/10.1016/S0021-9673(98)00007-7.

[85] C.F. Poole, Selection of calibration compounds for selectivity evaluation of wall-coated, open-tubular columns for gas chromatography by the solvation parameter model, J. Chromatogr. A 1629 (2020) 461500. https://doi.org/10.1016/j.chroma.2020.461500.

[86] N. Ulrich, S. Endo, T.N. Brown, N. Watanabe, G. Bronner, M.H. Abraham, K.-U. Goss, UFZ-LSER database v 3.2. http://www.ufz.de/lserd, 2017 (accessed 28 October 2021).

[87] T. Brehmer, B. Duong, M. Marquart, L. Friedemann, P.J. Faust, P. Boeker, M. Wüst, J. Leppert, Retention Database for Prediction, Simulation, and Optimization of GC Separations, ACS Omega 8 (2023) 19708–19718. https://doi.org/10.1021/acsomega.3c01348.

[88] T. Brehmer, P. Boeker, M. Wüst, J. Leppert, Relation between characteristic temperature and elution temperature in temperature programmed gas chromatography - part I: Influence of initial temperature and heating rate, J. Chromatogr. A 1707 (2023) 464301. https://doi.org/10.1016/j.chroma.2023.464301.

References

[89] C.F. Poole, Gas chromatography system constant database for 52 wall-coated, open-tubular columns covering the temperature range 60-140 °C, J. Chromatogr. A 1604 (2019) 460482. https://doi.org/10.1016/j.chroma.2019.460482.

[90] T. Brehmer, B. Duong, P. Boeker, M. Wüst, J. Leppert, Simulation of gas chromatographic separations and estimation of distribution-centric retention parameters using linear solvation energy relationships, J. Chromatogr. A 1717 (2024) 464665. https://doi.org/10.1016/j.chroma.2024.464665.

[91] J. Leppert, T. Brehmer, RetentionData: v0.2.0 (2023). https://doi.org/10.5281/zenodo.7793225.

[92] J. Leppert, T. Brehmer, RetentionData: v0.3.1 (2024). https://doi.org/10.5281/zenodo.11126972.

[93] J. Leppert, T. Brehmer, M. Wüst, P. Boeker, Estimation of retention parameters from temperature programmed gas chromatography, J. Chromatogr. A (2023) 464008. https://doi.org/10.1016/j.chroma.2023.464008.

[94] M.H. Abraham, G.S. Whiting, R.M. Doherty, W.J. Shuely, Hydrogen bonding. Part 13. A new method for the characterisation of GLC stationary phases—the laffort data set, J. Chem. Soc., Perkin Trans. 2 (1990) 1451–1460. https://doi.org/10.1039/P29900001451.

[95] N. Ulrich, G. Schüürmann, W. Brack, Prediction of gas chromatographic retention indices as classifier in non-target analysis of environmental samples, J. Chromatogr. A 1285 (2013) 139–147. https://doi.org/10.1016/j.chroma.2013.02.037.

[96] C.E. Freye, H.D. Bahaghighat, R.E. Synovec, Comprehensive two-dimensional gas chromatography using partial modulation via a pulsed flow valve with a short modulation period, Talanta 177 (2018) 142–149. https://doi.org/10.1016/j.talanta.2017.08.095.

[97] H. Cai, S.D. Stearns, Comprehensive two-dimensional gas chromatography using direct flow modulation to extend the secondary dimension separation time, J. Chromatogr. A 1669 (2022) 462930. https://doi.org/10.1016/j.chroma.2022.462930.

[98] N. Ulrich, A. Böhme, A.B. Strobel, T. Egert, Predicting partitioning from low density polyethylene to blood and adipose tissue by linear solvation energy relationship models, J. Biomed. Mater. Res. B Appl. Biomater. 111 (2023) 2044–2054. https://doi.org/10.1002/jbm.b.35304.

[99] K. Pokajewicz, Enhancing terpene and other plant volatiles analysis – A free spreadsheet tool "Retentify" for GC–MS data processing, Microchemical Journal 193 (2023) 108977. https://doi.org/10.1016/j.microc.2023.108977.

[100] S. Mazraedoost, P. Žuvela, S. Ulenberg, T. Bączek, J.J. Liu, Cross-column density functional theory-based quantitative structure-retention relationship model development powered by machine learning, Fresenius J Anal Chem (2024). https://doi.org/10.1007/s00216-024-05243-7.

[101] Le Peng, X. Gao, L. Wang, A. Zhu, X. Cai, P. Li, W. Li, Design of experiment techniques for the optimization of chromatographic analysis conditions: A review, Electrophoresis 43 (2022) 1882–1898. https://doi.org/10.1002/elps.202200072.

[102] M. Gaida, P.-H. Stefanuto, J.-F. Focant, Theoretical modeling and machine learning-based data processing workflows in comprehensive two-dimensional gas chromatography-A review, J. Chromatogr. A 1711 (2023) 464467. https://doi.org/10.1016/j.chroma.2023.464467.

[103] J. Boelrijk, B. Ensing, P. Forré, B.W.J. Pirok, Closed-loop automatic gradient design for liquid chromatography using Bayesian optimization, Anal. Chim. Acta 1242 (2023) 340789. https://doi.org/10.1016/j.aca.2023.340789.

[104] J. Boelrijk, B. Pirok, B. Ensing, P. Forré, Bayesian optimization of comprehensive two-dimensional liquid chromatography separations, J. Chromatogr. A 1659 (2021) 462628. https://doi.org/10.1016/j.chroma.2021.462628.

[105] D.R. Struk, R. Ilhamsyah, C.A. Heist, J.-M.D. Dimandja, P.J. Hesketh, A Semi-Automated Pipeline for Nontargeted Compound Analysis via GC×GC-MS, Journal of Chromatography Open (2024) 100118. https://doi.org/10.1016/j.jcoa.2024.100118.

[106] ChromSwordAuto®Developer, 2023. https://www.chromsword.com/.

[107] P.G. Boswell, P.W. Carr, J.D. Cohen, A.D. Hegeman, Easy and accurate calculation of programmed temperature gas chromatographic retention times by back-calculation of temperature and hold-up time profiles, J. Chromatogr. A 1263 (2012) 179–188. https://doi.org/10.1016/j.chroma.2012.09.048.

[108] T.M. McGinitie, J.J. Harynuk, Considerations for the automated collection of thermodynamic data in gas chromatography, J. Sep. Sci. 35 (2012) 2228–2232. https://doi.org/10.1002/jssc.201200192.

[109] T.M. McGinitie, H. Ebrahimi-Najafabadi, J.J. Harynuk, Rapid determination of thermodynamic parameters from one-dimensional programmed-temperature gas

chromatography for use in retention time prediction in comprehensive multidimensional chromatography, J. Chromatogr. A 1325 (2014) 204–212. https://doi.org/10.1016/j.chroma.2013.12.008.

[110] T.M. McGinitie, H. Ebrahimi-Najafabadi, J.J. Harynuk, A standardized method for the calibration of thermodynamic data for the prediction of gas chromatographic retention times, J. Chromatogr. A 1330 (2014) 69–73. https://doi.org/10.1016/j.chroma.2014.01.019.

[111] C. Stultz, R. Jaramillo, P. Teehan, F. Dorman, Comprehensive two-dimensional gas chromatography thermodynamic modeling and selectivity evaluation for the separation of polychlorinated dibenzo-p-dioxins and dibenzofurans in fish tissue matrix, J. Chromatogr. A 1626 (2020) 461311. https://doi.org/10.1016/j.chroma.2020.461311.

[112] N. Ulrich, J. Mühlenberg, H. Retzbach, G. Schüürmann, W. Brack, Linear solvation energy relationships as classifiers in non-target analysis - a gas chromatographic approach, J. Chromatogr. A 1264 (2012) 95–103. https://doi.org/10.1016/j.chroma.2012.09.051.

[113] F. van der Plas, M. Dral, P. Berg, Π. Γεωργακόπουλος, R. Huijzer, N. Bochenski, A. Mengali, B. Lungwitz, C. Burns, H. Priyashan, J. Ling, E. Zhang, F.S.S. Schneider, I. Weaver, Rogerluo, S. Kadowaki, Z. Wu, J. Gerritsen, R. Novosel, Supanat, Z. Moon, luis-mueller, M. Abbott, N. Bauer, P. Bouffard, S. Terasaki, S. Polasa, TheCedarPrince, Pluto.jl, 2022. https://doi.org/10.5281/zenodo.7226553.

[114] J. Bezanson, A. Edelman, S. Karpinski, V.B. Shah, Julia: A Fresh Approach to Numerical Computing, SIAM Review 59 (2017) 65–98. https://doi.org/10.1137/141000671.

[115] E. Castelani, R. Lopes, W. Shirabayashi, F. Sobral, RAFF.jl: Robust Algebraic Fitting Function in Julia, Journal of Open Source Software 4 (2019) 1385. https://doi.org/10.21105/joss.01385.

[116] T. Brehmer, B. Duong, J. Leppert, P. Boeker, M. Wüst, Computersimulation von GC-Trennungen unterstützt die Methodenentwicklung zur Analyse von Polyzyklischen Aromatischen Kohlenwasserstoffen, Lebensmittelchemie 76 (2022). https://doi.org/10.1002/lemi.202259106.

[117] F.L. Dorman, P.D. Schettler, L.A. Vogt, J.W. Cochran, Using computer modeling to predict and optimize separations for comprehensive two-dimensional gas

chromatography, J. Chromatogr. A 1186 (2008) 196–201.
https://doi.org/10.1016/j.chroma.2007.12.039.

[118]   H.D. Tolley, S. Avila, B.D. Iverson, A.R. Foster, A.R. Hawkins, S.E. Tolley, M.L. Lee, Simulating Capillary Gas Chromatographic Separations including Thermal Gradient Conditions, Anal. Chem. 93 (2021) 2291–2298. https://doi.org/10.1021/acs.analchem.0c04160.

[119]   D.W. Marquardt, An Algorithm for Least-Squares Estimation of Nonlinear Parameters, Journal of the Society for Industrial and Applied Mathematics 11 (1963) 431–441. https://doi.org/10.1137/0111030.

[120]   K. Levenberg, A Method for the Solution of Certain Non-Linear Problems in Least Squares, Quarterly of Applied Mathematics 2 (1944) 164–168.

[121]   A. Burel, M. Vaccaro, Y. Cartigny, S. Tisse, G. Coquerel, P. Cardinael, Retention modeling and retention time prediction in gas chromatography and flow-modulation comprehensive two-dimensional gas chromatography: The contribution of pressure on solute partition, J. Chromatogr. A 1485 (2017) 101–119. https://doi.org/10.1016/j.chroma.2017.01.011.

[122]   M.H. Abraham, R.A. McGill, P.L. Grellier, Determination of olive oil–gas and hexadecane–gas partition coefficients, and calculation of the corresponding olive oil–water and hexadecane–water partition coefficients, J. Chem. Soc., Perkin Trans. 2 (1987) 797–803. https://doi.org/10.1039/P29870000797.

[123]   P. Siriviboon, C. Tungkaburee, N. Weerawongphrom, C. Kulsing, Direct equations to retention time calculation and fast simulation approach for simultaneous material selection and experimental design in comprehensive two dimensional gas chromatography, J. Chromatogr. A 1602 (2019) 425–431. https://doi.org/10.1016/j.chroma.2019.05.059.

[124]   J.G. Speight (Ed.), Reaction mechanisms in environmental engineering: Analysis and prediction, Butterworth-Heinemann an imprint of Elsevier, Kidlington, Oxford, United Kingdom, 2018.

[125]   D. Bates, A. Noack, S. Kornblith, M. Bouchet-Valat, M.K. Borregaard, A. Arslan, J.M. White, D. Kleinschmidt, P. Alday, G. Lynch, I. Dunning, P.K. Mogensen, S. Lendle, D. Aluthge, pdeffebach, J.B.S. Calderón, A. Patnaik, B. Born, B. Setzler, C. DuBois, J. Quinn, M. Dutta, O. Slámečka, P. Bastide, V.B. Shah, A. Blaom, B. König, B. Kamiński, GLM.jl, 2023. https://doi.org/10.5281/Zenodo.7734970.

References

[126] P. Kakanopas, P. Janta, S. Vimolmangkang, F. Hermatasia, C. Kulsing, Retention index based approach for simulation of results and application for validation of compound identification in comprehensive two-dimensional gas chromatography, J. Chromatogr. A 1679 (2022) 463394. https://doi.org/10.1016/j.chroma.2022.463394.

Content

A. Publication 1

Retention Database for Prediction, Simulation, and Optimization of GC Separations

Tillman Brehmer,* Benny Duong, Manuela Marquart, Luise Friedemann, Peter J. Faust, Peter Boeker, Matthias Wüst, and Jan Leppert

ACCESS | 📊 Metrics & More | 📧 Article Recommendations | 🆘 Supporting Information
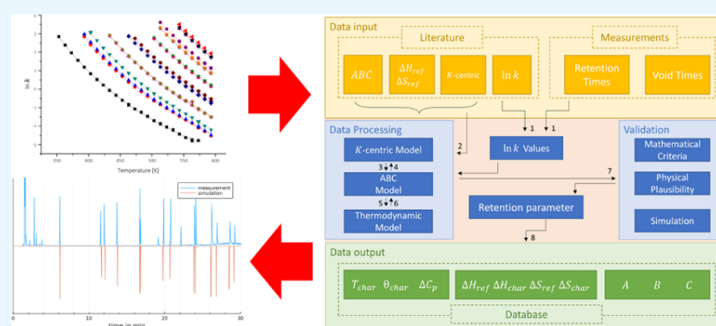
ABSTRACT: This work presents an open source database with suitable retention parameters for prediction and simulation of GC separations and gives a short introduction to three common retention models. Useful computer simulations play an important role to save resources and time in method development in GC. Thermodynamic retention parameters for the ABC model and the *K*-centric model are determined by isothermal measurements. This standardized procedure of measurements and calculations, presented in this work, have a useful benefit for all chromatographers, analytical chemists, and method developers because it can be used in their own laboratories to simplify the method development. The main benefits as simulations of temperature-programed GC separations are demonstrated and compared to measurements. The observed deviations of predicted retention times are in most cases less than 1%. The database includes more than 900 entries with a large range of compounds such as VOCs, PAHs, FAMEs, PCBs, or allergenic fragrances over 20 different GC columns.

1. INTRODUCTION

Method developments in gas (liquid) chromatography can often require a lot of time and resources. More efficient, less expensive, and resource-saving perspectives are opened up by the use of appropriate computer simulations to simplify the optimization process and solve separation problems. In method development, even simple retention models and calculations can be very helpful, for example, to estimate elution orders, retention times, or resolution. Retention models and simulations need substance-specific retention parameters, for example, for the model of Clarke and Glew[1] or the *K*-centric model of Blumberg.[2−4] Because the determination of those substance-specific and stationary-phase-specific parameters is also elaborate, it is constructive to collect them in databases and share them with the scientific community.

There are other retention databases existing, such as the retention index (RI) database for example of NIST[5] or the linear solvation energy relationship (LSER) database of UFZ.[6] These retention data are primarily suitable for prediction of retention phenomena and the distribution in the chromatographic phases. With *K*-centric data, the characteristic temperature may also be

suitable for identification. Via simulation, those retention data can also be used for prediction of retention indices similar to the LSER approach.[7] The retention data presented in this work are temperature-independent and can therefore be used for prediction of temperature programs.[8] Therefore, compared to the LSER[9] approach *K*-centric retention data can describe the change of retention factor *k* with the temperature.

This work presents an available open source retention database for three common retention models and gives a short overview for the calculation of the corresponding data. All three retention models describe the temperature dependence of the retention factor with different parameter sets and can be converted into each other. To save the user of the database a
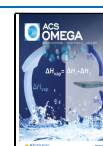
conversion, the data for each of the three retention models are presented in the corresponding parameter set, which is very convenient. The benefit of the data, for example, for simulation of GC separations is demonstrated. The standardized procedure of the determination can be useful for every gas chromatographer or analytical chemist to get predictions for their own measurements.

1.1. Thermodynamic Retention Model. In gas chromatography, the partition of a solute between the mobile phase (gas) and the stationary phase (liquid) is measured by the distribution coefficient K, defined as the ratio of the concentration of the solute in the stationary phase and in the mobile phase. It can be measured by isothermal measurements of the retention factor k and the phase ratio β of the column.

$$K = \beta k \tag{1}$$

The distribution coefficient K depends on the temperature T and the Gibbs free energy ΔG of the evaporation of the solute from the stationary phase.[10]

$$K = \exp\left(\frac{\Delta G}{RT}\right) \tag{2}$$

with R being the molar gas constant. The Gibbs free energy ΔG can be expressed by enthalpy ΔH and entropy ΔS changes of the solute from the stationary into the mobile phase as

$$\Delta G = \Delta H - T\Delta S \tag{3}$$

and therefore

$$k = \frac{1}{\beta}\exp\left(\frac{\Delta H}{RT} - \frac{\Delta S}{R}\right) \tag{4}$$

Both ΔH and ΔS depend on the temperature T itself. To compensate for this temperature dependency, a third parameter ΔC_p (change of the isobaric molar heat capacity) can be introduced and the enthalpy ΔH_{ref} and entropy ΔS_{ref} at a reference temperature T_{ref} are used. Equations 2 and 3 lead to the classic van't Hoff model and further to

$$\ln K = \frac{\Delta S_{\text{ref}}}{R} - \frac{\Delta H_{\text{ref}} + \Delta C_p(T - T_{\text{ref}})}{RT} + \frac{\Delta C_p}{R}\ln\left(\frac{T}{T_{\text{ref}}}\right) \tag{5}$$

which can be converted in a 3-parameter model of Clarke and Glew[1,4] for curve fitting

$$\ln K = A + \frac{B}{T} + C\ln\left(\frac{T}{T_1}\right) \tag{6}$$

It was shown[11] that using a 3-parameter model results in a better fit of k over a wider temperature range than using a 2-parameter model with constant ΔH and ΔS.

The parameters A, B, and C can be converted to enthalpy ΔH_{ref} and entropy ΔS_{ref} for a chosen reference temperature T_{ref} and the change of the isobaric molar heat capacity ΔC_p.

$$\Delta H_{\text{ref}} = R(CT_{\text{ref}} - B) \tag{7}$$

$$\Delta S_{\text{ref}} = R\left(A + C + C\ln\left(\frac{T_{\text{ref}}}{T_1}\right)\right) \tag{8}$$

$$\Delta C_p = RC \tag{9}$$

It seems reasonable to set up a model that normalizes its reference variables to a certain temperature. In adsorption phenomena, especially in chromatography, the distribution of an analyte depends to a large extent on the temperature conditions but not on the same temperature for each analyte. Choosing one reference temperature T_{ref} for all analytes leads to physically meaningless conditions for substances with extreme retention, such as highly volatile compounds or low volatile substances like triglycerides. For chromatography, it is more appropriate to normalize the model to the same distribution of the analyte over the stationary phase, expressed by the distribution coefficient K.[4]

A fully equivalent model to describe the distribution of a solute between stationary and mobile phases in a 3-parameter model is the distribution-centric 3-parameter model of Blumberg,[4] the short K-centric model. In this model, the retention factor k of a solute in a GC system is defined by three parameters:

- T_{char} characteristic temperature
- θ_{char} characteristic thermal constant
- ΔC_p change of the isobaric molar heat capacity (eq 7)

and the equation

$$\ln k = \left(\frac{\Delta C_p}{R} + \frac{T_{\text{char}}}{\theta_{\text{char}}}\right)\left(\frac{T_{\text{char}}}{T} - 1\right) + \frac{\Delta C_p}{R}\ln\left(\frac{T}{T_{\text{char}}}\right) \tag{10}$$

These parameters, especially T_{char} and θ_{char}, have a direct chromatographic meaningful interpretation. The characteristic temperature T_{char} is the temperature, where $\ln k = 0$ and $k = 1$.[4] At this temperature, the amount of the solute is evenly distributed between stationary and mobile phases. The characteristic thermal constant is the inverse declining slope of the function $\ln k(T)$ at $T = T_{\text{char}}$. Therefore, an increase of the temperature around T_{char} by θ_{char} reduces k by a factor of $e \approx 2.72$. The interpretation of ΔC_p is not straightforward, but it generally defines the deviation of k from a 2-parameter model for temperature significantly lower/higher than T_{char}.

The parameters T_{char}, θ_{char}, and ΔC_p are specific for the phase ratio β_0 used to determine these parameters. Using a column with the same stationary phase but different phase ratio β_1 requires a correction factor for the retention factor calculated from eq 10.

$$k_1 = \frac{\beta_0}{\beta_1}k_0 \tag{11}$$

The retention factor k can be determined using the retention time from the chromatogram at the known void time t_M of the GC column, which is the time the carrier gas or a substance with no retention requires to pass the column.

$$\ln k = \ln\left(\frac{t_R - t_M}{t_M}\right) \tag{12}$$

The void time t_M can be measured by detection of a non-interacting gas, for example, methane or air. For wall-coated cylindrical GC columns with length L, internal diameter d, and temperature T, t_M can also be determined with

$$t_M = \frac{128}{3}\cdot\frac{L^2}{d^2}\cdot\eta(T)\cdot\frac{p_i^3 - p_o^3}{(p_i^2 - p_o^2)^2} \tag{13}$$

where p_i is the pressure at the inlet of the column, p_o at the column outlet, and η is the viscosity of the carrier gas.[10]

2. MATERIALS AND METHODS

2.1. Chemicals. To create the database, 260 substances were measured, such as homologous alkanes, alcohols, ketones, phenones, BTEXs, halogen-phenols, and others. Relevant substances for the analytic in food and cosmetics were also measured, for example, 37 FAMEs, 58 allergenic fragrances, 16 EPA-PAHs, 6 PCBs, 6 triglycerides, and other volatile compounds. All used standard substances were purchased by Sigma-Aldrich with a purity of higher than 99.9%. Therefore, dilutions of the compounds were used to determine retention parameters of these substances and to measure chromatograms with different temperature programs.

2.2. Columns. Measurements for determination of the retention parameters were performed on different GC separation columns: 30 m × 0.25 mm × 0.25 μm Rxi17SilMS (75% phenyl−25% methylpolysiloxane, Restek. USA), 30 m × 0.25 mm × 0.25 μm Rxi5SilMS (75% phenyl−25% methyl-polysiloxane, Restek. USA), 30 m × 0.25 mm × 0.5 μm Rxi5SilMS, and 10 m × 0.1 mm × 0.1 μm ZB-PAH-CT (proprietary stationary phase, Phenomenex, USA). Void times were measured with injections of air and detection of the oxygen signal in the TOF-MS. The L/d ratios of the columns were determined from void time measurements by using eq 13 and are shown in Table 1.

Table 1. Determined L/d Ratios for the Investigated Separation Columns

stationary phase	d [mm]	d_f [μm]	L/d	L [m]
Rxi17SilMS	0.25	0.25	120,889.6 ± 170.4	30.222 ± 0.043
Rxi5SilMS	0.25	0.25	121,606.8 ± 1475.7	30.40 ± 0.37
Rxi5SilMS	0.25	0.5	119,084.0 ± 1276.0	29.77 ± 0.32
ZB-PAH-CT	0.1	0.1	102,300.0 ± 4700.0	10.23 ± 0.47

2.3. Instrumentals. A HP 6890 series GC system from Hewlett Packard/Agilent with split/splitless injector (300 °C, 1:100 split ratio) coupled with a BenchTOF-dx time-of-flight mass spectrometer from Markes, UK, was used. The allergen fragrances on the Rxi17SilMS were measured using an internal flame ionization detector of the GC (HP), with void time measurements using methane. Carrier gas was helium with purity of 99.9%. A PAL RSI Chronect Robotic autosampler (CTC Analytics AG, Switzerland) was used for injection of 1 μL of each sample. Isothermal measurements were made in the range from 60 to 300 °C with 10 °C increments and a constant flow of 1 mL/min of the carrier gas.

To validate the parameters, temperature-programed measurements were performed on the HP 6890 GC and a flow field gradient GC (FF-TG-GC)[12] (HyperChrom SA, Luxembourg). The measured chromatograms were compared to simulated data.

2.4. Literature Data. 13 data sets with retention parameters were found in the literature. Table 2 gives an overview about the size of the data sets, the number of compounds and columns that are included, and the reference of the literature.

2.5. Software. For calculation of void times and ln k values, MS Office Professional Plus 2019 Excel was used. All other calculations were performed in a Pluto notebook[23] using the programming language Julia.[24] The notebook is available in the project "RetentionData" via GitHub.[25] For robust fitting and outlier detection, the package RAFF.jl was used.[26] For linear and multivariate fits, the package LsqFit.jl was used.[27,28] Simulation

Table 2. Data sets with Retention Data Found in the Literature That are Included in the Database

data set	size of data set	number of compounds	number of columns	references
1	88	88	1	13
2	47	45	1	14
3	5	5	1	3
4	7	7	1	15
5	51	17	3	11
6	22	22	1	2
7	76	12	3	16
8	6	6	1	17
9	25	11	3	18
10	11	11	1	19
11	25	19	1	20
12	34	16	2	21
13	135	19	8	22

of GC separations and chromatograms were performed with the open source software GasChromatographySimulator.jl.[29] Detailed information to the simulation can be found elsewhere.[2]

3. CREATION OF THE DATABASE

3.1. Calculations and Processing Steps. A schematic overview of the calculation and processing steps is given in Figure 1.

K-centric parameters of each compound were determined by fitting the ln k values, calculated by eq 12, against the temperature of the investigated temperature range by using the K-centric model by Blumberg (eq 10) (see Figure 1 no. 1).

K-centric parameters were converted into the ABC parameters using eq 14 (see Figure 1 no. 3) with knowledge of nominal β.[4]

$$A = \ln \beta - \frac{T_{char}}{\theta_{char}} - \frac{\Delta C_p}{R}\left(1 + \ln\frac{T_{char}}{T_1}\right),$$
$$B = \frac{\Delta C_p T_{char}}{R} + \frac{T_{char}^2}{\theta_{char}}, \qquad C = \frac{\Delta C_p}{R} \qquad (14)$$

Enthalpy ΔH_{ref} and entropy ΔS_{ref} were determined from the ABC parameters by using eq 7 and 8, respectively, with a reference temperature of 90 °C (Figure 1 no. 5). 90 °C for T_{ref} was chosen because other the literature data are determined at these reference temperatures. With $T_{ref} = T_{char}$, the K-centric equivalents ΔH_{char} and ΔS_{char}, enthalpy, and entropy at the solute specific characteristic temperature were determined, which are more meaningful for chromatography.[4]

Data from the literature were converted into K-centric parameters by using the following steps (Figure 1 no. 2).

ABC parameters can be converted to K-centric data by using eqs 15 and 16[4] (Figure 1 no. 4).[4]

$$T_{char} = \frac{-B}{CW(x)}, \qquad \theta_{char} = \frac{B}{C^2(1 + W(x))W(x)},$$
$$C \neq 0 \qquad (15)$$

with

$$x = \frac{-Be^{A/C}}{CT_1\beta^{1/C}} \qquad (16)$$
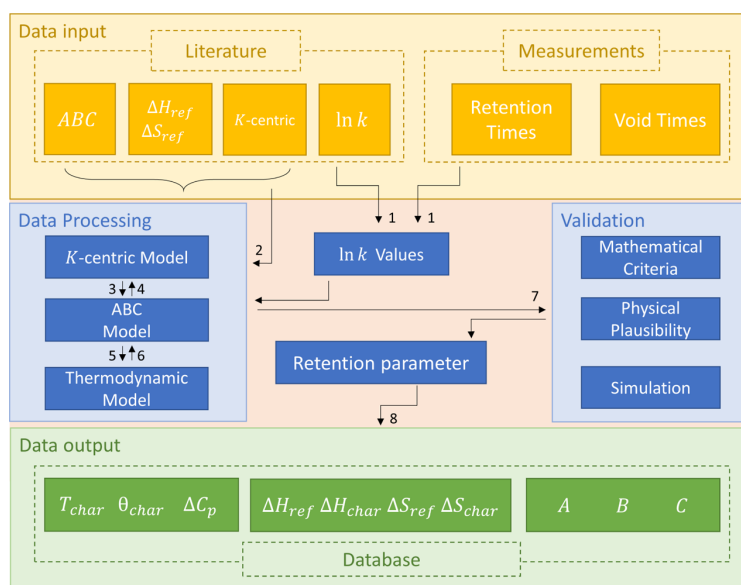
Figure 1. Schematic overview of the main tasks for calculation and converting of the retention parameters and creation of the database.

where $T_1 = 1$ K and $W(x)$ is the Lambert W function (also known as product log function). Per definition, the argument x has to be larger than $-1/e$. The Lambert W function has two branches W_0 and W_{-1}, as shown in Supporting Information, Figure S1. All data so far, show that only the branch W_{-1} is used; therefore, the value of x, eq 16, has to be between $-1/e$ and 0.

With knowledge of the reference temperature T_{ref}, thermodynamic data as ΔS_{ref} and ΔH_{ref} can be converted into ABC parameters[4] (Figure 1 no. 6). As shown above, they can be converted into K-centric data (Figure 1 no. 4).

3.2. Validation and Quality Control. The calculated values have to be validated (Figure 1 no. 7). For acceptance of the compound data the following criteria are defined:

(a) The data set includes three data points as minimum for non-linear multivariate fit, ideally four data points or more. As a recommendation, the data should contain points around $\ln k = 0$ to achieve accurate fitting results.

(b) $\ln k$ values range between -2.0 and 3.5, too high $\ln k$ values are associated with too broad peaks, increased signal-to-noise, and inaccurate retention times. Since low $\ln k$ values often result in analyte peaks merging into the solvent peak, retention does not only depend on the stationary phase.

(c) $0 < \theta_{char} < 100$, a negative θ_{char} cannot be accepted because it would mean that a temperature increase leads to higher retention times than to lower. Based on available data, the parameter θ_{char} tends to be lower than 100 °C, in most cases around 30 °C.[10]

(d) $T_{char} > -273.15$ °C, a value of T_{char} below the absolute zero is not possible.

(e) $C > 0$, negative C shows a lower bending of the fit curve, the curve becomes more linear and causes also to the wrong branch of the Lambert W function (W_0).

(f) $A < 0$, based on available data the parameter A tends to be negative.

(g) $W(x) < -1$ and $-1/e < x < 0$, data are inacceptable if the value of the argument x of the Lambert W function gets lower than $-1/e$ or $W(x) > -1$. Available data shows a

value of $W(x)$ lower than -1 and is on the W_{-1} branch, therefore $-1/e < x < 0$.

Data that failed one of the criteria will be flagged in the database. The reason of the failure will be documented.

To create the final database after validation as shown in Figure 1 no. 8, the parameters of each compound related to the stationary phase are collected in a table. For many substances, a substance category is added, for example "n-alkanes" for homologous series of alkanes, "FAMEs" for fatty acid methyl esters (FAMEs), or "Grob", if the substance is part of the Grob mix for evaluation of GC columns. The structure of the final table is shown in Table 3.

4. RESULTS AND DISCUSSION

4.1. Determined Parameters. The determined retention factors from isothermal measurements are plotted against the isothermal temperature. The detailed $\ln k$ values for each compound can be found in the GitHub project.[25] The internet link to the data is available in the Supporting Information. The plots and fits as $\ln k$ over T for allergenic compounds, 16 EPA-PAH, FAMEs, and triglycerides on the Rxi17SilMS are shown in Figure 2. The determined retention parameters for the thermodynamic model, the ABC model and the K-centric model are shown in the Supporting Information. A selection is shown in Table 3. The value of N gives the number of measurements for the fit of each compound.

Figure 3 shows the relationship between the characteristic temperature T_{char} and the characteristic thermal constant θ_{char} and to ΔC_p. The general relationship is consistent with observations of Blumberg.[10] A strong influence of different phase ratios on the correlation of θ_{char} on T_{char}, as described in ref 8 could not be observed in this data. Interactive 3D figures of the K-centric and the ABC parameters can be found in Supporting Information, Figures S3 and S4. The ABC data show a nearly straight line in the parameter space. In the parameter space of all three K-centric parameters, a general trend can be estimated, whereas some compounds from comparable substance classes show characteristic regions in the space, Figure 3. Aliphatic

Table 3. Structure of the Retention Database and Determined Values of the Retention Parameters of a Selection of Allergenic Fragrances, Triglycerides, PCBs, and PAHs[a]

name	CAS	phase	φ_0	A	$error_A$	B	$error_B$	C	$error_C$	ΔH_{ref}	$error_{\Delta H_{ref}}$	ΔS_{ref}	$error_{\Delta S_{ref}}$	T_{ref}
cinnamaldehyde	104-55-2	Rxi17SilMS	0.001	−82.062	0.65699	10,505	41.611	10.503	0.092476	−55,627	74.286	−80.181	0.17972	90
farnesol A	4602-84-0	Rxi17SilMS	0.001	−108.94	5.955	13,698	402.29	13.933	0.82925	−71,825	876.98	−107.01	2.0583	90
farnesol B	4602-84-0	Rxi17SilMS	0.001	−143.29	4.9454	15,819	337.2	18.806	0.68763	−74,741	757.59	−113.34	1.7679	90
geraniol	106-24-1	Rxi17SilMS	0.001	−88.825	2.3832	10,625	143.78	11.451	0.33807	−53,770	199.92	−82.087	0.49881	90
glyceryl tridecanoate	621-71-6	Rxi17SilMS	0.001	−394.74	65.672	41,657	5590.7	51.841	8.8180	−189,820	20186	−310.16	41.164	90
glyceryl trihexanoate	621-70-5	Rxi17SilMS	0.001	−188.84	20.960	22,064	1588.2	24.456	2.8654	−109,610	4636.7	−168.13	10.181	90
glyceryl trilaurate	538-24-9	Rxi17SilMS	0.001	−543.67	127.33	55,893	11394	71.568	16.969	−248,630	44256	−417.58	87.316	90
glyceryl trimyristin	555-45-3	Rxi17SilMS	0.001	−655.14	198.66	66,369	27435	86.428	25.872	−290,860	181970	−492.57	265.34	90
glyceryl trioctanoate	538-23-8	Rxi17SilMS	0.001	−211.38	27.344	25,948	2197.4	27.112	3.7033	−133,880	7159.8	−203.29	15.197	90
glyceryl tripalmitin	555-44-2	Rxi17SilMS	0.001	−493.02	661.79	53,703	529250	64.545	23.508	−251,620	4398400	−399.00	5293.9	90
iso E super A	54464-	Rxi17SilMS	0.001	−94.965	2.4567	12,303	167.07	12.154	0.34177	−65,595	375.22	−92.836	0.87513	90
iso E super B	54464-	Rxi17SilMS	0.001	−96.736	3.5892	12,420	243.95	12.407	0.49917	−65,801	531.2	−93.049	1.2494	90
iso E super C	54464-	Rxi17SilMS	0.001	−96.021	5.5070	12,334	376.07	12.331	0.76535	−65,315	833.99	−91.485	1.9543	90
iso E super D	54464-	Rxi17SilMS	0.001	−101.18	5.3862	12,802	368.57	13.014	0.74834	−67,148	823.79	−95.219	1.9272	90
limonene	138-86-3	Rxi17SilMS	0.001	−75.098	4.3818	83,93.5	240.6	9.8499	0.63146	−40,046	205.41	−59.733	0.54245	90
linalool	78-70-6	Rxi17SilMS	0.001	−83.176	2.6778	95,08.6	151.66	10.803	0.38383	−46,441	140.04	−72.290	0.36234	90
PCB 101	37680-	Rxi5SilMS	0.002	−111.16	0.85969	14,804	66.924	14.179	0.11708	−80,277	209.05	−111.41	0.44911	90
PCB 138	35065-	Rxi5SilMS	0.002	−107.39	2.4739	15,187	200.61	13.561	0.33499	−85,325	685.92	−115.53	1.4259	90
PCB 153	35065-	Rxi5SilMS	0.002	−106.02	3.2438	14,985	260.39	13.377	0.43993	−84,199	874.59	−114.60	1.8301	90
PCB 180	35065-29-3	Rxi5SilMS	0.002	−95.041	5.9211	14,747	489.4	11.783	0.79956	−87,035	1731	−114.72	3.5510	90
PCB 28	7012-37-5	Rxi5SilMS	0.002	−101.55	2.2747	13,300	169.51	13.001	0.31176	−71,330	474.46	−98.992	1.0547	90
PCB 52	35693-	Rxi5SilMS	0.002	−108.61	2.3285	14,057	175.54	13.925	0.31859	−74,832	506.49	−104.77	1.1160	90
benz[a]anthracene	56-55-3	ZB-PAH-CT	0.001	−17.543	48.568	9795.2	3816.2	0.92277	6.6114	−78,656	12497	−92.960	26.368	90
benzo[g,h,i]perylene	191-24-2	ZB-PAH-CT	0.001	−15.308	13.044	10,841	1125.3	0.57344	1.7504	−88,404	4257.1	−94.403	8.4867	90
dibenzo[a,h]anthracene	53-70-3	ZB-PAH-CT	0.001	−93.497	26.461	16,475	2300.0	11.327	3.5481	−10,2780	8853.9	−128.05	17.501	90
indeno[1,2,3-cd]pyrene	193-39-5	ZB-PAH-CT	0.001	−55.231	39.696	13,583	3436.5	6.0911	5.3263	−94,547	13175	−110.03	26.091	90

name	CAS	phase	φ_0	T_{char}	$error_{T_{char}}$	θ_{char}	$error_{\theta_{char}}$	ΔC_p	$error_{\Delta C_p}$	vH_{char}	$error_{\Delta H_{char}}$	ΔS_{char}	$error_{\Delta S_{char}}$
cinnamaldehyde	104-55-2	Rxi17SilMS	0.001	174.33	0.012622	34.497	0.025762	87.329	0.76889	−48262	36.144	−61.944	0.0806
farnesol A	4602-84-0	Rxi17SilMS	0.001	210.18	0.075096	33.545	0.16568	115.85	6.8948	−57,903	286.56	−73.892	0.59201
farnesol B	4602-84-0	Rxi17SilMS	0.001	215.35	0.069363	35.982	0.15936	156.36	5.7173	−55,141	244.72	−66.971	0.50020
geraniol	106-24-1	Rxi17SilMS	0.001	150.5	0.032493	31.082	0.067725	95.209	2.8109	−48,010	104.87	−67.417	0.24708
glyceryl tridecanoate	621-71-6	Rxi17SilMS	0.001	357.50	1.20	44.375	2.8054	431.03	73.317	−74,520	4719.7	−72.255	7.4737
glyceryl trihexanoate	621-70-5	Rxi17SilMS	0.001	279.28	0.36766	35.679	0.53451	203.34	23.824	−71,117	1069.6	−82.828	1.9305
glyceryl trilaurate	538-24-9	Rxi17SilMS	0.001	393.69	3.3938	54.435	8.6086	595.05	141.09	−67,920	10764	−55.946	16.116
glyceryl trimyristin	555-45-3	Rxi17SilMS	0.001	471.37	130.28	274.27	2095.4	718.60	215.11	−16,804	128520	23.337	172.49
glyceryl trioctanoate	538-23-8	Rxi17SilMS	0.001	318.75	0.27448	35.386	0.54949	225.42	30.791	−82,318	1280.5	−93.167	2.1606
glyceryl tripalmitin	555-44-2	Rxi17SilMS	0.001	556.97	5727.5	5634.7	17350000	536.66	195.45	−10,16.8	3131000	44.683	3771.7
iso E super A	54464-	Rxi17SilMS	0.001	213.41	0.043614	37.053	0.092552	101.05	2.8417	−53,123	133.03	−63.273	0.27289
iso E super B	54464-	Rxi17SilMS	0.001	214.72	0.025811	37.385	0.084073	103.16	4.1503	−52,935	119.17	−62.594	0.24407
iso E super C	54464-	Rxi17SilMS	0.001	217.20	0.046149	38.245	0.14648	102.52	6.3635	−52,274	200.45	−60.696	0.40842
iso E super D	54464-	Rxi17SilMS	0.001	218.27	0.047197	37.694	0.14396	108.20	6.222	−53,269	203.7	−62.489	0.41412
limonene	138-86-3	Rxi17SilMS	0.001	106.20	0.05929	30.903	0.1486	81.897	5.2502	−38,719	186.58	−56.158	0.49107

Table 3. continued

name	CAS	phase	φ_0	T_{char}	$error_{T_{char}}$	θ_{char}	$error_{\theta_{char}}$	ΔC_p	$error_{\Delta C_p}$	vH_{char}	$error_{\Delta H_{char}}$	ΔS_{char}	$error_{\Delta S_{char}}$
linalool	78-70-6	Rxi17SilMS	0.001	120.72	0.029744	29.529	0.067299	89.817	3.1914	−43,682	99.774	−64.996	0.25290
PCB 101	37680-	Rxi5SilMS	0.002	294.81	0.023455	47.780	0.053172	117.89	0.97344	−56,132	62.638	−58.687	0.11006
PCB 138	35065-	Rxi5SilMS	0.002	318.7	0.12712	48.915	0.20645	112.75	2.7853	−59,539	252.59	−60.455	0.42514
PCB 153	35065-	Rxi5SilMS	0.002	312.05	0.16064	47.854	0.25766	111.22	3.6578	−59,502	322.03	−61.532	0.54816
PCB 180	35065-	Rxi5SilMS	0.002	330.90	0.33185	47.826	0.48932	97.972	6.6479	−63,433	652.73	−64.868	1.0760
PCB 28	7012-37-5	Rxi5SilMS	0.002	269.33	0.052128	47.105	0.085008	108.10	2.5921	−51,944	94.272	−55.609	0.17305
PCB 52	35693-	Rxi5SilMS	0.002	276.10	0.050548	47.072	0.10184	115.78	2.6489	−53,285	115.7	−56.871	0.21008
benz[a]anthracene	56-55-3	ZB-PAH-CT	0.001	296.00	2.5171	34.944	2.3759	7.6724	54.97	−77,075	5284.5	−89.513	9.2267
benzo[g,h,i]perylene	191-24-2	ZB-PAH-CT	0.001	359.69	0.82067	38.222	0.71626	14.553	4.7678	−87,118	1648.1	−91.755	2.5859
dibenzo[a,h]anthracene	53-70-3	ZB-PAH-CT	0.001	362.95	2.0216	43.648	2.0490	94.176	29.501	−77,076	3651.2	−75.261	5,7012
indeno[1,2,3-cd]pyrene	193-39-5	ZB-PAH-CT	0.001	359.73	3.0879	41.172	2.7876	50.644	44.285	−80,886	5533.2	−81.899	8.6760

name	CAS	phase	φ_0	N	R^2	χ^2	$\overline{\chi}^2$	source	flag	category 1	category 2
cinnamaldehyde	104-55-2	Rxi17SilMS	0.001	8	1	6.5340×10^{-7}	1.3068×10^{-7}	this work		aldehyde	allergenic fragrances
farnesol A	4602-84-0	Rxi17SilMS	0.001	8	0.99999	3.6088×10^{-5}	7.2175×10^{-6}	this work		allergenic fragrances	
farnesol B	4602-84-0	Rxi17SilMS	0.001	9	0.99999	5.2339×10^{-5}	8.7231×10^{-6}	this work		allergenic fragrances	
geraniol	106-24-1	Rxi17SilMS	0.001	9	1	2.2404×10^{-5}	3.7340×10^{-6}	this work		terpene	allergenic fragrances
glyceryl tridecanoate	621-71-6	Rxi17SilMS	0.001	24	0.99636	8.3195×10^{-2}	3.9617×10^{-3}	this work		triglyceride	
glyceryl trihexanoate	621-70-5	Rxi17SilMS	0.001	14	0.99968	9.3626×10^{-3}	8.5115×10^{-4}	this work		triglyceride	
glyceryl trilaurate	538-24-9	Rxi17SilMS	0.001	13	0.99883	3.9493×10^{-3}	3.9493×10^{-4}	this work		triglyceride	
glyceryl trimyristin	555-45-3	Rxi17SilMS	0.001	13	0.99916	9.1803×10^{-3}	9.1803×10^{-4}	this work	$\theta_{char} > 100\ °C$	triglyceride	
glyceryl trioctanoate	538-23-8	Rxi17SilMS	0.001	20	0.99958	1.4787×10^{-2}	8.6984×10^{-4}	this work		triglyceride	
glyceryl tripalmitin	555-44-2	Rxi17SilMS	0.001	9	0.99897	3.4491×10^{-3}	5.7485×10^{-4}	this work	$\theta_{char} > 100\ °C$	triglyceride	
iso E super A	54464-57-2	Rxi17SilMS	0.001	10	1	2.7114×10^{-5}	3.8735×10^{-6}	this work		allergenic fragrances	
iso E super B	54464-57-2	Rxi17SilMS	0.001	7	1	4.5734×10^{-6}	1.1434×10^{-6}	this work		allergenic fragrances	
iso E super C	54464-57-2	Rxi17SilMS	0.001	7	1	1.0752×10^{-5}	2.6879×10^{-6}	this work		allergenic fragrances	
iso E super D	54464-57-2	Rxi17SilMS	0.001	7	1	1.0279×10^{-5}	2.5697×10^{-6}	this work		allergenic fragrances	
limonene	138-86-3	Rxi17SilMS	0.001	5	1	4.0222×10^{-6}	2.0111×10^{-6}	this work		terpene	allergenic fragrances
linalool	78-70-6	Rxi17SilMS	0.001	8	1	1.7043×10^{-5}	3.4086×10^{-6}	this work		allergenic fragrances	terpene
PCB 101	37680-73-2	Rxi5SilMS	0.002	10	1	5.0424×10^{-6}	7.2034×10^{-7}	this work		PCB	
PCB 138	35065-28-2	Rxi5SilMS	0.002	11	1	4.0017×10^{-5}	5.0021×10^{-6}	this work		PCB	
PCB 153	35065-27-1	Rxi5SilMS	0.002	10	1	4.1581×10^{-5}	5.9401×10^{-6}	this work		PCB	
PCB 180	35065-29-3	Rxi5SilMS	0.002	9	0.99999	8.5642×10^{-5}	1.4274×10^{-5}	this work		PCB	
PCB 28	7012-37-5	Rxi5SilMS	0.002	11	0.99999	5.4783×10^{-5}	6.8479×10^{-6}	this work		PCB	
PCB 52	35693-99-3	Rxi5SilMS	0.002	12	0.99999	6.5045×10^{-5}	7.2273×10^{-6}	this work		PCB	
benz[a]anthracene	56-55-3	ZB-PAH-CT	0.001	8	0.99975	1.5696×10^{-3}	3.1392×10^{-4}	this work		PAH	
benzo[g,h,i]perylene	191-24-2	ZB-PAH-CT	0.001	8	0.99999	7.7010×10^{-5}	1.5402×10^{-5}	this work		PAH	
dibenzo[a,h]anthracene	53-70-3	ZB-PAH-CT	0.001	8	0.99994	3.1643×10^{-4}	6.3287×10^{-5}	this work		PAH	
indeno[1,2,3-cd]pyrene	193-39-5	ZB-PAH-CT	0.001	15	0.9996	4.1942×10^{-3}	3.4952×10^{-4}	this work		PAH	

^{a}For each entry, N gives the number of measurement points which were used for the fit. φ_0 is the dimensionless film thickness with $\varphi_0 = 1/4\beta$.

Appendix

Appendix
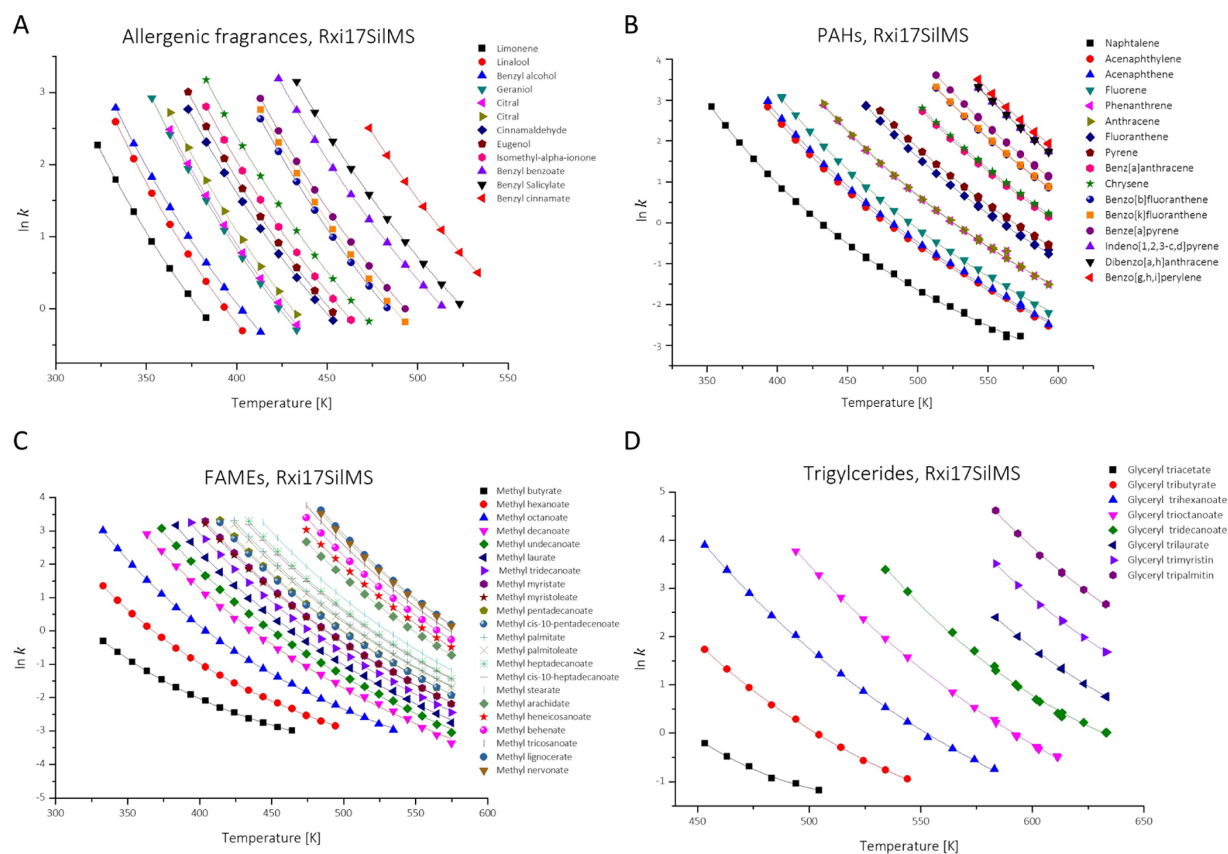
Figure 2. Determined ln k values over T with fits of the K-centric model for each substance for a selection of allergen fragrances (A), EPA-PAHs (B), FAMEs (C), and triglycerides (D) on Rxi17SilMS (β = 250) as the stationary phase.

Figure 3. Relationships between K-centric parameters and influence of substance category. 2D projection from the 3D parameter space for T_{char} against θ_{char} (A) and ΔC_p against T_{char} (B).

62

Figure 4. PCA for all three *K*-centric parameters of different compound categories. PC1 explains 82.7% of the data and variance explained = 99.6562.

Table 4. Data sets After the Validation Process Including the Literature Data and Own Determined Data

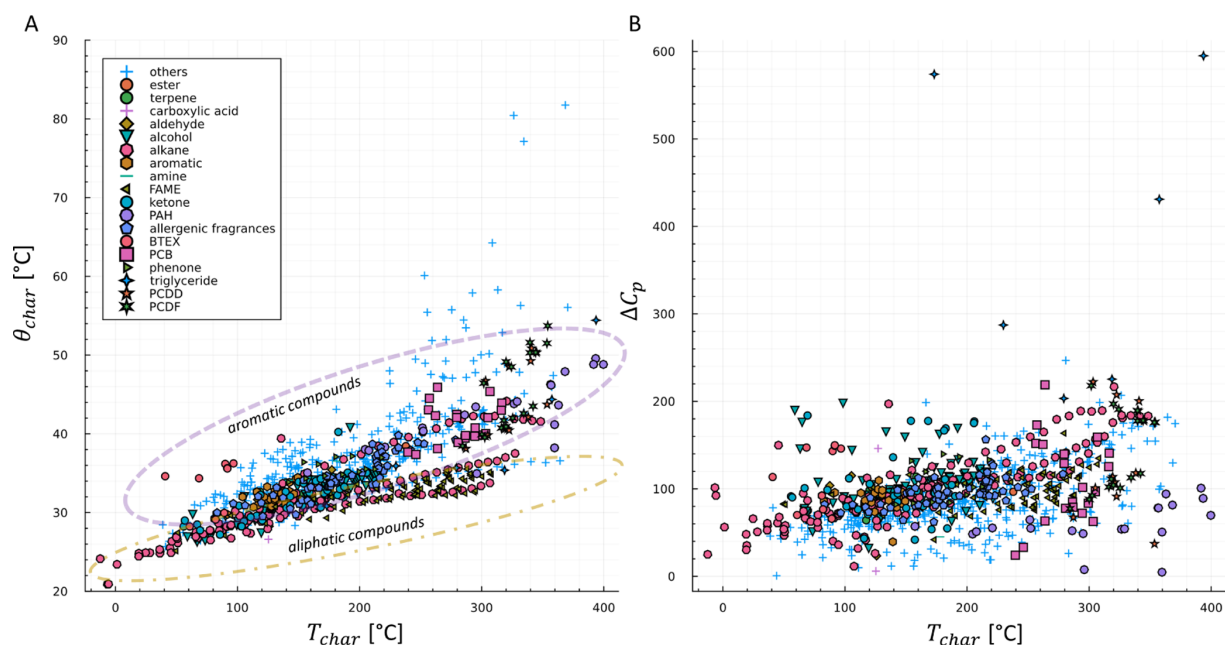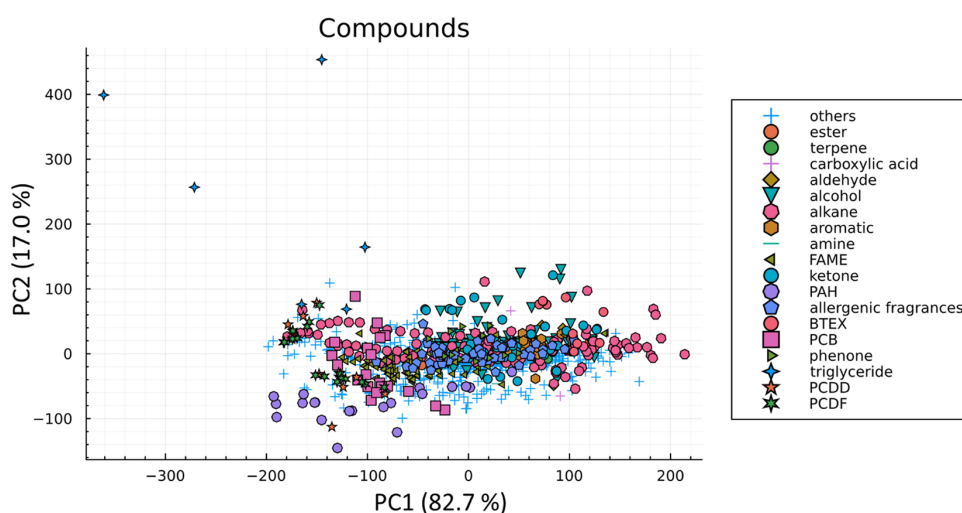| data set	size of data set before validation	size of data after validation	number of compounds	number of columns	references
1	88	88	88	1	13
2	47	47	45	1	14
3	5	5	5	1	3
4	7	7	7	1	15
5	51	51	17	3	11
6	22	22	22	1	2
7	76	76	12	3	16
8	6	6	6	1	17
9	25	25	11	3	18
10	11	11	11	1	19
11	25	0	0	0	20
12	34	29	15	2	21
13	135	117	19	8	22
14	32	22	16	2	this work
15	85	85	70	1	this work
16	355	351	128	3	this work
Total	1031	967	289	20	

Figure 5. Distribution of different substance categories included in the database (absolute values, substances).

compounds such as *n*-alkanes, *n*-alcohols, or FAMEs lie in other regions than aromatic compounds such as PAHs, PCBs, or dioxins but even high volatiles like BETXs. The region of the triglycerides is close to FAMEs. Glyceryl trimyristin and glyceryl tripalmitin did not pass the validation because their arguments *x* of the Lambert *W* function are $x < -1/e$. A problem during the determination are data measured at high temperature far away from $\ln k = 0$, if the parameters, especially T_{char}, are determined as extrapolation with high standard errors. This can be observed for triglycerides but for some PAHs as well.

A principal compound analysis (PCA) provides a model that can describe the relationships between the *K*-centric parameters, Figure 4. PCA of the ABC parameters reduces the data to one principal compound (variance explained = 99.9985%), which is close to the approximately linear trend that could be observed. These PCA models can also be used for further validation of new data and exclusion of data from the database.
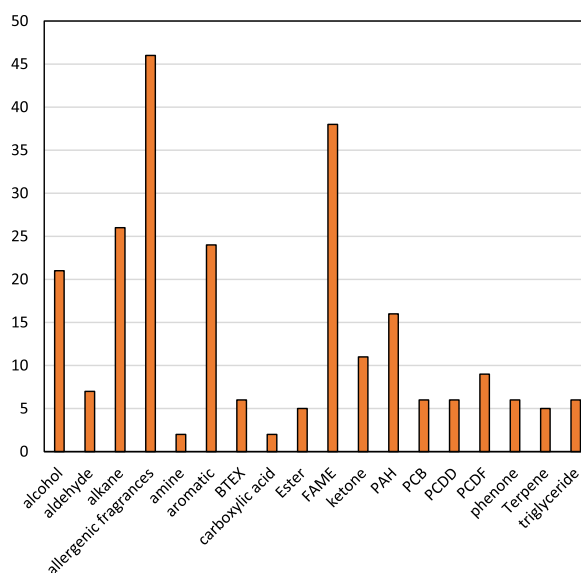
4.2. Results of the Validation Process. Table 4 shows the final data sets after the validation process. The total size of the database was reduced from 1031 to 967 listings. It is notable, that all of the compounds found by Stevenson et al., did not pass the validation.[20] This data, obtained by temperature-programed rather than isothermal measurements, show nearly linear ln *k* over *T* curves, so that the Lambert *W* criteria could not be accepted. A similar trend is observed for some of the PAHs measured on the ZB-PAH-Column, which also show very linear curves in the investigated conditions. Figure 5 shows the primary substance categories and the number of compounds in the final database. To review the quality of the determined data, in the next step randomized GC measurements were performed and compared to simulated chromatograms.

4.3. Benefit of the Data. The data can be used for prediction and simulation of GC separations. The determined characteristic temperatures of the substances can be directly
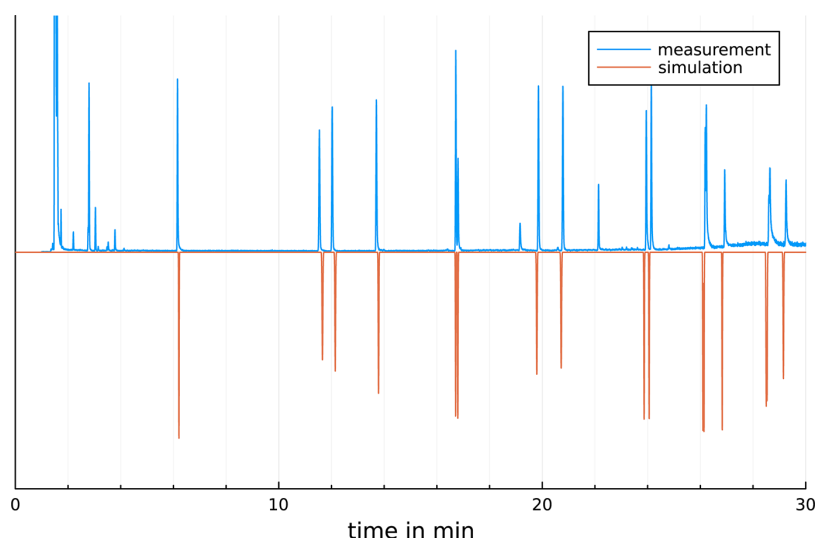
Appendix

Figure 6. Measured and simulated chromatogram of a temperature-programed GC separation of 16 polycyclic aromatic hydrocarbons (EPA-PAH) on a Rxi17SilMs. GC conditions: T_{init} = 70 °C; first ramp: 20 °C/min, T_1 = 150 °C, hold time = 5 min; second ramp: 12 °C/min, T_2 = 250 °C, hold time = 2 min; third ramp: 15 °C/min, T_{end} = 360 °C, hold time = 5 min, rmse = 0.1425 min.

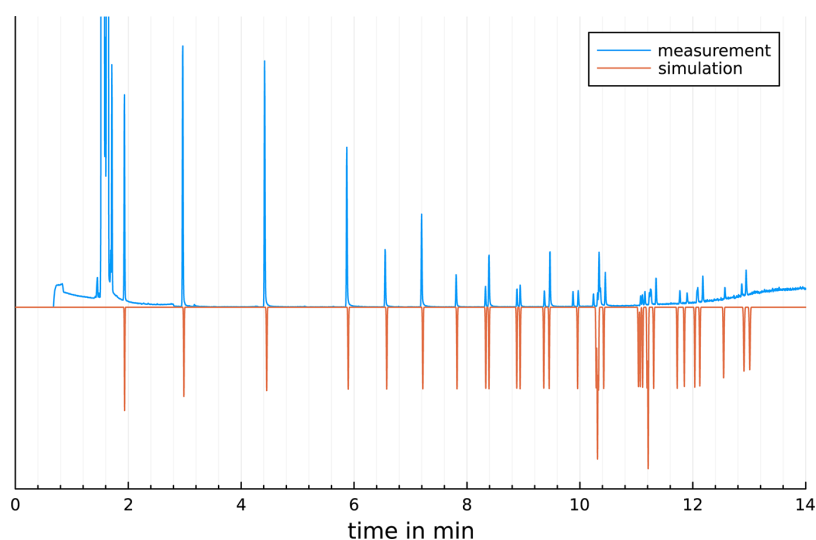**Figure 7.** Measured and simulated chromatogram of a temperature-programed GC separation of FAMEs on a Rxi5SilMs. GC conditions: T_{init} = 60 °C, first ramp: 20 °C/min, T_{end} = 300 °C, rmse = 0.03532 min.

used to estimate the general elution order of a composition. Most compounds elute in order of their characteristic temperatures. For close T_{char} values, the values of θ_{char} and heating rates also have influence on the elution order.[4] Simulated chromatograms of PAHs and FAMEs compared to measurements on the same GC system are shown in Figures 6 and 7. As demonstrated the simulations well accords to measurements. The average deviation for each compound is less than 1%. The rmse (root-mean-square error) is 0.1425 min for the PAHs and 0.03532 min for the FAMEs. Figure 8 shows a simulation computed by ABC retention parameter from the literature[14] on a Rxi5 compared to measurements on our own GC system on a Rxi5SilMS. These two stationary phases are similar but do not have exactly same composition; however, the deviations between the retention times for n-alkanes are almost

less than 2%, which are almost equivalent to a shift by one to three peak widths. In this case, the data are transferable to different GC systems. To check the transferability of the data from one GC system to another, the authors are highly interested in data from the community to compare retention data for similar compounds and phases. As another example for a transferability, the simulation is also suitable for prediction of fast GC measurements such as FF-TG-GC.[2] Measurements with PAHs[30] on a FF-TG-GC system show a good match of elution order but a systematic shift in retention times, which result by a lack of knowledge of the exact gradient profile and the different used GC system. A simulation of FF-TG-GC measurements of PAHs compared to measurements is shown in Supporting Information, Figure S5.

Figure 8. Measured chromatogram of n-alkanes (C8−C20) on a Rxi5SilMS compared to simulation by using ABC retention parameters from Gaida et al.[14] on Rxi5. GC conditions: T_{init} = 40 °C, first ramp: 10 °C/min, T_{end} = 300 °C, rmse = 0.2646 min.

5. CONCLUSIONS

The retention parameter for a huge number of compounds, for example, allergenic fragrances, PAHs, FAMEs, and other volatile substances were determined and collected in a database. The presented calculation procedure is even suitable for method developers on their own GC systems to generate own databases for simple predictions. The presented database now includes data for more than 280 substances on up to 20 different stationary phases. The full database is available at GitHub https://github.com/JanLeppert/RetentionData.[25] The data are suitable for prediction, simulation, and optimization of GC separations.

To reduce the elaborate isothermal measurements, further investigations will focus on development of easier estimation methods for the retention parameters than via isothermal measurements. The most important *K*-centric parameter T_{char} can be well-estimated from the elution temperature. Similar to the estimations of RI or boiling points from LSER data[7] from the literature, the other *K*-centric parameters can also be estimated. First results are promising. With suitable optimization algorithms, efficient estimates by simulation will be possible from temperature-programed measurements .

■ ASSOCIATED CONTENT

ⓈⒾ Supporting Information

The Supporting Information is available free of charge at https://pubs.acs.org/doi/10.1021/acsomega.3c01348.

> Plot of Lambert W function, ln *k* values of measurements, 3D plots of retention parameters, chromatograms, and results of PCA (PDF)

> Databases described in this work before and after validation, and new data measured without any literature data (XLS)

■ AUTHOR INFORMATION

Corresponding Author

Tillman Brehmer − *Institute of Nutritional and Food Sciences, Food Chemistry, University of Bonn, 53115 Bonn, Germany;*
Ⓞ orcid.org/0000-0001-7252-3589; Email: brehmer@uni-bonn.de

Authors

Benny Duong − *Institute of Nutritional and Food Sciences, Food Chemistry, University of Bonn, 53115 Bonn, Germany*
Manuela Marquart − *Institute of Nutritional and Food Sciences, Food Chemistry, University of Bonn, 53115 Bonn, Germany*
Luise Friedemann − *Institute of Nutritional and Food Sciences, Food Chemistry, University of Bonn, 53115 Bonn, Germany; Department for Applied Sciences, Hochschule Bonn-Rhein-Sieg, 53359 Rheinbach, Germany*
Peter J. Faust − *Institute of Nutritional and Food Sciences, Food Chemistry, University of Bonn, 53115 Bonn, Germany; HyperChrom GmbH Germany, 53115 Bonn, Germany*
Peter Boeker − *Institute of Nutritional and Food Sciences, Food Chemistry, University of Bonn, 53115 Bonn, Germany; HyperChrom GmbH Germany, 53115 Bonn, Germany*
Matthias Wüst − *Institute of Nutritional and Food Sciences, Food Chemistry, University of Bonn, 53115 Bonn, Germany;* Ⓞ orcid.org/0000-0001-6808-5555
Jan Leppert − *Institute of Nutritional and Food Sciences, Food Chemistry, University of Bonn, 53115 Bonn, Germany;* Ⓞ orcid.org/0000-0001-8857-8103

Complete contact information is available at:
https://pubs.acs.org/10.1021/acsomega.3c01348

Notes

The authors declare no competing financial interest.

■ ACKNOWLEDGMENTS

■ REFERENCES

(1) Clarke, E. C. W.; Glew, D. N. Evaluation of thermodynamic functions from equilibrium constants. *Trans. Faraday Soc.* **1966**, *62*, 539.

Appendix

(2) Leppert, J.; Müller, P. J.; Chopra, M. D.; Blumberg, L. M.; Boeker, P. Simulation of spatial thermal gradient gas chromatography. *J. Chromatogr. A* **2020**, *1620*, 460985.

(3) Hou, S.; Stevenson, K. A. J. M.; Harynuk, J. J. A simple, fast, and accurate thermodynamic-based approach for transfer and prediction of gas chromatography retention times between columns and instruments Part I: Estimation of reference column geometry and thermodynamic parameters. *J. Sep. Sci.* **2018**, *41*, 2544−2552.

(4) Blumberg, L. M. Distribution-centric 3-parameter thermodynamic models of partition gas chromatography. *J. Chromatogr. A* **2017**, *1491*, 159−170.

(5) Babushok, V. I.; Linstrom, P. J.; Reed, J. J.; Zenkevich, I. G.; Brown, R. L.; Mallard, W. G.; Stein, S. E. Development of a database of gas chromatographic retention properties of organic compounds. *J. Chromatogr. A* **2007**, *1157*, 414−421.

(6) Ulrich, N.; Endo, S.; Brown, T. N.; Watanabe, N.; Bronner, G.; Abraham, M. H.; Goss, K.-U. UFZ-LSER database v 3.2 [Internet]. http://www.ufz.de/lserd (accessed Apr 19, 2023).

(7) Ulrich, N.; Schüürmann, G.; Brack, W. Prediction of gas chromatographic retention indices as classifier in non-target analysis of environmental samples. *J. Chromatogr. A* **2013**, *1285*, 139−147.

(8) Blumberg, L. M. Chromatographic parameters: Characteristic parameters of solute retention - an insightful description of column properties. *J. Chromatogr. A* **2022**, *1685*, 463594.

(9) Poole, C. F. Solvation parameter model: Tutorial on its application to separation systems for neutral compounds. *J. Chromatogr. A* **2021**, *1645*, 462108.

(10) Blumberg, L. M. *Temperature-programmed Gas Chromatography*; Wiley-VCH, 2010.

(11) Karolat, B.; Harynuk, J. Prediction of gas chromatographic retention time via an additive thermodynamic model. *J. Chromatogr. A* **2010**, *1217*, 4862−4867.

(12) Boeker, P.; Leppert, J. Flow field thermal gradient gas chromatography. *Anal. Chem.* **2015**, *87*, 9033−9041.

(13) Boswell, P. G.; Carr, P. W.; Cohen, J. D.; Hegeman, A. D. Easy and accurate calculation of programmed temperature gas chromatographic retention times by back-calculation of temperature and hold-up time profiles. *J. Chromatogr. A* **2012**, *1263*, 179−188.

(14) Gaida, M.; Franchina, F. A.; Stefanuto, P.-H.; Focant, J.-F. Modeling approaches for temperature-programmed gas chromatographic retention times under vacuum outlet conditions. *J. Chromatogr. A* **2021**, *1651*, 462300.

(15) Hou, S.; Stevenson, K. A. J. M.; Harynuk, J. J. A simple, fast, and accurate thermodynamic-based approach for transfer and prediction of gas chromatography retention times between columns and instruments Part III: Retention time prediction on target column. *J. Sep. Sci.* **2018**, *41*, 2559−2564.

(16) McGinitie, T. M.; Karolat, B. R.; Whale, C.; Harynuk, J. J. Influence of carrier gas on the prediction of gas chromatographic retention times based on thermodynamic parameters. *J. Chromatogr. A* **2011**, *1218*, 3241−3246.

(17) McGinitie, T. M.; Harynuk, J. J. Considerations for the automated collection of thermodynamic data in gas chromatography. *J. Sep. Sci.* **2012**, *35*, 2228−2232.

(18) McGinitie, T. M.; Ebrahimi-Najafabadi, H.; Harynuk, J. J. Rapid determination of thermodynamic parameters from one-dimensional programmed-temperature gas chromatography for use in retention time prediction in comprehensive multidimensional chromatography. *J. Chromatogr. A* **2014**, *1325*, 204−212.

(19) McGinitie, T. M.; Ebrahimi-Najafabadi, H.; Harynuk, J. J. A standardized method for the calibration of thermodynamic data for the prediction of gas chromatographic retention times. *J. Chromatogr. A* **2014**, *1330*, 69−73.

(20) Stevenson, K. A. J. M.; Blumberg, L. M.; Harynuk, J. J. Thermodynamics-based retention maps to guide column choices for comprehensive multi-dimensional gas chromatography. *Anal. Chim. Acta* **2019**, *1086*, 133−141.

(21) Stultz, C.; Jaramillo, R.; Teehan, P.; Dorman, F. Comprehensive two-dimensional gas chromatography thermodynamic modeling and selectivity evaluation for the separation of polychlorinated dibenzo-p-dioxins and dibenzofurans in fish tissue matrix. *J. Chromatogr. A* **2020**, *1626*, 461311.

(22) Ulrich, N.; Mühlenberg, J.; Retzbach, H.; Schüürmann, G.; Brack, W. Linear solvation energy relationships as classifiers in non-target analysis - a gas chromatographic approach. *J. Chromatogr. A* **2012**, *1264*, 95−103.

(23) van der Plas, F.; Dral, M.; Berg, P.; Georgakopoulos, P.; Huijzer, R.; Bochenski, N.; Mengali, A.; Lungwitz, B.; Burns, C.; Priyashan, H.; Ling, J.; Zhang, E.; Schneider, F. S. S.; Weaver, I.; Rogerluo; Kadowaki, S.; Wu, Z.; Gerritsen, J.; Novosel, R.; Supanat; Moon, Z.; Luis-mueller; Abbott, M.; Bauer, N.; Bouffard, P.; Terasaki, S.; Polasa, S. *TheCedarPrince fonsp/Pluto.jl: v0.19.14*; Zenodo, 2022.

(24) Bezanson, J.; Edelman, A.; Karpinski, S.; Shah, V. B. Julia: A Fresh Approach to Numerical Computing. *SIAM Rev.* **2017**, *59*, 65−98.

(25) Leppert, J.; Brehmer, T. *RetentionData: v0.2.0*, 2023. https://github.com/JanLeppert/RetentionData (accessed Apr 19, 2023).

(26) Castelani, E.; Lopes, R.; Shirabayashi, W.; Sobral, F. RAFF.jl: Robust Algebraic Fitting Function in Julia. *J. Open Source Softw.* **2019**, *4*, 1385.

(27) White, J. M.; et al. *LsqFit.jl*, 2012. https://github.com/JuliaNLSolvers/LsqFit.jl (accessed Apr 19, 2023).

(28) K Mogensen, P.; N Riseth, A. Optim: A mathematical optimization package for Julia. *J. Open Source Softw.* **2018**, *3*, 615.

(29) Leppert, J. GasChromatographySimulator.jl. *J. Open Source Softw.* **2022**, 7, 4565.

(30) Brehmer, T.; Duong, B.; Leppert, J.; Boeker, P.; Wüst, M. Computersimulation von GC-Trennungen unterstützt die Methodenentwicklung zur Analyse von Polyzyklischen Aromatischen Kohlenwasserstoffen. *Lebensmittelchemie* **2022**, *76*, S2-149.

B. Publication 2

Relation between characteristic temperature and elution temperature in temperature programmed gas chromatography - part I: Influence of initial temperature and heating rate

Tillman Brehmer [a,*], Peter Boeker [a,b], Matthias Wüst [a], Jan Leppert [a,*]

[a] University of Bonn, Institute of Nutritional and Food Sciences, Chair of Food Chemistry - Department Fast GC, Endenicher Allee 11 - 13, 53115 Bonn, Germany
[b] Hyperchrom GmbH Germany, Endenicher Allee 11 -13, 53115, Bonn, Germany

ARTICLE INFO

ABSTRACT

The development of new analytical methods can save resources, time and costs if there are prediction tools like computer simulation which support the optimization process. In GC the distribution-centric 3-parameter model (K-centric model) is well established for prediction of retention factors k and retention times but laborious isothermal measurements for determination of the characteristic parameters are needed. For the most important parameter, the characteristic temperature T_{char}, the search for simpler determination methods or even estimates is an interesting research topic.

In this work the elution temperatures for 37 fatty acid methyl esters, 6 BTEXs and 40 other volatile substances are determined by measurements under variable heating rates, initial temperatures, constant pressure mode and constant flow mode. The relationship between the measured elution temperature and the characteristic temperature was investigated. The novel multivariate curve fit model presented in this study describes accurately the relation between the characteristic temperature T_{char} and elution temperatures T_{elu} under variable heating rates R_T, respectively, and initial temperature T_{init} conditions. The novel model shows good accordance to earlier estimation models and expands the prediction range, especially for high volatile compounds. The model is suitable for determination of T_{char} by estimated T_{elu} and vice versa. Predictions of retention times of simple temperature programs were also possible by using the model with relative deviations < 5% compared to measurements.

1. Introduction

Method developments in gas chromatography can be time-consuming. Depending on the amount of substances to be analysed, many test measurements have to be performed before a method can be used in an analytical application. Higher requirements, e.g. in food safety or environmental protection, increase the sample throughput and increase the need of analytical methods for novel analytes [1]. More efficient, cost-effective, and resource-saving perspectives are opened up by the use of suitable computer simulations [2,3] to adequately address separation problems and simplify the optimisation process.

Important fields for simulations are the description of complex GC-systems like modular GC Systems such as GC × GC [4,5], higher dimensional GC or thermal gradient GC [6,7]. This simulation [8], which describes spatial thermal gradients, uses the so called 'distribution-centric 3-parameter model' of Blumberg also known as K-centric model. Like other thermodynamic based models, data describing the interaction of the analytes and the stationary phase are needed. To determine this data, many laborious isothermal measurements for each analyte of interest have to be performed. Alternatives to prediction or methods to more easily obtain the thermodynamic retention parameters are needed, e.g. by substance data from the literature [9] or simpler temperature programmed measurements [10].

One known relationship based on the K-centric model is the dependence of elution temperature on the characteristic temperature T_{char} [11–13]. This relationship permits an estimate of one thermodynamic parameter from less laborious temperature programmed measurements [10]. Since simulations are based on models, it is necessary to review and extend the existing models to ensure the correct prediction of retention times and thus improve the optimization process. This also
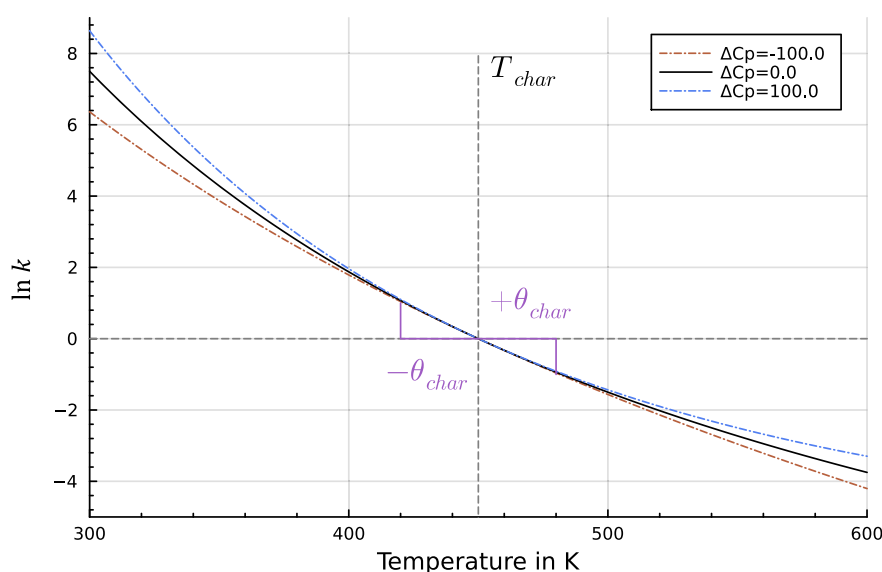
Appendix

Fig. 1. Plot of the **K**-centric model by Blumberg which describes the dependence of temperature to **ln k** under varied **ΔC_p** values.

applies to the prediction of elution temperatures. Depending on the measurement conditions e.g. initial temperature, the trend between T_{char} and T_{elu} deviate from a general linear relationship for low retained substances like volatile alcohols, aldehydes or short fatty acids and others [11]. Low retained volatile compounds are interesting for analytics since they can be found as aroma active compounds in food, cosmetics or other consumer products and are relevant for assessment of authenticity or safety e.g. as allergenic fragrances or toxicological relevant residual solvents [14,15].

A more precise knowledge of the influences of heating rate and initial temperature on elution temperatures opens the possibility of estimating thermodynamic parameters in simpler ways especially from temperature programmed measurements [10]. This can help to propose conditions that allow optimal GC separation of compounds whose thermodynamic parameters are known. The aim of the study presented in this paper is to investigate the elution temperature depending on its influence factors and to develop a model that describes the relationship for a large set of T_{char} values, even for low retained volatile compounds. Therefore, a large amount of measurements is performed for different heating rates and initial temperatures for FAMEs, BETXs and other volatiles on the same GC column. In addition simulations of GC separations for a larger set up of GC columns and compounds [16] were performed and presented in a second part. The model will be investigated, and properties will be estimated that are relevant as well for the usual GC method developers.

2. Theory

It is to be mentioned, that in the following equations and models, the Temperature T and associated parameters are given in Kelvin, even if they are expressed in °C in examples or figures.

2.1. Retention model

In gas chromatography the partition of a solute between the mobile phase and the stationary phase is measured by the distribution coefficient K, defined as the ratio of the concentration of the solute in stationary phase and in the mobile phase. It can be measured by isothermal measurements of the retention factor k and the phase ratio β of the column.

$$K = \beta k \tag{1}$$

The phase ratio is defined as the ratio of the volume of the mobile phase V_m to the volume of the stationary phase V_s [17]. Because internal diameter and the diameter of the column are much higher than the film thickness, β is approximately equal to the ratio of column diameter d and quadruple of the film thickness d_f [11,17].

$$\beta = \frac{V_m}{V_s} \approx \frac{d}{4d_f} \tag{2}$$

A model to describe the distribution of a solute between stationary and mobile phase in a 3-parameter model is the distribution-centric 3-parameter model of Blumberg [11], in short *K*-centric model. In this model, the retention factor k of a solute in a GC system is defined as

$$\ln k = \left(\frac{\Delta C_p}{\mathbb{R}} + \frac{T_{char}}{\theta_{char}} \right) \left(\frac{T_{char}}{T} - 1 \right) + \frac{\Delta C_p}{\mathbb{R}} \ln \left(\frac{T}{T_{char}} \right) \tag{3}$$

with the characteristic temperature T_{char}, the characteristic thermal constant θ_{char} and the change of the isobaric molar heat capacity ΔC_p and the molar gas constant $\mathbb{R}$. The model is an alternative to the ABC model of Clark and Glew [18] and stays in relationship to enthalpy, entropy and Gibbs free energy, which is discussed elsewhere [11,13,16]. Unlike in the ABC-model, the parameters of the *K*-centric model, especially T_{char} and θ_{char}, have a direct chromatographic meaningful interpretation. The characteristic temperature T_{char} is the temperature at $k = 1$ respectively $\ln k = 0$ [11]. At this temperature the amount of the analyte is evenly distributed between stationary and mobile phase. The characteristic thermal constant θ_{char} is the inverse decreasing slope of the function $\ln k(T)$ at $T = T_{char}$. Therefore, an increase of the temperature around T_{char} by θ_{char} reduces $\ln k$ by 1.0. The interpretation of ΔC_p is not straightforward, but it generally defines the deviation of k from a two-parameter model for temperature significantly lower/higher than T_{char}, see Fig. 1 [11].

The parameters T_{char}, θ_{char} and ΔC_p are specific for the phase ratio β_0 used to determine these parameters. Using a column with the same stationary phase, but different phase ratio β_1 requires a correction factor for the retention factor calculated from Eq. (3)

$$k_1 = \frac{\beta_0}{\beta_1} k_0 \tag{4}$$

The retention factor k of an analyte can be determined experimentally at isothermal and isobaric conditions by using the retention time of the analyte from the chromatogram at the known void time t_M of the GC column, which is the time the carrier gas or a substance with no retention requires to pass through the column.

$$\ln k = \ln\left(\frac{t_R - t_M}{t_M}\right) \tag{5}$$

For a wall coated cylindrical GC column with length L, internal diameter d and temperature T, the void time t_M required for a gas with the viscosity η can be calculated by

$$t_M = \frac{128}{3}\cdot\frac{L^2}{d^2}\cdot\eta(T)\cdot\frac{p_i^3 - p_o^3}{\left(p_i^2 - p_o^2\right)^2} \tag{6}$$

where p_i is the pressure at the inlet of the column and p_o at the column outlet [16].

2.2. Temperature programmed GC

The heating rate R_T is the temporal change of the oven temperature during a temperature programmed GC separation. To compare heating rates on different GC systems the heating rate in units of temperature per time can be defined as a normalised heating rate r in units of temperature per void time, which eliminates column specific influences such as column length or diameter or applied pressures/flow [19].

$$r = R_T\cdot t_M = T_M \tag{7}$$

In accordance to Blumberg r as the product $R_T\cdot t_M$ is a fundamental value in method translation and can be referred as void temperature T_M [20]. It is a synonym term for the normalised heating rate r.

Another standardised form to express heating rates is the dimensionless heating rate

$$r_T = \frac{R_T\cdot t_{M,ref}}{\theta_{ref}} \tag{8}$$

with the average thermal constant $\theta_{ref} = 30\ ^{\circ}\mathrm{C}$ and the reference void time at a defined temperature usually 150 °C [12,21]. A dimensionless heating rate of $r_T = 0.4$ e.g., is equivalent to a heating rate of $R_T = 0.4\bullet30\ ^{\circ}\mathrm{C}/t_M = 12\ ^{\circ}\mathrm{C}$ per void time at 150 °C. With a reference void time of 4 min the corresponding heating rate is $R_T = 3\ ^{\circ}\mathrm{C}\ \mathrm{min}^{-1}$. By reducing the length of the GC column to the half value Eq. (6) leads to void time of ¼ of the original void time ($t_M = 1$ min). Under these conditions the equivalent heating rate is $R_T = 12\ ^{\circ}\mathrm{C}\ \mathrm{min}^{-1}$. This shows that a change in the system condition causes a change in the heating rates, but not the dimensionless heating rate. This is meaningful for the method translation where the methods should be comparable. Note that the void temperature in the example has a constant value of 12 °C for both conditions.

2.3. Elution temperature

The elution temperature T_{elu} of an analyte is defined as the temperature of the GC oven when the analyte is passing the outlet of the GC column and arrives at the detector of the separation system.

In a given single ramp temperature program that starts with the initial temperature of the GC oven T_{init} and with the heating rate R_T the elution temperature is defined as [12]

$$T_{elu} = T_{init} + t_R\cdot R_T \tag{9}$$

where t_R is the retention time of the analyte which is passing the column outlet.

It is known that there is a relation between the characteristic temperature T_{char} of a substance and its elution temperature T_{elu} during temperature programmed GC separation with a single ramp [11]. For a

GC system one heating rate $R_{T,0}$ exists where T_{elu} is equal to T_{char} [11, 12]. If T_{elu} or T_{char} is much higher than the initial temperature T_{init}, the dependence can be described as a simple linear function:

$$T_{elu} = T_{char} + T_0 \tag{10}$$

where T_0 is the intercept which determine the shift from the heating rate $R_{T,0}$ where T_{char} is equal to T_{elu}. In the case of an initial temperature of e. g. 30 °C, the linear relationship can be assumed for an elution temperature above 90 °C [11]. However, this relationship does not fit for low retained volatile compounds that elute at the beginning of the chromatogram and whose elution temperatures are close to the initial temperature. The measured elution temperatures are usually much higher than the linear dependence would predict.

2.4. Describing the dependence of T_{elu} on T_{char} (Curve fit model)

To approach a description of the phenomenon, basic properties of the model must be defined: For T_{char} values much larger than the initial temperature, the function must transform into a simple linear equation, as it can already be derived from Blumberg's data [11]. For T_{char} values tending towards the initial temperature, the function should assume a constant T_{elu} value T_1. This constant value is to be expected in the order of magnitude of the initial temperature. Physically it cannot be lower than the initial temperature.

A model, that describes the phenomena could be a combination of constant, linear, exponential or logarithmic functions. At first, we will define the constant part of the model as $g(x)$ and a linear part as a function $h(x)$. It is notable that the transition between a constant or approximately constant part $g(x)$ and the linearly increasing branch $h(x)$ should be continuous and values lower than the constant $g(x)$ or linear function $h(x)$ are not possible in reality. In other words, the function should not have a local respectively global minimum. A possible smooth differentiable function $f(x)$ which modulates continuously between any two different functions $g(x)$ and $h(x)$ is described in Eq. (11). This function has the property, that it approximates values of $h(x)$ or $g(x)$ above or below the interception of both functions.

$$f(x) = \frac{1}{\gamma}\ln\left(e^{\gamma g(x)} + e^{\gamma h(x)}\right) \tag{11}$$

The modulation of the transition between the two functions is realised by a modulation factor γ. For absolute values of γ higher than 1, transition will be very close to both functions, but with steep transition. Values of γ between zero and 1 generate a smoother transition from the constant to the linear part which should better fit to reality. The sign of γ has influence if the values above or below the interception will be approximated.

To investigate the influence of T_{char} on T_{elu} the function $h(x)$ can be substituted as the linear relationship between T_{char} and T_{elu} for high volatile compounds, where T_0 is the intercept of the linear function and m the slope. The function $g(x)$ can be substituted as constant temperature T_1, Eq. (12), and then $f(x)$ becomes T_{elu} as a function of T_{char}. Fig. 2 shows the fit function and its parts compared to first measured data.

$$T_{elu}(T_{char}) = \frac{1}{\gamma}\ln\left(e^{\gamma(m\cdot T_{char} + T_0)} + e^{\gamma T_1}\right) \tag{12}$$

3. Materials & methods

3.1. Chemicals

A standard solution with 37 fatty acid methyl esters (FAME) from butyric acid methyl ester (C4:0) to tetracosanoic acid methyl ester (C24:0) with concentrations between 200 and 600 µg mL^{-1} per component in dichloromethane was purchased from Sigma-Aldrich. A standard solution of benzene, toluene, ethylbenzene, *o*-xylene, *m*-xylene and *p*-xylene (BTEX standard) with concentrations of 2000 µg mL^{-1} each

Appendix
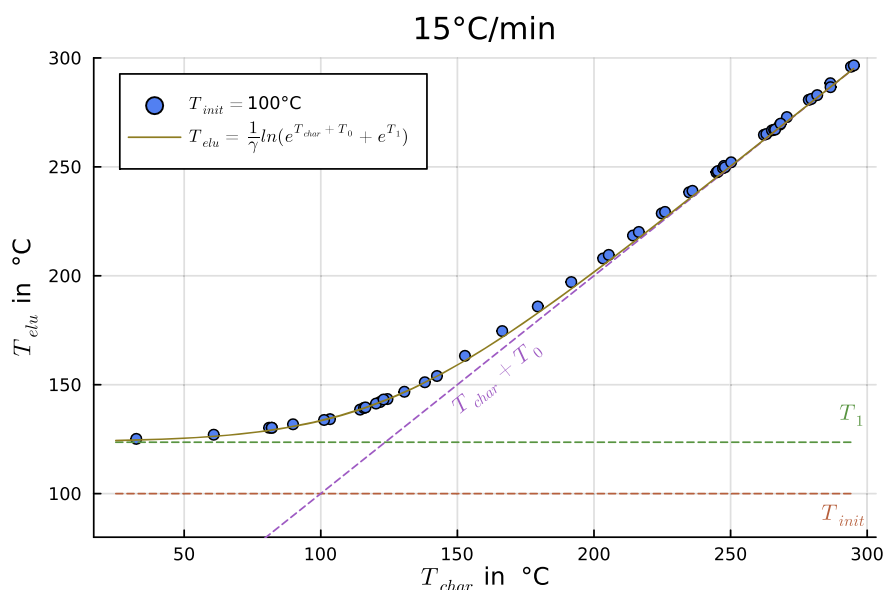
Fig. 2. Presented curve fit model with its sub models, the constant part T_1 and the linear function $\mathbf{T_{char}} + \mathbf{T_0}$ and comparison to measured data. Conditions: initial temperature of 100 °C, heating rate of 15 °C min^{-1} and constant flow of 1 mL min^{-1}.

was purchased from Sigma Aldrich. The BTEX standard mixture was used because the BTEXs are a higher volatile fraction with lower retention and should have elution temperatures near the investigated initial temperatures. For these substances a nonlinear dependence of characteristic temperature and elution temperature would be expectable in accordance with current models.

A composition of various alcohols, phenols, halogen alkyls and others were diluted in dichloromethane and contain 10 µg/mL of each compound. All these substances had a purity of more than 98%. The substances were selected because they are related to studies on the determination of linear solvent energy relationship models (LSER) and are also volatile compounds with expected low to medium elution temperatures [22]. Detailed information about the substances and its LSER descriptors are shown in the supplemental part.

For evaluation of the model, mixtures of phenones (including pro-piophenone, butyrophenone, valerophenone, hexanophenone, hepta-nophenone, octanophenone) all from Sigma-Aldrich and primary alcohols (C5 to C11, Sigma-Aldrich) are used.

Dilutions of the described compounds were used to determine retention parameters of these substances and to measure chromatograms with different temperature programs to determine the elution temperatures of the substances. The BTEX-Mix was diluted in methanol (99.8%, VWR, Germany), FAME-Mix and LSER-Mix were diluted in dichloromethane (99.9%, Fischer Chemical, Germany).

3.2. Instrumental

All measurements to determine the retention parameters and to measure the elution temperature are performed on a 30 m × 0.25 mm × 0.25 µm Rxi17SilMS column (75% Phenyl-25% Methylpolysiloxane, Restek. USA) in a HP 6890 Series GC System from Hewlett Packard/ Agilent with split/splitless injector (300 °C, 1:100 split ratio) coupled with a BenchTOF-dx Time-Of-Flight Mass Spectrometer (TOF-MS) from Markes, UK. Carrier gas was helium with purity of 99.9%. The length of the column was calculated as 29.125 ± 0.253 m and the internal diameter of the column was calculated as 0.244 ± 0.001 mm from flow measurements and void time measurements at different inlet pressures and temperatures. Void times are measured with injections of air and detection of oxygen signal in the TOF-MS.

A PAL RSI Chronect Robotic autosampler (CTC Analytics AG, Switzerland) was used for injection of 1 µL of each sample.

To investigate a relation between the characteristic temperature T_{char} of the analytes and their elution temperature T_{elu}, temperature programs were made, with four different heating rates: 5, 10, 15 and 20 °C min^{-1}. The measurements were performed also with varied initial temperatures at 40, 60, 80, 100, 120 °C under constant pressure (83 kPa) conditions and at 40, 60, 80, 100, 120 and 140 °C under constant flow (1 mL min^{-1}) conditions.

To evaluate the curve fit model temperature programmed measurements with standard solutions of phenones and alcohols were performed.

Measurements of temperature in the GC oven and the ambient temperature were performed with external temperature thermocouples from Ahlborn, Germany. The ambient pressure was measured by an external sensor from Ahlborn whereas the inlet pressure was measured with an external sensor type PAA-33X/10 bar from Keller, Switzerland, connected to the split outlet of the injector. All external sensors were connected to an ALMEMO 8990–6 V5 data logger (Ahlborn, Germany). The elution temperature was determined by comparing of the data of the oven temperature with the retention times of each measurement.

3.3. Calculations

The K-centric parameters, especially the data of the characteristic temperature of the substances, were found in an open source retention parameter database [23]. The details of the determination of the parameters can be found in [16].

The measured elution temperatures were analysed separately for each condition, constant flow respectively constant pressure, initial temperature and heating rate. The characteristic temperatures and the elution temperatures were plotted against each other. For linear and non-linear fits of the data, the Julia package LsqFit.jl [24,25] was used, which uses the Levenberg-Marquardt algorithm for non-linear fitting [26,27]. For all heating rates and initial temperatures, the parameters of the model presented in Eq. (12) T_0 and T_1 were determined. The influence of the initial temperature and the heating rate was investigated to find a systematic relationship between the parameters and the conditions. The correlations were described and inserted into the model. To

Table 1
Determined Characteristic Temperatures of the BTEX. FAMES and LSER-MIX in accordance to the **K**-centric model of Blumberg on a Rxi17SilMS.

Compound	CAS	T_{char} [°C]			Class
Benzene	71–43–2	32.46	±	2.17	BTEX
Ethylbenzene	100–41–4	81.08	±	0.09	BTEX
Toluene	108–88–3	60.80	±	0.18	BTEX
o-Xylene	95–47–6	89.83	±	0.73	BTEX
m-Xylene	108–38–3	82.06	±	0.08	BTEX
p-Xylene	106–42–3	32.46	±	2.17	BTEX
Methyl butyrate	623–42–7	49.70	±	0.64	FAMES
Methyl hexanoate	106–70–7	89.32	±	0.10	FAMES
Methyl octanoate	111–11–5	122.96	±	0.10	FAMES
Methyl decanoate	110–42–9	152.75	±	0.05	FAMES
Methyl undecanoate	1731–86–8	166.41	±	0.05	FAMES
Methyl laurate	111–82–0	179.40	±	0.05	FAMES
Methyl tridecanoate	1731–88–0	191.67	±	0.04	FAMES
Methyl myristate	124–10–7	203.33	±	0.05	FAMES
Methyl myristoleate	56,219–06–8	205.38	±	0.05	FAMES
Methyl pentadecanoate	7132–64–1	214.28	±	0.06	FAMES
Methyl cis-10-pentadecenoate	90,176-52–6	216.40	±	0.05	FAMES
Methyl palmitate	112–39–0	224.78	±	0.07	FAMES
Methyl palmitoleate	1120–25–8	225.98	±	0.05	FAMES
Methyl heptadecanoate	1731–92–6	234.82	±	0.06	FAMES
cis-10-Heptadecenoic acid methyl ester	75,190–82–8	236.03	±	0.05	FAMES
Methyl stearate	112–61–8	244.82	±	0.35	FAMES
trans-9-Elaidic acid methyl ester	1937–62–8	245.35	±	0.06	FAMES
cis-9-Oleic acid methyl ester	112–62–9	245.31	±	0.07	FAMES
Methyl linolelaidate	2566–97–4	247.19	±	0.05	FAMES
Methyl linoleate	112–63–0	247.54	±	0.25	FAMES
Methyl arachidate	1120–28–1	262.19	±	0.06	FAMES
Methyl gamma linolenate	16,326–32–2	247.93	±	0.07	FAMES
Methyl cis-11-eicosenoate	2390–09–2	263.07	±	0.12	FAMES
Methyl alpha linolenate	301–00–8	250.18	±	0.07	FAMES
Methyl heneicosanoate	6064–90–0	270.58	±	0.07	FAMES
cis-11,14-Eicosadienoic acid methyl ester	2463–02–7	265.13	±	0.08	FAMES
Methyl behenate	929–77–1	278.61	±	0.08	FAMES
cis-8,11,14-Eicosatrienoic acid methyl ester	21,061–10–9	265.89	±	0.08	FAMES
Methyl erucate	1120–34–9	279.54	±	0.36	FAMES
cis-11,14,17-Eicosatrienoic acid methyl ester	55,682–88–7	268.05	±	0.06	FAMES
cis-5,8,11,14-Eicosatetraenoic acid methyl ester	2566–89–4	266.29	±	0.05	FAMES
Methyl tricosanoate	2433–97–8	286.49	±	0.09	FAMES
cis-13,16-Docosadienoic acid methyl ester	–	281.68	±	0.07	FAMES
Methyl lignocerate	2442–49–1	294.06	±	0.06	FAMES
cis-5,8,11,14,17-Eicosapentaenoic acid methyl ester	2734–47–6	268.28	±	0.38	FAMES
Methyl nervonate	2733–88–2	295.09	±	0.07	FAMES
cis-4,7,10,13,16,19-Docosahexaenoic acid methyl ester	301–01–9	286.57	±	0.10	FAMES
n-Octanal	124–13–0	105.34	±	0.12	LSER-MIX
2-Octanone	111–13–7	103.35	±	0.12	LSER-MIX
Octan-2-ol	123–96–6	99.50	±	0.23	LSER-MIX
Benzyl alcohol	100–51–6	128.55	±	0.06	LSER-MIX
4-Fluoroaniline	371–40–4	124.39	±	0.07	LSER-MIX
Phenyl acetate	122–79–2	130.06	±	0.08	LSER-MIX
1-Phenyl ethanol	98–85–1	130.84	±	0.05	LSER-MIX
2,6-Dimethylphenol	576–26–1	138.07	±	0.06	LSER-MIX
2-Chlorophenol	95–57–8	115.88	±	0.09	LSER-MIX
2-Methylphenol	95–48–7	126.96	±	0.04	LSER-MIX
Cyclohexanol	108–93–0	90.04	±	0.11	LSER-MIX
Bromobenzene	108–86–1	104.09	±	0.07	LSER-MIX
n-Heptanal	111–71–7	87.46	±	0.11	LSER-MIX
Benzaldehyde	100–52–7	116.25	±	0.11	LSER-MIX
Acetophenone	98–86–2	135.77	±	0.06	LSER-MIX
Methyl benzoate	93–58–3	136.74	±	0.05	LSER-MIX
Styrene	100–42–5	91.67	±	0.12	LSER-MIX
3-Methylphenol	108–39–4	130.37	±	0.07	LSER-MIX
Octan-1-ol	111–87–5	114.37	±	0.08	LSER-MIX
1,3-Dichlorobenzene	541–73–1	115.80	±	0.11	LSER-MIX
Cyclohexanone	108–94–1	101.20	±	0.08	LSER-MIX
4-Methylphenol	106–44–5	130.58	±	0.07	LSER-MIX
1,2-Dichlorobenzene	95–50–1	124.28	±	0.05	LSER-MIX
Linalool	78–70–6	120.04	±	0.11	LSER-MIX
Aniline	62–53–3	121.66	±	0.09	LSER-MIX
n-Butylbenzene	104–51–8	116.35	±	0.08	LSER-MIX
Heptan-2-one	110–43–0	85.53	±	0.16	LSER-MIX
Nonan-2-one	821–55–6	120.20	±	0.13	LSER-MIX
Nitrobenzene	98–95–3	142.41	±	0.06	LSER-MIX
n-Nonanal	124–19–6	122.12	±	0.07	LSER-MIX
1-Phenyl-2-propanol	698–87–3	142.50	±	0.06	LSER-MIX

5

Table 1 (*continued*)

Compound	CAS	T_{char} [°C]			Class
Hexan-1-ol	111–27–3	77.98	±	0.12	LSER-MIX
Chlorobenzene	108–90–7	82.79	±	0.09	LSER-MIX
2-Nitrophenol	88–75–5	147.83	±	0.06	LSER-MIX
3,5-Dimethylphenol	108–68–9	146.21	±	0.07	LSER-MIX
2-Chloroaniline	95–51–2	149.33	±	0.05	LSER-MIX
Phenol	108–95–2	113.06	±	0.10	LSER-MIX
Pentanol	71–41–0	58.93	±	0.13	Alcohols
Heptanol	111–70–6	98.42	±	0.17	Alcohols
Nonanol	143–08–8	133.60	±	0.15	Alcohols
Decanol	112–30–1	149.10	±	0.08	Alcohols
Undecanol	112–42–5	163.77	±	0.17	Alcohols
Dodecanol	112–53–8	177.53	±	0.14	Alcohols
Propiophenone	93–55–0	154,16	±	0.07	Phenones
Butyrophenone	495–40–9	166.13	±	0.12	Phenones
Valerophenone	1009–14–9	180.55	±	0.078	Phenones
Hexanophenone	942–92–7	193.72	±	0.13	Phenones
Heptanophenone	1671–75–6	206.14	±	0.23	Phenones
Octanophenone	1674–37–9	217.92	±	0.35	Phenones

validate the final model, the data was fitted again with multivariate regression using LsqFit.jl [24].

To analyse the data an interactive notebook is programmed by using the Julia package Pluto.jl [28,29]. The algorithm is available via the GitHub project 'Elutiontemperature' or can be found in the supplemental materials. For multivariate fits the package LsqFit.jl was used [24,25]. For simulation of GC separations GasChromatographySimulator.jl was used [30].

4. Results & discussion

Detailed results of the determination of the *K*-centric retention parameters of the substances are shown in the supplemental material. The determined characteristic temperatures of the substances are shown in Table 1. The reference void time at 150 °C at 83 kPa was determined with $t_{M,150} = 1.3808$ min.

4.1. Measurements of elution temperatures and curve fit

4.1.1. Measurements in constant pressure mode

The measured elution temperatures are shown in Fig. 3. A detailed interactive 3D-Chart of the data is given in the supplementals. As expected, all conditions show a linear trend at high characteristic temperatures and deviation from the linear trend for low characteristic temperatures close to the initial temperature. The slope of the linear

Table 2

Experimental determined parameters after multivariate fit for constant pressure and constant flow mode. The slopes $\mathbf{m_0}$ and $\mathbf{m_1}$ can be expressed for absolute heating Rate $\mathbf{R_T}$ respectively dimensionless heating rate $\mathbf{r_T}$ ($\tilde{\mathbf{m}}$) or for void temperature $\mathbf{T_M}$ ($\overline{\mathbf{m}}$) also known as normalised heating rate.

Parameter	Const. pressure ($p_{in} = 83$ kPa)	Const. flow (F = 1 mL min^{-1})
γ	0.0548 ± 0.0015 K^{-1}	0.03608 ± 0.0005 K^{-1}
	T_0 term	
m_0	3.365 ± 0.019 min	3.062 ± 0.016 min
$\tilde{m}_0$	73.11 ± 0.41 K	66.51 ± 0.35 K
$\overline{m}_0$	2.437 ± 0.014	2.217 ± 0.012
n_0	-43.12 ± 0.27 K	-45.90 ± 0.23 K
	T_1 term	
m_1	1.766 ± 0.033 min	1.573 ± 0.025 min
$\tilde{m}_1$	38.36 ± 0.71 K	34.18 ± 0.54 K
$\overline{m}_1$	1.279 ± 0.024	1.139 ± 0.018
$R_{T,0}$	12.81 ± 0.11 K min^{-1}	14.99 ± 0.12 K min^{-1}
$r_{T,0}$	0.5898 ± 0.0049	0.6900 ± 0.0055
R^2	0.999835	0.999933
$rmse$	3.10 K	2.81 K

trend is for all conditions is approximately 1.0. The shift from the heating rate $R_{T,0}$ at which T_{char} is equal to T_{elu} is proportional to the heating rate R_T and nearly equal for all T_{init} at same heating rate. For a given heating rate, the elution temperatures span a plane at high values
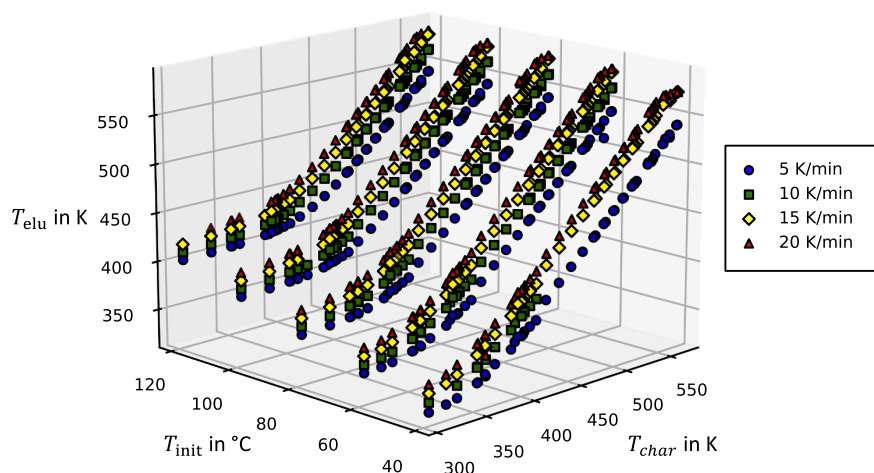
Fig. 3. Dependence of $\mathbf{T_{elu}}$ on $\mathbf{T_{char}}$ at different initial temperatures and different heating rates for the investigated data set.

6

of T_{char} for all T_{init}. The increasing of the initial temperature also increases the deviation from the linear trend for volatile compounds such as BTEX even for compounds with medium T_{char} values.

For the quantity T_1, which determines the constant asymptote of the model given in Eq. (12), a systematic influence of initial temperature and heating rate could be found and is shown in Fig. 5C. T_1 is not equal to the initial temperature but depends linearly on it. This is plausible because the lowest measurable elution temperature must be a higher temperature than the initial temperature of the program, like the temperature reached after the void time. Please note: If the initial temperature is held for specific times, the elution temperature of an analyte eluting during this holding time, is equal to the initial temperature. But in this case no correlation between T_{char} and T_{elu} exists.

Linear regressions examining the influences of the initial temperature show that T_1 also depends linearly on the heating rate, Fig. 5D. The linear function describing the dependence could have an independent intercept n_1. When the initial temperature is given in units of °C, the value of n_1 is approximately equal to -273 °C and changing the units to K changes the intercept n_1 to almost zero. For the multivariate regression described below, the intercept n_1 was no longer used.

For the intercept T_0 which determines the shift from the heating rate $R_{T,0}$ where T_{char} is equal to T_{elu} the influence of the heating rate also could be described and is shown in Fig. 5B. In the investigated range, T_0 depends approximately linearly to R_T. The data also show that under the investigated conditions T_0 is approximately independent from the initial temperature (Fig. 5A and B).
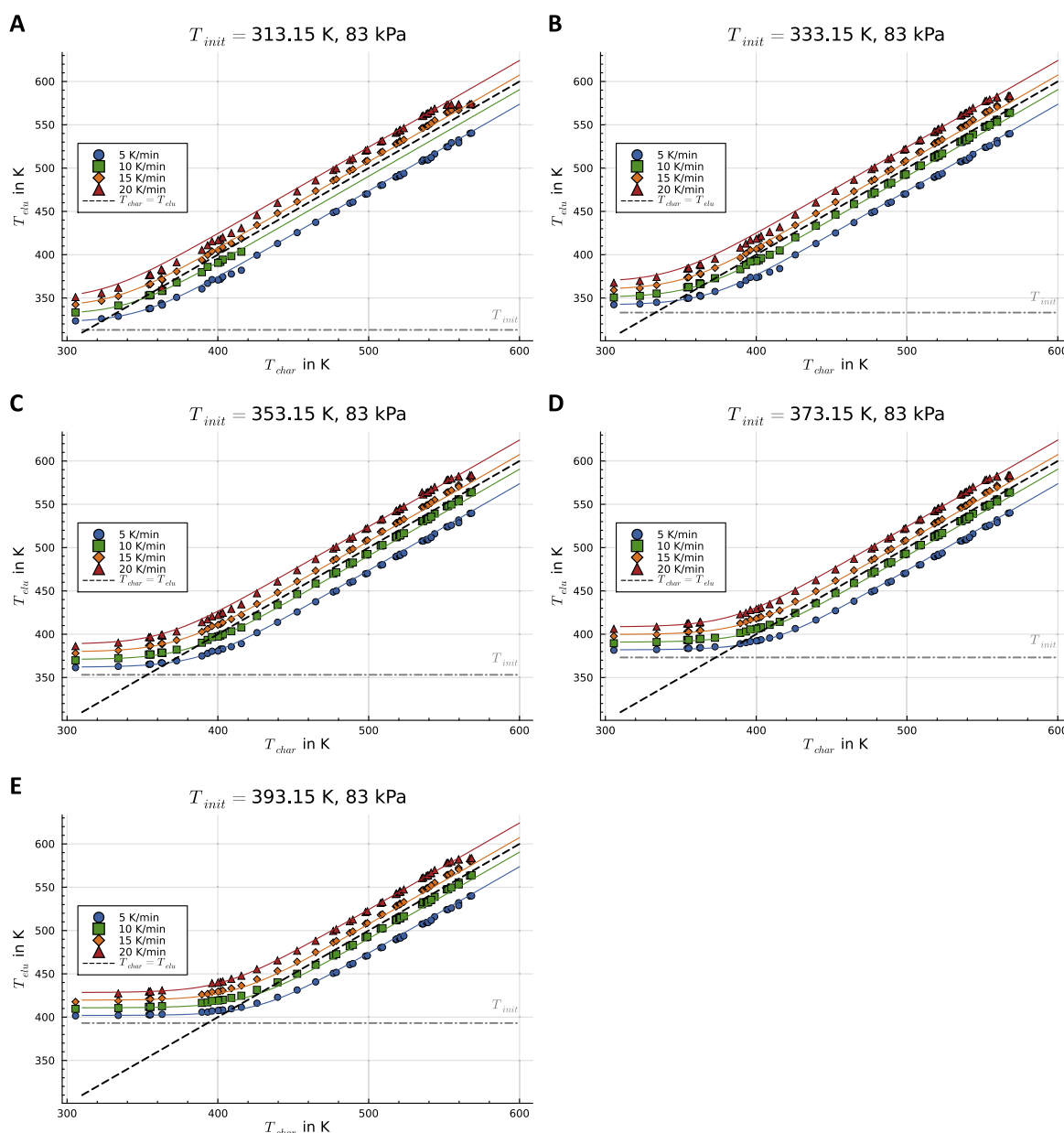
Fig. 4. Measured elution temperature depending on characteristic temperature at different initial temperatures (A-G) and heating rates (5 K min^{-1}= blue, 10 K min^{-1}=green, 15 K min^{-1}= orange, 20 K min^{-1}= red) in constant pressure mode of 83 kPa carrier gas and curve fits.

Appendix

For the parameter γ which modulates the transition from the constant part to the linear part for each condition, values between 0.04 and 0.1 were found. A systematic dependence on the heating rate or the initial temperature was not found. To simplify the model for γ the averaged value 0.05967 for all condition is used.

To assess the values and find the best values of the parameters, the model given in Eq. (12) was modified by adding the influence of heating rate and initial temperature to the model such as shown in Eqs. (14) and (15).

$$T_{elu}(T_{char}, R_T, T_{init}) = \frac{1}{\gamma}\ln\left(e^{\gamma(T_{char}+T_0)} + e^{\gamma(T_1)}\right) \tag{13}$$

with

$$T_0 = m_0 \cdot R_T + n_0 \leftrightarrow \widetilde{m}_0 \cdot r_T + n_0 \tag{14}$$

$$T_1 = T_{init} + m_1 \cdot R_T \leftrightarrow T_{init} + \widetilde{m}_1 \cdot r_T \tag{15}$$

In the next step the values of the parameters where redetermined by using a multivariate regression. The final values of the parameters of the model are shown in Table 2. The coefficient of determination R^2 of the determined model has a value of 0.9998. Detailed results and conditions of the determination via multivariate regression are shown in supplemental material. The calculated data correlate well to the measured ones as shown in the supplemental material, Fig. S1. The final fits of the determined model in relation to the measured data also are shown in Fig. 4 and prove the well accordance to the data. For most of the compounds the deviation from the measured data is lower than 2% even for the early volatile compounds. Fig. 4 also shows, that an average value for γ is acceptable to describe the dependence of elution temperature on

characteristic temperature. The proportionality factors m_0 and m_1 for the heating rate can also be expressed for dimensionless heating rate or heating rate per void time and are also listed in Table 2.

The intercept of the linear term T_0 can be described as $T_0 = (3.365 \pm 0.019)$ min$\cdot R_T - (43.12 \pm 0.27)$ °C respectively $T_0 = (2.437 \pm 0.014)$ min$\cdot T_M - (43.12 \pm 0.27)$ °C by using the void temperature. Using the data of Blumberg and calculating the influence of heating rate to the intercept of the linear part, the shift T_0 can be described as $T_0 = 2.5 \cdot T_M - 43.5°C$ [11]. At one heating rate the term $m_0 R_T$ is equal to n_0 and T_0 becomes zero. This defines the heating rate $R_{T,0}$ as the ratio between n_0 and m_0 (Eq. (16)).

$$R_{T,0} = -\frac{n_0}{m_0} \tag{16}$$

$R_{T,0}$ can be determined as 12.81 ± 0.11 °C min^{-1} respectively $r_{T,0} = 0.5898 \pm 0.0049$ as dimensionless heating rate. Expressed as void temperature the value amounts to $T_M = 17.69 \pm 0.15$ °C and accords to early estimations - using a simple linear relationship - with $T_M = 17.4$ °C respectively $r_T = 0.58$ [11]. For a heating rate of 10 °C/t_M the model gives a shift from $R_{T,0}$ of -18.75 ± 0.3 °C which well accords to early determinations with $- 18.5$ °C [11]. For $T_M = 20$ °C the model determined a intercept of 5.62 ± 0.38 °C whereas Blumberg estimated it as nearly 4.5 °C [11]. Overall, this shows, that the new model agrees with the current theory and converges in known models for high values.

4.1.2. Measurements in constant flow mode

For most GC chromatographers the use of constant flow is more common than constant pressure mode [31]. For the conditions at a constant flow of 1 mL min^{-1} the results of the measurements are rather
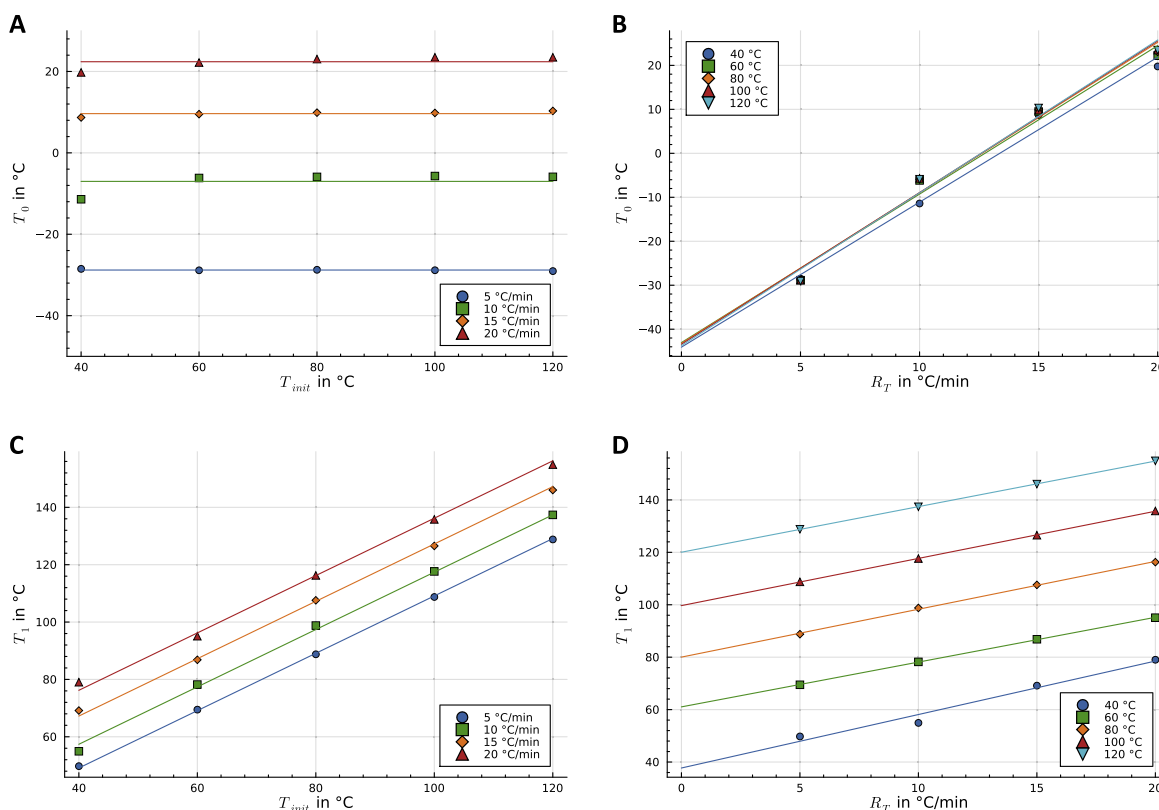
Fig. 5. Influence of initial temperature and heating rate to fit parameters T_0 and T_1 in constant pressure mode of 83 kPa. The intercept T_0 is almost constant for different values of T_{init} (A) but depends approximately linear to heating rate (B). Parameter T_1 depends strong linear on the investigated initial temperatures (C) and depends also linear on heating rate (D).

8

similar to the measurements of constant pressure (Fig. 6). The measured elution temperatures for the same compounds are between 1 and 5 K lower than in the constant pressure mode with 83 kPa.

Plotting the elution temperature against the characteristic temperature also shows a similar profile as in constant pressure mode. It also can be described with Eq. (12) and the slope of the linear region can approximate with a value of 1. To fit the data with multiple regression by using Eq. (13) shows well accordance. The coefficient of determination is R^2 =0.999933. The determined values of the coefficients are also listed in Table 2.

The determined value for the curvature parameter γ=0.03609 $\pm$ 0.0005 is different and also the other determined parameters have lower values than in the constant pressure mode. Using Eq. (16) The heating rate where Tchar is equal to Telu can be predicted as $R_{T,0} = 14.99 \pm 0.12$ respectively $r_{t,0} = 0.6900 \pm 0.0055$ and is close to In 2 and accords to other observations found in the literature [12,21].

One reason of the similar results compared with the constant pressure results, can be the pressure of 83 kPa which is equal to the pressure in the middle of a temperature program at constant flow, starting at 60 °C and rising up to 200 °C. The Influence of the carrier gas pressure on the retention factor and thus also on the elution temperature should be negligible [32]. Simulations of GC separations carried out with different flows confirm that and show hardly any change in the parameters at different pressures, as it will be shown in the second part. However, minor changes were observed between different flows, while different values were observed between constant flow and constant pressure modes (see in part II).

4.2. Prediction of retention times

To predict the retention times only from a T_{char} of a compound, Eq. (9) can be converted to

$$t_R = \frac{T_{elu} - T_{init}}{R_T} \tag{17}$$

With knowledge of the found dependence of T_{elu} on T_{char}, given in Eq. (12), the retention time can be estimated as

$$t_R = \frac{1}{R_T} \left(\frac{1}{\gamma} \ln\left(e^{\gamma(T_{char}+T_0)} + e^{\gamma(T_1)}\right) - T_{init} \right) \tag{18}$$

To evaluate this equation, measurements of homologous phenols and alcohols were performed. The chromatograms were compared to the predicted retention time using the multivariate estimation, Eq. (18). Fig. 7 shows the chromatogram and the predictions visualised as sticks. The relative differences are between 1 and 6%. For the alcohols the root-mean-square error (rmse) is 0.1522 min and for the measurement of phenones the rmse is 0.2403 min.

For further comparison the retention times were also predicted using the simple linear relationship for T_{elu} given in Eq. (10). The measured values and the predicted values are given in Table 3. Compared to the relative differences of the prediction using the simple linear relationship, the prediction using the multivariate fit is closer to the measurements for high volatiles. Pentanol shows the highest difference between the two estimation methods, whereas the multivariate estimation is accurately compared to the measurement. As a high volatile compound, its elution temperature is close to the initial temperature. For $T_{char} > T_{init} + 100$ °C the multivariate estimations for the other substance, especially the phenones, are almost the same as the linear relationship.
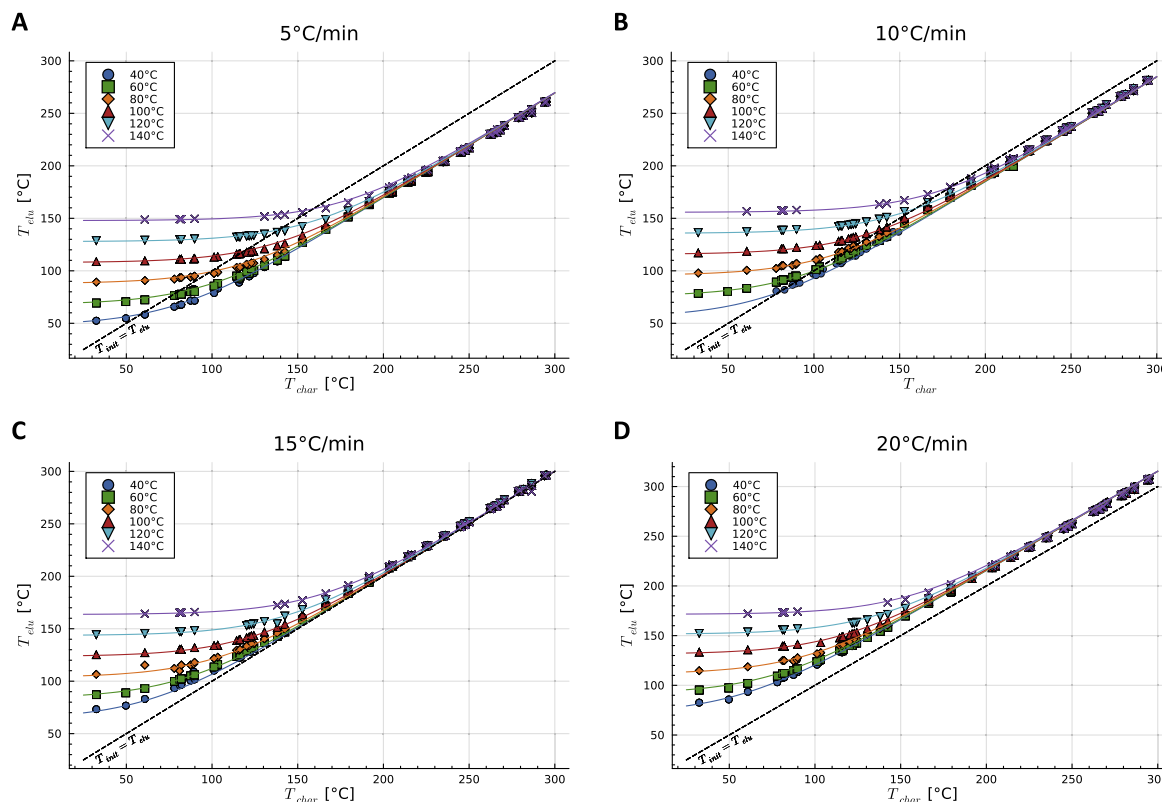
Fig. 6. Dependence of measured elution temperature on characteristic temperature at different heating rates (A-D) and initial temperatures in constant flow mode of 1 mL min^{-1} carrier gas. T_1 depends strongly on T_{init} whereas T_0 is depending on R_T. Slope of linear increase is almost close to 1.0 for every condition.
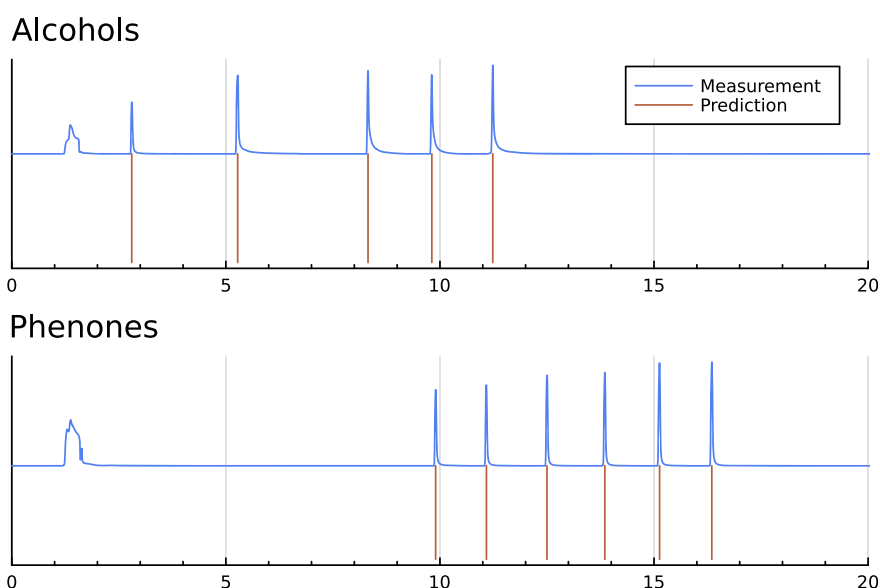
Fig. 7. Measured chromatograms compared to predicted retention times of alcohols (pentanol, heptanol, nonanol, decanol, undecanol) and phenones (propiophenone - octanophenone). The retention times are predicted only by the $\mathbf{T_{char}}$ values of the substances by using the novel model; Temperature program: $\mathbf{T_{init}}= 40$ °C, $\mathbf{R_T} = 10$ °C min^{-1}, $\mathbf{p_i} = 83$ kPa.

Table 3

Measured and predicted retention times of a various selection of alcohols and phenones. Measurement conditions: Constant pressure of 83 kPa, $\mathbf{T_{init}}= 40$ °C, Heating Rate $= 10$ °C min^{-1}.

Measurements Compound	t_R [min]	Multivariate Prediction t_R [min]	relative difference	Linear Prediction t_R [min]	relative difference
Alcohols					
Pentanol	2.8014	2.6667	−4.81%	0.9464	−66.22%
Heptanol	5.2747	5.1970	−1.47%	4.8950	−7.20%
Nonanol	8.3196	8.4597	1.68%	8.4125	1.12%
Decanol	9.8104	9.9831	1.76%	9.9628	1.55%
Undecanol	11.2333	11.4387	1.83%	11.4295	1.75%
$\overline{\chi}^2$		0.0232 min^2		0.7311 min^2	
rmse		0.1522 min		0.8551 min	
Phenones					
Propiophenone	9.8993	10.4842	5.91%	10.4687	5.75%
Butyrophenone	11.0851	11.6737	5.31%	11.6657	5.24%
Valerophenone	12.4996	13.0914	4.73%	13.0878	4.71%
Hexanophenone	13.8505	14.4264	4.16%	14.4246	4.15%
Heptanophenone	15.1295	15.6683	3.56%	15.6674	3.56%
Octanophenone	16.3492	16.8456	3.04%	16.8451	3.03%
$\overline{\chi}^2$		0.0577 min^2		0.0562 min^2	
rmse		0.2403 min		0.2370 min	

Using the simple linear branch for estimations is only recommended for high heating rates and low initial temperatures. For $T_{char} < T_{init} + 100$ °C this relationship gives physically meaningless results e.g. negative retention times or retention times lower than the void time. In contrast the multivariate relationship given in Eq. (18) expands the estimation range for $T_{char} < T_{init} + 100$ °C to values close to T_{init}. This shows it is suitable for simple method development especially for estimations of start values for T_{char}, as it is needed for the determination of the K-centric parameters from temperature-programmed measurements [10]. This opens up the opportunity to obtain an estimation of the thermodynamic parameters from only one rapid temperature-programmed measurement for a series of substances compared to the classic ABC or K-centric model

where four or more isothermal measurements are recommended per analyte, typically requiring about one hour for each measurement [16].

5. Conclusion

The dependence of the elution temperatures T_{elu} on the characteristic temperature T_{char} at variable heating rates and initial temperatures are shown. It was possible to describe the influence of the heating rate and the initial temperature in a model which accords well to the measured data and which expands the current relationship shown by Blumberg. For substances which elute near the start temperature like BTEX the curve fit model proposed in this report allows one to calculate the elution temperature more precise than a simple linear model would. The dimensionless heating $r_{T,0}$, where the elution temperature is equal to the characteristic temperature, can be estimated as 0.59 for constant pressure and 0.69 for constant flow. The estimation of retention times of simple temperature programs by the characteristic temperature using the fit was demonstrated.

In a second part more fits for a larger range of initial temperatures and heating rates using computer simulation of GC separations of a large set of analytes and stationary phases will be performed. Further, more influences of the heating rate will be discussed. It will be shown that the model is suitable to predict T_{char} values from temperature programmed measurements, which will reduce the expense of isothermal measurements to determine the characteristic temperature and can be an estimation value for GC method optimization.

CRediT authorship contribution statement

Tillman Brehmer: Conceptualization, Methodology, Software, Validation, Investigation, Writing – original draft, Visualization. **Peter Boeker:** Conceptualization, Resources, Supervision, Project administration, Funding acquisition. **Matthias Wüst:** Methodology, Writing – review & editing, Supervision. **Jan Leppert:** Conceptualization, Methodology, Software, Validation, Investigation, Writing – original draft, Visualization, Project administration.

Declaration of Competing Interest

The authors declare the following financial interests/personal relationships which may be considered as potential competing interests: Tillman Brehmer reports financial support was provided by German Research Foundation (DFG). Jan Leppert reports financial support was provided by German Research Foundation (DFG).

Data availability

Data will be made available on request.

Supplementary materials

Supplementary material associated with this article can be found, in the online version, at doi:10.1016/j.chroma.2023.464301.

References

[1] K. Jurica, I. Brčić Karačonji, D. Lasić, D. Bursać Kovačević, P. Putnik, Unauthorized food manipulation as a criminal offense: food authenticity, legal frameworks, analytical tools and cases, Foods 10 (2021), https://doi.org/10.3390/foods10112570.

[2] H. Snijders, H.-G. Janssen, C. Cramers, Optimization of temperature-programmed gas chromatographic separations I. Prediction of retention times and peak widths from retention indices, J. Chromatogr. A 718 (1995) 339–355, https://doi.org/10.1016/0021-9673(95)00692-3.

[3] Pro EZGC, Chromatogram modeler, Restek (2023).

[4] F.L. Dorman, P.D. Schettler, L.A. Vogt, J.W. Cochran, Using computer modeling to predict and optimize separations for comprehensive two-dimensional gas chromatography, J. Chromatogr. A 1186 (2008) 196–201, https://doi.org/10.1016/j.chroma.2007.12.039.

[5] M. Gaida, F.A. Franchina, P.-H. Stefanuto, J.-F. Focant, Top-down approach to retention time prediction in comprehensive two-dimensional gas chromatography-mass spectrometry, Anal. Chem. 94 (2022) 17081–17089, https://doi.org/10.1021/acs.analchem.2c03107.

[6] P. Boeker, J. Leppert, Flow field thermal gradient gas chromatography, Anal. Chem. 87 (2015) 9033–9041, https://doi.org/10.1021/acs.analchem.5b02227.

[7] H.D. Tolley, S. Avila, B.D. Iverson, A.R. Foster, A.R. Hawkins, S.E. Tolley, M.L. Lee, Simulating capillary gas chromatographic separations including thermal gradient conditions, Anal. Chem. 93 (2021) 2291–2298, https://doi.org/10.1021/acs.analchem.0c04160.

[8] J. Leppert, P.J. Müller, M.D. Chopra, L.M. Blumberg, P. Boeker, Simulation of spatial thermal gradient gas chromatography, J. Chromatogr. A 1620 (2020), 460985, https://doi.org/10.1016/j.chroma.2020.460985.

[9] N. Ulrich, G. Schüürmann, W. Brack, Prediction of gas chromatographic retention indices as classifier in non-target analysis of environmental samples, J. Chromatogr. A 1285 (2013) 139–147, https://doi.org/10.1016/j.chroma.2013.02.037.

[10] J. Leppert, T. Brehmer, M. Wüst, P. Boeker, Estimation of retention parameters from temperature programmed gas chromatography, J. Chromatogr. A 464008 (2023), https://doi.org/10.1016/j.chroma.2023.464008.

[11] L.M. Blumberg, Distribution-centric 3-parameter thermodynamic models of partition gas chromatography, J. Chromatogr. A 1491 (2017) 159–170, https://doi.org/10.1016/j.chroma.2017.02.047.

[12] K.A.J.M. Stevenson, L.M. Blumberg, J.J. Harynuk, Thermodynamics-based retention maps to guide column choices for comprehensive multi-dimensional gas chromatography, Anal. Chim. Acta 1086 (2019) 133–141, https://doi.org/10.1016/j.aca.2019.08.011.

[13] L.M. Blumberg, Chromatographic parameters: characteristic parameters of solute retention - an insightful description of column properties, J. Chromatogr. A 1685 (2022), 463594, https://doi.org/10.1016/j.chroma.2022.463594.

[14] M.D. Chopra, P.J. Müller, J. Leppert, M. Wüst, P. Boeker, Residual solvent analysis with hyper-fast gas chromatography-mass spectrometry and a liquid carbon dioxide cryofocusing in less than 90 s, J. Chromatogr. A 1648 (2021), 462179, https://doi.org/10.1016/j.chroma.2021.462179.

[15] A. Wilson, J.B. Johnson, R. Batley, P. Lal, L. Wakeling, M. Naiker, Authentication using volatile composition: a proof-of-concept study on the volatile profiles of Fourteen Queensland Ciders, Beverages 7 (2021) 28, https://doi.org/10.3390/beverages7020028.

[16] T. Brehmer, B. Duong, L. Friedemann, P.J. Faust, P. Boeker, M. Wüst, J. Leppert, Retention database for prediction, simulation, and optimization of GC separations, ACS Omega (2023), https://doi.org/10.1021/acsomega.3c01348.

[17] L.S. Ettre, Nomenclature for chromatography (IUPAC recommendations 1993), Pure Appl. Chem. 65 (1993) 819–872, https://doi.org/10.1351/pac199365040819.

[18] E.C.W. Clarke, D.N. Glew, Evaluation of thermodynamic functions from equilibrium constants, Trans. Faraday Soc. 62 (1966) 539, https://doi.org/10.1039/tf9666200539.

[19] L.M. Blumberg, M.S. Klee, Optimal heating rate in gas chromatography, J. Micro. Sep. 12 (2000) 508–514, https://doi.org/10.1002/1520-667X(2000)12:9<508:AID-MCS5>3.0.CO;2-Y.

[20] L.M. Blumberg, M.S. Klee, Method Translation and Retention Time Locking in Partition GC, Anal. Chem. 70 (1998) 3828–3839, https://doi.org/10.1021/ac971141v.

[21] L.M. Blumberg, Temperature-Programmed Gas Chromatography, Wiley-VCH, Weinheim, 2010.

[22] C.F. Poole, Selection of calibration compounds for selectivity evaluation of wall-coated, open-tubular columns for gas chromatography by the solvation parameter model, J. Chromatogr. A 1629 (2020), 461500, https://doi.org/10.1016/j.chroma.2020.461500.

[23] J. Leppert, T. Brehmer, RetentionData.jl. https://github.com/JanLeppert/RetentionData/tree/v0.2.0.

[24] J.M. White, P.K. Mogensen, et al., LsqFit.jl (2012). https://github.com/JuliaNLSolvers/LsqFit.jl.

[25] P.K. Mogensen, A.N. Riseth, Optim: a mathematical optimization package for Julia, JOSS 3 (2018) 615, https://doi.org/10.21105/joss.00615.

[26] D.W. Marquardt, An algorithm for least-squares estimation of nonlinear parameters, J. Soc. Ind. Appl. Math. 11 (1963) 431–441, https://doi.org/10.1137/0111030.

[27] K. Levenberg, A method for the solution of certain non-linear problems in least squares, Q. Appl. Math. 2 (1944) 164–168.

[28] F. van der Plas, M. Dral, P. Berg, Παναγιώτης Γεωργακόπουλος, R. Huijzer, N. Bochenski, A. Mengali, B. Lungwitz, C. Burns, H. Priyashan, J. Ling, E. Zhang, F.S. S. Schneider, I. Weaver, Rogerluo, S. Kadowaki, Z. Wu, J. Gerritsen, R. Novosel, Supanat, Z. Moon, luis-mueller, M. Abbott, N. Bauer, P. Bouffard, S. Terasaki, S. Polasa, TheCedarPrince, Pluto.jl: v0.19.14, https://github.com/fonsp/Pluto.jl, (2022).

[29] J. Bezanson, A. Edelman, S. Karpinski, V.B. Shah, Julia: a fresh approach to numerical computing, SIAM Rev. 59 (2017) 65–98, https://doi.org/10.1137/141000671.

[30] J. Leppert, GasChromatographySimulator.jl, J. Open Source Softw. 7 (2022) 4565, https://doi.org/10.21105/joss.04565.

[31] S. Hou, K.A.J.M. Stevenson, J.J. Harynuk, A simple, fast, and accurate thermodynamic-based approach for transfer and prediction of gas chromatography retention times between columns and instruments part III: retention time prediction on target column, J. Sep. Sci. 41 (2018) 2559–2564, https://doi.org/10.1002/jssc.201701345.

[32] A. Burel, M. Vaccaro, Y. Cartigny, S. Tisse, G. Coquerel, P. Cardinael, Retention modeling and retention time prediction in gas chromatography and flow-modulation comprehensive two-dimensional gas chromatography: the contribution of pressure on solute partition, J. Chromatogr. A 1485 (2017) 101–119, https://doi.org/10.1016/j.chroma.2017.01.011.

C.   Publication 3

Simulation of gas chromatographic separations and estimation of distribution-centric retention parameters using linear solvation energy relationships

Tillman Brehmer [a,*], Benny Duong [b], Peter Boeker [a,b], Matthias Wüst [a], Jan Leppert [a,*]

[a] University of Bonn, Institute of Nutritional and Food Sciences, Chair of Food Chemistry - Department Fast GC, Endenicher Allee 11 - 13, 53115 Bonn, Germany
[b] Hyperchrom GmbH Germany, Konrad-Zuse-Straße, 53115 Alfter, Germany

ARTICLE INFO

ABSTRACT

For method development in gas chromatography, suitable computer simulations can be very helpful during the optimization process. For such computer simulations retention parameters are needed, that describe the interaction of the analytes with the stationary phase during the separation process. There are different approaches to describe such an interaction, e.g. thermodynamic models like Blumberg's distribution-centric 3-parameter model (K-centric model) or models using chemical properties like the Linear Solvation Energy Relationships (LSER).

In this work LSER models for a Rxi-17Sil MS and a Rxi-5Sil MS GC column are developed for different temperatures. The influences of the temperature to the LSER system coefficients are shown in a range between 40 and 200 °C and can be described with Clark and Glew's ABC model as fit function. A thermodynamic interpretation of the system constants is given and its contribution to enthalpy and entropy is calculated. An estimation method for the retention parameters of the K-centric model via LSER models were presented. The predicted retention parameters for a selection of 172 various compounds, such as FAMEs, PCBs and PAHs are compared to isothermal determined values. 40 measurements of temperature programmed GC separations are compared to computer simulations using the differently determined or estimated K-centric retention parameters. The mean difference (RSME) between the measured and predicted retention time is less than 8 s for both stationary phases using the isothermal retention parameters. With the LSER predicted parameters the difference is 20 s for the Rxi-5Sil MS and 38 s for the Rxi-17Sil MS. Therefore, the presented estimation method can be recommended for first method development in gas chromatography.

1. Introduction

Higher requirements, e.g. in environmental protection or food safety, increase the sample throughput and the need of novel methods for novel analytes in analytical chemistry at the same time [1,2]. Often, a large number of preliminary measurements have to be performed before a method could be used in an analytical application.

For method development in GC, suitable computer simulation can be a powerful instrument to support the optimization process and to safe time, costs and chemical resources [3]. For such computer simulations of GC separations, retention parameters are needed, which describe the interactions of the analytes and the stationary phase of the column [4]. A precise retention model for prediction of retention factor k is the 'distribution-centric 3-parameter model' ('K-centric model') proposed by

Blumberg[5,6]. Based on this model a numeric computer simulation was developed which can be used for prediction of retention times of temperature programmed measurements but even for complex systems such as GC × GC or spatial thermal gradient GC (FF-TG-GC) [7,8].

Many laborious isothermal measurements for each analyte have to be performed and there are just a small number of available retention databases existing [9]. Therefore, it is necessary to find easier and more efficient alternatives for prediction of the retention parameters.

The characteristic temperature, one of the most important retention parameters, can be estimated from measurable elution temperatures [10]. In a novel approach the K-centric parameters can be determined by faster temperature programmed measurements [9].

As mentioned above, there is just a small number of available thermodynamic data for gas chromatography. But there are also other

substance specific data that can be used for prediction of GC separation, e.g. data from the Retention Index database of NIST [11], Flavornet [12] or UFZ database LSERD [11,13].

Another common retention model for prediction of retention factor k [14] or RI [15] under isothermal conditions is the 'Linear Solvation Energy Relationships model' (LSER) or 'solvation parameter model' [16, 17]. For this model there are a lot of literature data available in libraries [18,19]. Since the system describing constants of the model strongly depend on temperature [20]. Therefore, they are not suitable for prediction of retention times of temperature programmed measurements.

The aim of this work is to combine LSER models and the K-centric 3-parameter model to perform precise temperature independent predictions of temperature programmed GC separations by available LSER substance data from literature databases. Thus, a model to describe the temperature-dependence of the system constants will be developed.

2. Theory

In the following equations and models, temperature T and associated parameters are given in Kelvin, even if they are expressed in Celsius in examples or figures.

2.1. Thermodynamic retention model

In gas chromatography, the partition of an analyte between the mobile phase and the stationary phase is described by the distribution coefficient K [21] (also called partition coefficient [22]), defined as the ratio of the solute concentration in the stationary phase and in the mobile phase. It can be measured by isothermal measurements of the retention factor k and the phase ratio β of the column.

$$K = \beta k \tag{1}$$

The retention factor k is defined as the ratio of the reduced retention time $t_R - t_M$ and void time t_M of the GC column.

$$k = \frac{t_R - t_M}{t_M} \tag{2}$$

The void time t_M is the required time of the carrier gas for passing through the column. The distribution coefficient K depends on the temperature T and the Gibbs free energy ΔG of the solute evaporation from the stationary phase [21].

$$K = exp\left(\frac{\Delta G}{RT}\right) \tag{3}$$

with the molar gas constant R. Due to the change of the solute from the stationary into the mobile phase, the Gibbs free energy ΔG can be expressed by enthalpy ΔH and entropy ΔS and therefore applies

$$\ln K = \frac{\Delta H}{RT} - \frac{\Delta S}{R} \tag{4}$$

Both ΔH and ΔS depend on the temperature T itself and its dependence can be accounted for using a 3-parameter mode [6,23] with the change of the isobaric molar heat capacity ΔC_p as third parameter. At a given reference temperature T_{ref} Clark and Glew proposed a curve fit model, known as ABC-model. To avoid confusion with the symbols of the LSER, here A, B, C are written as α, β, γ:

$$\ln K = \alpha + \frac{\beta}{T} + \gamma \ln T \tag{5}$$

with

$$\Delta C_p = R\gamma \tag{6}$$

$$\Delta H = R\left(\gamma T_{ref} - \beta\right) + R\gamma\left(T - T_{ref}\right) \tag{7}$$

$$\Delta S = R\left(\alpha + \gamma + \gamma \ln \frac{T_{ref}}{T_1}\right) + R\gamma \ln \frac{T}{T_{ref}} \tag{8}$$

2.2. Distribution-centric 3-parameter model (K-centric model)

A precise model resulting from classic van't Hoff model to describe the distribution of a compound between the stationary and mobile phase is the so called 'Distribution-centric 3-parameter' model of Blumberg [5, 6], also known as the 'K-centric' model. The temperature dependence of the retention factor k of an analyte in a GC system can be described as

$$\ln k = \left(\frac{\Delta C_p}{R} + \frac{T_{char}}{\theta_{char}}\right)\left(\frac{T_{char}}{T} - 1\right) + \frac{\Delta C_p}{R}\ln\left(\frac{T}{T_{char}}\right) \tag{9}$$

whereby T_{char} is the characteristic temperature and θ_{char} is the characteristic thermal constant.

These parameters, especially T_{char} and θ_{char}, have a direct chromatographic impact. The characteristic temperature T_{char} is the temperature, where the amount of the analyte is evenly distributed between stationary and mobile phase ($k = 1$) [5]. The characteristic thermal constant is the inverse slope of the function $\ln k(T)$ at $T = T_{char}$: an increase of the temperature around T_{char} by θ_{char} reduces $\ln k$ by 1.0. The quantity ΔC_p defines the deviation of k from a two-parameter model for temperature significantly lower/higher than T_{char}.

2.3. Solvation parameter model

An alternative to the above mentioned thermodynamic retention models is the '*Linear Solvation Energy Relationship*' model (LSER), also known as the 'Abraham model' [24,25]. LSER models are very common e.g. in environmental chemistry to predict distribution phenomena of a target analyte with any kind of matrix [26]. Typically applications are e.g. prediction of pollutant adsorption in soils or migration of mobile additives from or into package materials [27]. The principle of adsorption phenomena prediction can also be used for the prediction of retention in chromatography [18,19]. In this model, the logarithm of the retention factor $\ln k$ at a defined temperature is expressed as a multiple linear regression of chemical properties of the analyte (descriptors E, S, A, B, L) and properties of the stationary phase (system constants e, s, a, b, l) [14].

$$\ln k = eE + sS + aA + bB + lL + c \tag{10}$$

The individual system constants (lower case letters) represent different individual intermolecular interactions of the stationary phase that have an influence on the substance described by its substance specific descriptors (capital letters).

These are:

- e, the electron lone pair interactions (the excess dispersion interactions that result from the presence of polarizable electrons),
- s, interactions of a dipole-type, known as induction and orientation,
- a, the interactions of the hydrogen-bonding in which the stationary phase acts as a hydrogen-bond acceptor
- b, interactions in which the stationary phase acts as hydrogen-bond donor. In GC the value of b can be approximated as zero.
- l, the size dependent interactions, which are the cavity formation in the stationary phase and the setup of dispersion interactions.
- c, the intercept contains deviations from the model, but also information about the phase ratio. It is a system property required to estimate retention factors for a specific column and temperature but is not a characteristic property of the solvation properties of the stationary phase. [14]

The substance specific descriptors are experimental values and are defined as

- *E*, the excess molar refraction
- *S*, the capability for interactions of a dipole-type (orientation and induction)
- A, overall resp. effective hydrogen-bond acidity
- B, overall resp. effective hydrogen-bond basicity
- *L* the gas-liquid partition constant at 25 °C on n-hexadecane as stationary phase. [14]

The system constants depend on the temperature, while the substance descriptors have fixed, substance-stationary phase-specific values. For individual temperatures, the system constants can be determined by a multivariate regression using selected calibration substances whose descriptors are known. A small number of 30 to 40 substances (with different functional groups and structures) is sufficient to determine the system coefficients [20].

For any analyte, for which the substance descriptors (capital letters) are known, the ln*k* values for the defined temperature can be calculated with the systems coefficients without any other measurement on the GC column. Substance coefficients can be found in the literature and are collected in databases such as the LSER database (LSERD) of the Helmholtz Centre for Environmental Research (UFZ) [13] or the Wayne State University (WSU) database [19]. The determination can be found elsewhere [28–30].

3. Materials and methods

3.1. Chemicals

A standard solution containing 40 compounds (see Table 2), e.g. various alcohols, phenols, halogen alkyls and others with a concentration of 10 µg/mL was prepared in dimethyl chloride (VWR). All the substances had a purity > 98 % and were purchased from Sigma-Aldrich.

For validation a standard solution, with 37 fatty acid methyl esters (FAMEs) from butyric acid methyl ester (C4:0) to tetracosanoic acid methyl ester (C24:0), with concentrations between 200 and 600 µg/mL per component in *n*-hexane was purchased from Sigma-Aldrich. A PCB-Mix from Sigma-Aldrich including 10 ng/µL of PCB 28, PCB 52, PCB 101, PCB 138, PCB 153, PCB 180 in isooctane was used.

3.2. Instrumentation

Isothermal measurements to determine *K*-centric retention parameters and to develop the LSER-models were performed on a 30 m x 0.25 mm x 0.25 µm Rxi-17Sil MS column (50 %-Phenyl-50 % Methyl-polysiloxane) and a 30 m x 0.25 mm x 0.25 µm Rxi-5Sil MS (5 %-Phenyl-95 % Methylpolysiloxane), both from Restek, USA.

The measurements were performed on a HP 6890 Series GC System from Hewlett Packard/Agilent with split/splitless injector (300 °C, 1:100 split ratio) coupled with a BenchTOF-dx Time-Of-Flight Mass Spectrometer (TOF-MS) from Markes, UK. The carrier gas was helium. For injection of 1 µL of each sample a PAL RSI Chronect Robotic autosampler (Axel Semrau, Germany) was used.

The lengths of the columns and the internal diameters were calculated from flow measurements at different inlet pressures and void time measurements. Void times are measured by injections of air and detection of oxygen signal in the TOF-MS. The determined values of the column parameters are shown in Table 1.

Table 1
Determined column properties of the Rxi-17Sil MS and the Rxi-5Sil MS.

Stationary phase	*d* [mm]	d_f [µm]	*L/d*	*L* [m]
Rxi-17Sil MS	0.25	0.25	120,889.6 ± 170.4	30.222 ± 0.043
Rxi-5Sil MS	0.25	0.25	121,606.8 ± 1475.7	30.40 ± 0.37

3.3. Software

Calculations were performed using two Pluto notebooks [31] with the programming language Julia [32] and can be found as html document in the supporting information. For linear and multivariate least-squares fits the package LsqFit.jl was used [33–35]. LSER models were calculated with the generalized linear models package GLM.jl [36]. Simulation of GC separations and chromatograms were performed with the open source Julia package GasChromatographySimulator.jl [7].

3.4. Methods

3.4.1. Isothermal measurements

K-centric retention parameters for FAMEs, PAHs and PCBs were determined from isothermal measurements and using the *K*-centric model, eq. (9). Measurements were performed between 40 °C to 300 °C with incremental steps of 10 °C and a constant carrier gas flow of 1 mL min^{-1}. The *K*-centric data are published in a database. Further details to the measurements can be found there [3]. In order to clarify that the data were collected from isothermal measurements, the index 'iso' was introduced, e.g. $T_{char,iso}$.

3.4.2. LSER prediction

For both separation columns LSER models were calculated in a range between 60 °C and 200 °C with increment steps of 10 °C. 40 selected compounds with a wide range of functional groups are used, see Table 2. Basis was the selection proposed by Poole [20] for a temperature range of 40–140 °C. The LSER solute descriptors of these substances were

Table 2
Solute descriptors of 40 LSER substances from [18].

Compound	E	S	A	B	L
n-Octanal	0.148	0.629	0	0.415	4.364
2-Octanone	0.109	0.661	0	0.509	4.277
Octan-2-ol	0.176	0.413	0.275	0.528	4.335
Benzyl alcohol	0.804	0.872	0.409	0.557	4.248
1,2-Dimethylbenzene	0.663	0.547	0	0.178	3.948
4-Fluoroaniline	0.723	0.958	0.331	0.41	4.063
Phenyl acetate	0.661	1.13	0	0.54	4.414
1-Phenyl ethanol	0.782	0.725	0.424	0.66	4.473
2,6-Dimethylphenol	0.752	0.774	0.413	0.406	4.635
2-Chlorophenol	0.879	0.66	0.535	0.342	4.124
2-Methylphenol	0.772	0.748	0.607	0.355	4.281
Cyclohexanol	0.474	0.638	0.246	0.583	3.722
Methyl hexanoate	0.084	0.566	0	0.47	3.967
Bromobenzene	0.882	0.729	0	0.092	4.038
n-Heptanal	0.14	0.643	0	0.435	3.855
Benzaldehyde	0.813	1.027	0	0.395	4.003
Ethylbenzene	0.613	0.509	0	0.147	3.8
Acetophenone	0.806	1.057	0	0.496	4.488
Methyl benzoate	0.738	0.916	0	0.441	4.681
Styrene	0.845	0.671	0	0.166	3.856
3-Methylphenol	0.776	0.771	0.695	0.339	4.327
Octan-1-ol	0.199	0.464	0.327	0.543	4.635
1,3-Dichlorobenzene	0.852	0.692	0	0.004	4.421
Cyclohexanone	0.403	0.887	0	0.531	3.771
4-Methylphenol	0.828	0.791	0.664	0.364	4.314
1,2-Dichlorobenzene	0.872	0.775	0	0.04	4.507
Linalool	0.325	0.524	0.199	0.693	4.783
Aniline	0.955	1.021	0.239	0.424	3.944
n-Butylbenzene	0.595	0.484	0	0.139	4.75
Heptan-2-one	0.123	0.657	0	0.487	3.789
Nonan-2-one	0.113	0.676	0	0.467	4.764
Nitrobenzene	0.846	1.143	0	0.268	4.53
n-Nonanal	0.121	0.635	0	0.399	4.84
1-Phenyl-2-propanol	0.787	0.782	0.316	0.7	4.835
Hexan-1-ol	0.21	0.432	0.35	0.535	3.646
Chlorobenzene	0.718	0.656	0	0.058	3.622
2-Nitrophenol	0.942	1.107	0.033	0.374	4.731
3,5-Dimethylphenol	0.786	0.799	0.662	0.337	4.759
2-Chloroaniline	1.026	0.991	0.243	0.315	4.685
Phenol	0.776	0.772	0.713	0.317	3.83

found in [18,20] and are shown in Table 2. Temperature-dependent influences on the system coefficients were investigated. For the other investigated substances data were found in the UFZ database (LSERD) [13] and the Wayne State University Experimental Descriptor Database [19].

Using the determined LSER-models for each temperature, ln$k$ values of the investigated FAMEs, PAHs and PCBs were calculated via Eq. (10). After that, the predicted ln k values were used to determine the K-centric retention parameters via curve fit. These retention parameters were labelled with the index 'LSER', as $T_{char,\ LSER}$, $\theta_{char,\ LSER}$ and $\Delta C_{p,\ LSER}$.

For validation, measured chromatograms of a FAME standard mixture were compared to simulations of temperature programmed GC separations using the K-centric retention parameters determined by isothermal measurements on the one hand and predicted ones using the LSER-models on the other hand. The measurements were performed at 5 different initial temperatures (40, 60, 80, 100, 120 °C) and four heating rates (5, 10, 15, 20 °C/min). The PCB Mix was measured at a heating rate of 10 °C/min and an initial temperature of 60 °C.

3.4.3. Computer simulation of GC separations

For the computer simulations of the GC separation the package `GasChromatographySimulation.jl` for the programming language Julia [7,33,37] was used. Detail information about the simulation can be found in the literature [4]. In short, the migration of an analyte along the column as $t(x)$ and the development of the peak variance $\tau^2(x)$ during the migration is governed by the ordinary differential equations (ODEs):

$$\frac{dt}{dx} = \frac{1}{u(x,t)} \qquad (11)$$

$$\frac{d\tau^2}{dx} = \frac{H(x,t)}{u^2(x,t)} + 2\tau^2(x,t)\frac{\partial}{\partial x}\left(\frac{1}{u(x,t)}\right) \qquad (12)$$

with $u(x,t)$ the analyte velocity and $H(x,t)$ the local plate height at the end of the column, $x = L$, the solutions are given as the retention time $t_R = t(L)$ and the peak width $\tau_R = \sqrt{\tau^2(L)}$ (as standard deviation of the peak).

The system of ODEs, eq. (8) and (9), are solved numerically [7,38, 39]. The analyte velocity depends on the velocity of the mobile phase u_m and the retention factor k of the analyte, eq. (13).

$$u = \frac{u_m}{1+k} \qquad (13)$$

Whereby the mobile phase velocity is defined as

$$u_m(x) = \frac{1}{64}\frac{d^2}{\eta L}\frac{p_i^2 - p_o^2}{\sqrt{p_i^2 - \frac{x}{L}\left(p_i^2 - p_o^2\right)}} \qquad (14)$$

with d the column diameter, L the column length, η the viscosity of the mobile phase gas, p_i the inlet pressure and p_o the outlet pressure.

4. Results and Discussion

4.1. LSER model for Rxi-17Sil MS and Rxi-5Sil MS

The determined ln k values for the 40 LSER-calibration-substances can be found in the supplemental materials (Table S2). The determined system constants of the LSER models at different temperatures are shown as a system map, Fig. 1.

It shows that on both columns b tends to be zero for all temperatures, which reduces the multivariate model from five to four system coefficients. This is in accordance to other LSER models that are described for GC separations [18]. It is often discussed in literature [20,40,41] that stationary phases of poly(siloxane) and poly(ethylene glycol), which are commonly used in GC, do not contain hydrogen-bonding acid groups.
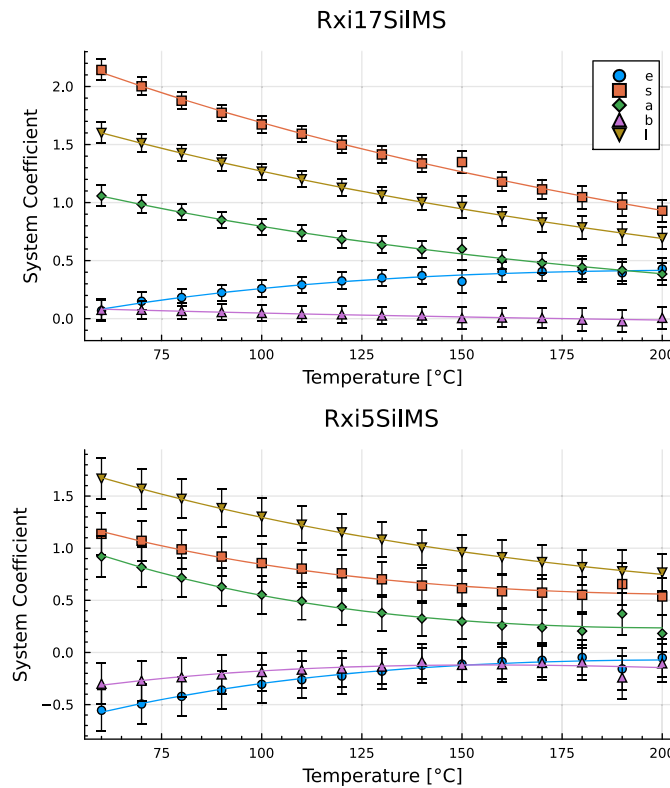
Fig. 1. Determined system coefficients of the LSER models for the Rxi-17Sil MS and Rxi-5Sil MS at different temperatures (system map).

Appendix

Therefore, b is negligible in GC.

A systematic temperature dependence of the coefficients can be estimated. Similar dependencies are also observed elsewhere [14,18]. Each system constant i can be described as a function f_i of Temperature T e.g. with Clarke and Glew's thermodynamic 3-parameter model given in eq. (5), (ABC-model) [23].

$$f_i(T) = \alpha_i + \frac{\beta_i}{T} + \gamma_i \ln T \tag{15}$$

The ABC model is a common approach to describe temperature dependencies of Gibbs-energy related quantities. It is an extension of the classic van't Hoff model [6,23]. The results of the curve fit and the coefficient of determination for each system constant is given in Table 3. Regarding on the data in this case, the ABC model is rather recommended for interpolation than for extrapolation. The function has an extremum at β_i / γ_i: e.g. the value of s (Rxi-5Sil MS) will decrease until 216 °C and then increase again, but this is not to be expected in a physico-chemical context. In contrast to polynomial curve fits proposed elsewhere [18], the ABC model offers an opportunity for a deeper thermodynamic understanding of the system constants and its contribution to enthalpy ΔH and entropy ΔS.

With the temperature model of the system constants the LSER model eq. (10) becomes

$$\ln k = \sum_i \left(\alpha_i + \frac{\beta_i}{T} + \gamma_i \ln T \right) I_i + c$$
$$= \left(\alpha_e + \frac{\beta_e}{T} + \gamma_e \ln T \right) E + \left(\alpha_s + \frac{\beta_s}{T} + \gamma_s \ln T \right) S + \ldots \tag{16}$$

with system constants $i = e, s, a, b, l$ and solute descriptors $I_i = E, S, A, B, L$.

In combination with the solute descriptors I, for each interaction term eE, sS, aA, bB or lL eqs. (7) and (8) can be used to determine the partition of entropy and enthalpy of the several solute interactions.

$$\Delta H_I = R(\gamma_I T_{ref} - \beta_I) + R\gamma_I (T - T_{ref}) \tag{17}$$

$$\Delta S_I = R\left(\alpha_I + \gamma_I + \gamma_I \ln \frac{T_{ref}}{T_1} \right) + R\gamma_I \ln \frac{T}{T_{ref}} \tag{18}$$

whereby $\alpha_I = \alpha_i I$, $\beta_I = \beta_i I$, $\gamma_I = \gamma_i I$.

The sum of all enthalpies ΔH_I and entropies ΔS_I should be equal to the overall ΔH and ΔS of the gas chromatographic distribution of the solute at a given temperature. For $T = T_{ref}$ the several ΔH_I and ΔS_I were calculated for 92 compounds, with descriptors from WSU, on both stationary phases and can be found in the supplemental materials (Table S3). For T_{ref} a value of 90 °C was chosen as literature data i are available for this temperature[3,42]. The sums of the entropies and enthalpies are in the same order of magnitude as data from isothermal measurements ΔH_{ref} and ΔS_{ref} for of a Rxi-5SilMS and a Rxi-17Sil MS column found in [3]. The median of the relative differences for ΔH_{ref} is 8 % and for ΔS_{ref} it is −1 % on the Rxi-5Sil MS. On the Rxi-17Sil MS ΔH_{ref} has a relative difference of 2 % and ΔS_{ref} of −8 %. Higher deviations can be observed for less volatile compounds. It should be mentioned, that the LSER models characterise the two columns only up to 200 °C. This might be an explanation for the uncertainty, as the range is too low for the less volatiles. The same applies to the chosen value of T_{ref}. For many

substances, e.g. Anthracene, $\Delta H_A = 0$ because the A descriptor is also zero. Compared to the other interactions, the values of ΔH_E are positive for all compounds on both phases. For n-alkanes, n-alcohols and ketones ΔH_L has the highest impact on ΔH_{ref}.

In the next step the temperature-dependent system coefficients will be used to predict the ln k values for different temperatures.

4.2. Prediction of K-centric retention parameters by LSER models

The LSER models where used to predict the logarithm of the retention factor at different temperatures.

Fig. 2 shows the ln k over T diagrams of Naphthalene, Benzo[a] pyrene, PCB 101, PCB 153, Methyl palmitate and Methyl butyrate including the isothermal determined ln k values and fit curves of the K-centric 3-parameter model. More plots can be found in the supplemental materials (Figure S1-S418). In most cases the fit curves of the K-centric model determined by retention factors coming from the LSER model are very close to the isothermal determined curves. For methyl butyrate e.g., the curves deviate at temperatures larger than 200 °C.

The K-centric parameters of all substances determined by isothermal measurement and predicted values by the LSER Models are shown in the supplemental materials (Table S1). Fig. 3 shows the difference of T_{char} predicted by LSER to the isothermal determinations. The relative difference between the predicted values of the retention parameters and the isothermal determinations are shown in the Boxplots in Fig. 4. For the prediction of the characteristic temperature T_{char}, the values resulting by the LSER models are close to the values calculated by isothermal measurements for both investigated GC columns. For the Rxi-17Sil MS the relative differences are about −3.95 to + 7.81 % (median= 1.27 %), for the Rxi-5SilMS -7.91 to 6.31 % (median = −0.91 %). Similar to the deviation of the ln k values there is also an increasing difference observed above 200 °C, especially for the Rxi17-Sil MS and for the data from LSERD. It is the nature of curve fit models that the fit results are better for interpolation than for extrapolation (here above 200 °C). For the determination of the characteristic temperature it is recommended to choose interpolation around ln $k = 0$ and so temperature T becomes T_{char} [3]. Estimations for less volatiles such as PCBs or PAHs show consequently higher deviations than for high volatiles.

The predicted θ_{char} and ΔC_p values show a larger deviation compared to the isothermal determinations. It is mentioned that ΔC_p also shows large variance by data from isothermal measurements and it is the less important parameter of the K-centric model [3]. Regarding the good prediction performance of the K-centric models it is possible that the deviation of θ_{char} and ΔC_p compensate each other which results in an acceptable prediction of ln k values.

Because there is a strong correlation between the T_{char} and the elution temperature [10] this procedure for prediction of the retention parameter using LSER models is also suitable to estimate the elution order respectively the elution temperature T_{elu}. This is important since the dependence between T_{char} and T_{elu} is influenced by heating rates. If there is a composition of different analytes and it is possible to estimate the T_{char} values it is also possible to estimate a heating rate which is suitable to solve the separation problem - only by substance specific data from databases without any test measurement. [10]

Table 3

Temperature dependence of the of the system constants e, s, a, b and l described by the ABC-model.

| System constant	Rxi-17Sil MS				Rxi-5Sil MS			
	α	β	γ	R^2	α	β	γ	R^2
e	30.1860	−2012.14	−4.14284	0.972171	49.1784	−3278.11	−6.87110	0.972112
s	−2.79802	1389.00	0.128983	0.99563	−50.8750	3500.20	7.14962	0.976791
a	−10.5530	1281.05	1.33651	0.996609	−69.1351	4608.02	9.68143	0.96762
b	−0.104547	98.3015	−0.0187212	0.934622	39.1624	−2387.19	−5.56258	0.757357
l	−2.02266	1055.74	0.0782387	0.999584	−24.6434	2354.67	3.31450	0.999218
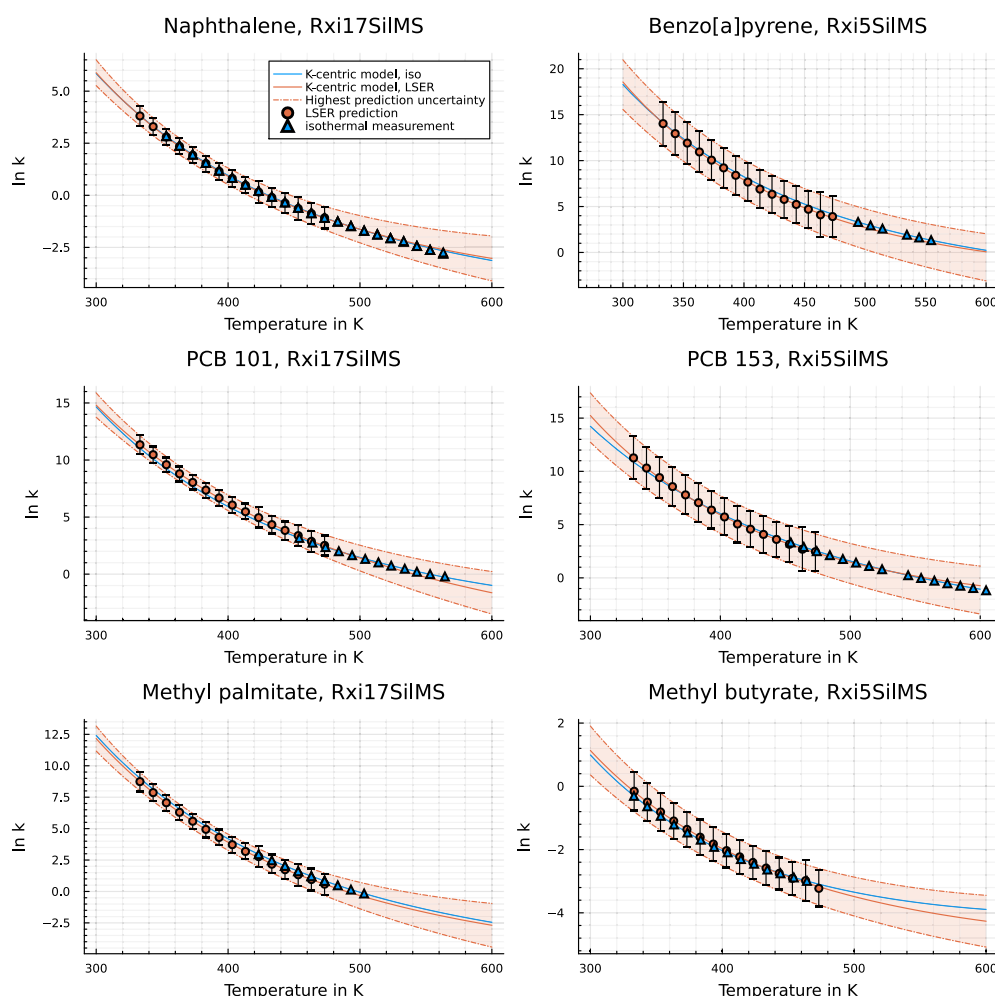
5

Fig. 2. Predicted ln k values for each temperature using the LSER models (orange, circle) and isothermal determined values (blue, triangle) and curve fit of the K-centric model for different compounds. The orange shadow indicates the prediction uncertainty by using the error bars for the curve fit.

4.3. Simulations of GC chromatograms

Detailed results from the simulations can be found in the supplemental materials. Fig. 5 shows the chromatogram of a measurement of 37 fatty acid methyl esters compared to the simulations using the K-centric parameters of both estimation approaches. Both simulations demonstrate good accordance to the measurement, whereby the isothermal parameters offer the best prediction. The root-mean-square-errors (RMSE), as parameters of the simulation performance have the value of 0.0345 min (for isothermal parameters) and 0.4753 min (for LSER parameters). Similar results can be observed for the simulation of a separation of 6 PCBs, where the RMSE for the simulation with isothermal parameters is 0.0880 min and with LSER approach it is 0.4403 min, Fig. 6. The chromatograms of the remainly validation measurements can be found in the supplemental materials (Figure S419-S460). They show similar simulation performances. The average RMSE for the simulation with the isothermal retention parameters is 0.1268 min in contrast to the average RMSE for the LSER parameters of RMSE= 0.5136 min. Fig. 7 presents the relative difference between the measured retention times and predicted values for both stationary phases over all measurements. The best results are obtained for the isothermal parameters. For most measurements the relative differences compared to the simulation are between ±5 % when using the isothermal retention

parameters. For Rxi-5Sil MS the median is −0.3 % and for the Rxi-17Sil MS it is −0.6 %. Using the LSER estimations results in a relative difference of −3.4 to 7.5 % on the Rxi-5Sil MS (median= 0.2 %). On the Rxi-17Sil MS the simulation underestimates the retention time and shows a larger range of the difference from –10.9 to + 0.65 % (median=−5.2). One reason for the better performance of the simulations with isothermal parameters could be that the K-centric parameters calculated with LSER also show higher deviations. Uncertainties in the LSER descriptors themselves would exacerbate this problem. For example, in the LSERD descriptor database [14], there are many values for the same substances and no indication of which data can be considered reliable and which cannot.

However, the predicted parameters via LSER can be recommended for first estimations and simulations during the method development process. In most cases the final optimization of a GC separation method has to be performed on the GC system. Start values for the GC method might be a benefit for the optimisation of complex mixtures e.g. essential oils. The simulation is valid and reliable for FAMEs with about 40 compounds. Predictions for 80 allergenic fragrances have been shown previously [3]. Limitations of the simulation are given by the quality of the input data. e.g. the thermodynamic parameters. Furthermore, the quality of the GC system is also important: reliability of the diameter, length and phase ratio. Blumberg [5] has shown that the ageing of the
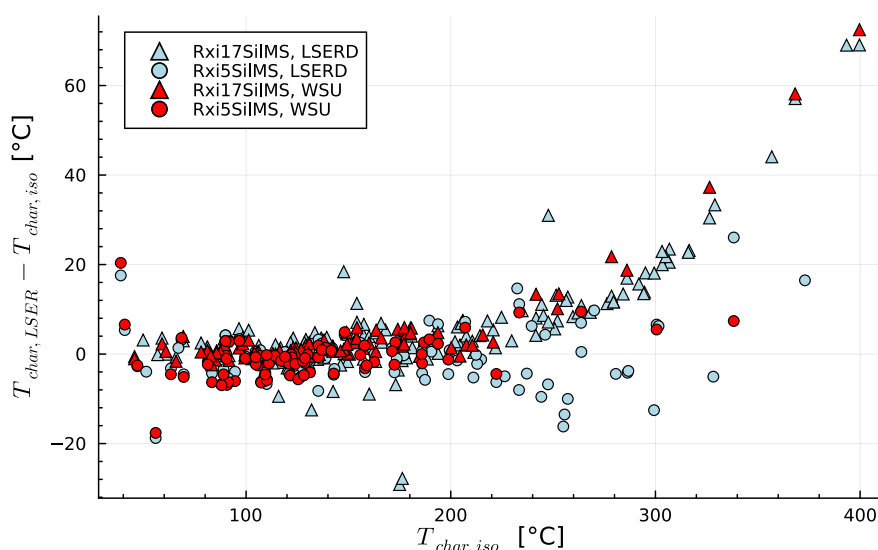
Fig. 3. Difference between the prediction of the characteristic temperature via LSER and isothermal determination sorted by stationary phase and data source.
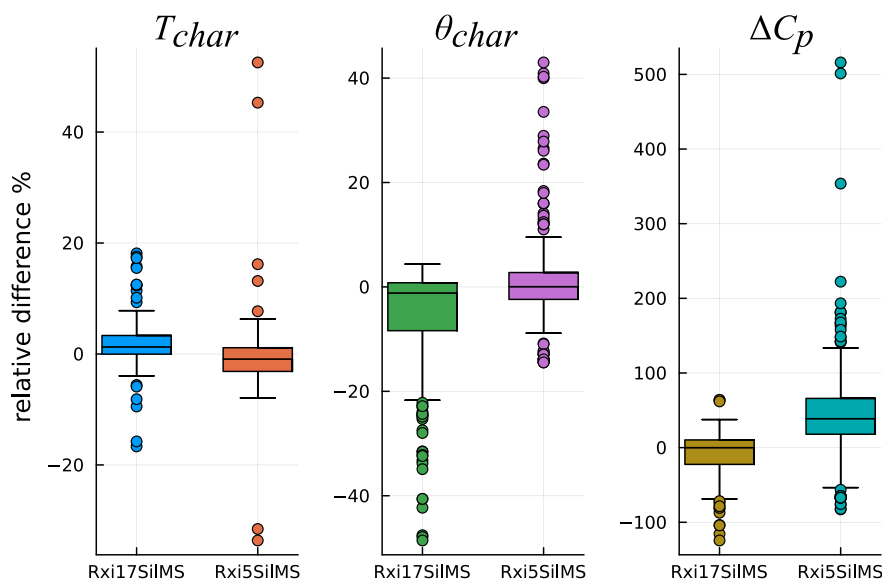
Fig. 4. Boxplots of the relative differences for each retention parameter T_{char}, θ_{char} and ΔC_p between the isothermal determined and the predicted values for both stationary phases.

column can change the stationary phase and thus the previous thermodynamic parameters are no longer correct. However, the procedure using the LSER models is less elaborated compared to conventional isothermal measurements as described above.

Some further investigations based on this work can be possible: LSER descriptors can be used to predict the *K*-centric parameters directly via multiple linear regression without the prediction of ln *k* values such as it can be used for the prediction of the retention index *RI* [15,43] Other approaches can link the LSER descriptor data to the *K*-centric data using graphical neural networks, similar to approaches for prediction of *RI*.

A benefit for other research areas than GC separation can be another approach by inversion of the regression. With the computer simulation of GC simulations it is even possible to estimate the LSER substance descriptors of a compound from temperature programmed measure-

ments similar to the estimation of the *K*-centric parameters by Leppert [9]. This data then are available for other LSER research such as environmental chemistry. There are substance classes whose solute descriptors are unknown, e.g. triacyl glycerides.

5. Conclusion

In this work the LSER system constants of two stationary phases at different temperatures were determined. The temperature impact on each system constant can be described with the ABC-model. For each system-constant-descriptor-interaction enthalpies and entropies could be calculated. Furthermore, the LSER models were used to predict the three parameters of the *K*-centric 3-parameter retention model. Simulations of temperature programmed GC separations using the predicted
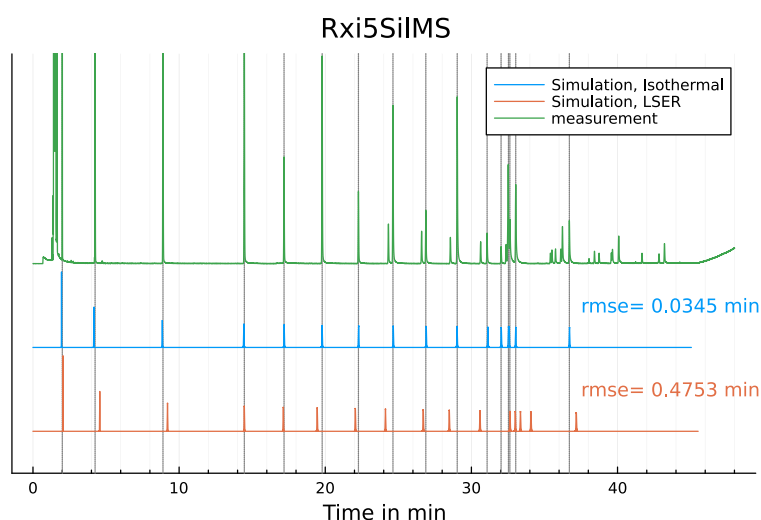
Fig. 5. Measured Chromatograms (green) of the FAMEs Mix compared to simulation using the isothermal determined retention parameters (blue) and using the retention parameters predicted by the LSER models (orange). GC settings: $T_{init} = 60$ °, Heating Rate= 5 °C/min.
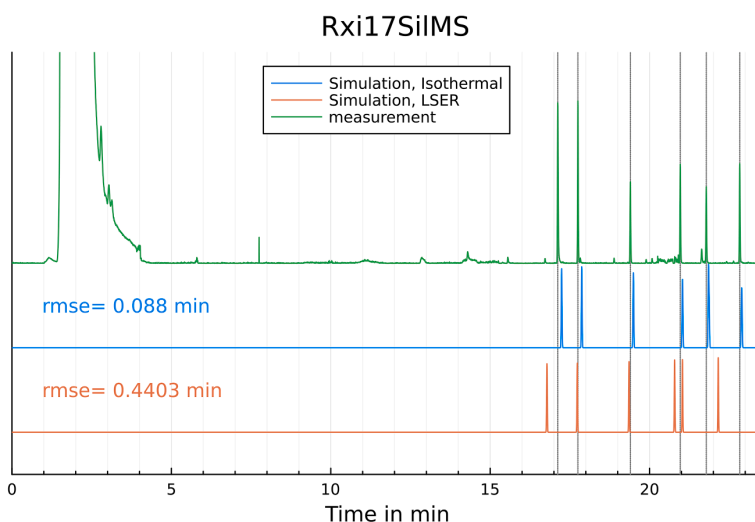
Fig. 6. Measured Chromatograms (green) of 6 PCBs compared to simulation using the isothermal determined retention parameters (blue) and using the retention parameters predicted by the LSER model (orange). GC settings: $T_{init} = 60$ °, Heating Rate= 10 °C/min.

retention parameters were demonstrated. The procedure can reduce the workload for the chromatographer during the optimization process since there is just a small number of substances, which has to be measured by isothermal measurements to calibrate the system.

The values of the predicted parameters are close to measured values given by isothermal measurements. LSER models can be used for the estimation of the characteristic temperature T_{char} and the elution order of the substances on the column, by literature data only.

Predicted T_{char} can also be used as start value for the determination of K-centric parameters from temperature programmed measurements [9]. For estimation of K-centric parameters by LSER data further approaches e.g. using graph neural networks can be investigated.

Using the simulation, LSER data from the literature also are suitable to recommend first temperature programs for a GC separation and can support the method development process. In addition, with machine learning the approach can be integrated into a workflow for a self-optimization of GC separations similar to liquid chromatography [44,

45]. Regarding on benefits for other research e.g. environmental research the link between the K-centric model and the LSER model can help to determine the LSER descriptors by temperature programmed measurements using the simulation software [9].

CRediT authorship contribution statement

Tillman Brehmer: Conceptualization, Data curation, Formal analysis, Investigation, Methodology, Software, Validation, Visualization, Writing – original draft. **Benny Duong:** Investigation. **Peter Boeker:** Funding acquisition, Project administration, Resources, Supervision. **Matthias Wüst:** Resources, Supervision, Writing – review & editing. **Jan Leppert:** Conceptualization, Data curation, Investigation, Methodology, Project administration, Software, Validation, Visualization, Writing – original draft.

Appendix
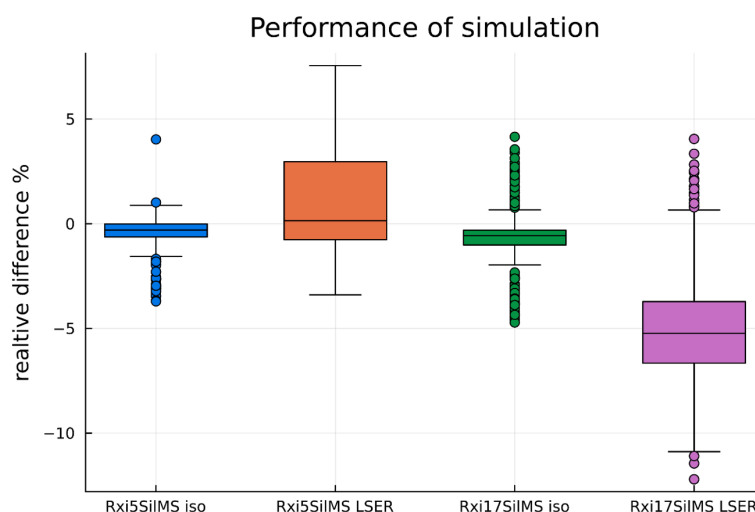
Fig. 7. Relative difference between the measured retention times of the FAMES and the simulated retention times using the isothermal retention parameters (iso) and the retention parameters estimated by the LSER models for both stationary phases.

Declaration of competing interest

The authors declare the following financial interests/personal relationships which may be considered as potential competing interests: Tillman Brehmer reports financial support was provided by German Research Foundation. Jan Leppert reports financial support was provided by German Research Foundation. If there are other authors, they declare that they have no known competing financial interests or personal relationships that could have appeared to influence the work reported in this paper.

Data availability

Data will be made available on request.

Acknowledgement

Supplementary materials

Supplementary material associated with this article can be found, in the online version, at doi:10.1016/j.chroma.2024.464665.

References

[1] K. Jurica, I. Brčić Karačonji, D. Lasić, D. Bursać Kovačević, P. Putnik, Unauthorized Food Manipulation as a Criminal Offense: Food Authenticity, Legal Frameworks, Analytical Tools and Cases, Foods 10 (2021), https://doi.org/10.3390/foods10112570.

[2] Y. Nolvachai, C. Kulsing, P.J. Marriott, Multidimensional gas chromatography in food analysis, TrAC Trends in Analytical Chemistry 96 (2017) 124–137, https://doi.org/10.1016/j.trac.2017.05.001.

[3] T. Brehmer, B. Duong, L. Friedemann, P.J. Faust, P. Boeker, M. Wüst, J. Leppert, Retention Database for Prediction, Simulation, and Optimization of GC Separations, ACS Omega, 2023, https://doi.org/10.1021/acsomega.3c01348.

[4] J. Leppert, P.J. Müller, M.D. Chopra, L.M. Blumberg, P. Boeker, Simulation of spatial thermal gradient gas chromatography, J. Chromatogr. A 1620 (2020) 460985, https://doi.org/10.1016/j.chroma.2020.460985.

[5] L.M. Blumberg, Chromatographic parameters: Characteristic parameters of solute retention - an insightful description of column properties, J. Chromatogr. A 1685 (2022) 463594, https://doi.org/10.1016/j.chroma.2022.463594.

[6] L.M. Blumberg, Distribution-centric 3-parameter thermodynamic models of partition gas chromatography, J. Chromatogr. A 1491 (2017) 159–170, https://doi.org/10.1016/j.chroma.2017.02.047.

[7] J. Leppert, GasChromatographySimulator.jl, Journal of Open Source Software 7 (2022) 4565, https://doi.org/10.21105/joss.04565.

[8] P. Boeker, J. Leppert, Flow field thermal gradient gas chromatography, Anal. Chem. 87 (2015) 9033–9041, https://doi.org/10.1021/acs.analchem.5b02227.

[9] J. Leppert, T. Brehmer, M. Wüst, P. Boeker, Estimation of retention parameters from temperature programmed gas chromatography, J. Chromatogr. A 464008 (2023), https://doi.org/10.1016/j.chroma.2023.464008.

[10] T. Brehmer, P. Boeker, M. Wüst, J. Leppert, Relation between characteristic temperature and elution temperature in temperature programmed gas chromatography - part I: Influence of initial temperature and heating rate, J. Chromatogr. A 1707 (2023) 464301, https://doi.org/10.1016/j.chroma.2023.464301.

[11] V.I. Babushok, P.J. Linstrom, J.J. Reed, I.G. Zenkevich, R.L. Brown, W.G. Mallard, S.E. Stein, Development of a database of gas chromatographic retention properties of organic compounds, J. Chromatogr. A 1157 (2007) 414–421, https://doi.org/10.1016/j.chroma.2007.05.044.

[12] T. Acree, H. Arn, Flavornet, 2004. https://www.flavornet.org/flavornet.html. accessed 20 September 2023.

[13] N. Ulrich, S. Endo, T.N. Brown, N. Watanabe, G. Bronner, M.H. Abraham, K.-U. Goss, UFZ-LSER database v 3.2, 2017. http://www.ufz.de/lserd. accessed 28 October 2021.

[14] C.F. Poole, Solvation parameter model: Tutorial on its application to separation systems for neutral compounds, J. Chromatogr. A 1645 (2021) 462108, https://doi.org/10.1016/j.chroma.2021.462108.

[15] N. Ulrich, G. Schüürmann, W. Brack, Prediction of gas chromatographic retention indices as classifier in non-target analysis of environmental samples, J. Chromatogr. A 1285 (2013) 139–147, https://doi.org/10.1016/j.chroma.2013.02.037.

[16] M.H. Abraham, R.A. McGill, P.L. Grellier, Determination of olive oil–gas and hexadecane–gas partition coefficients, and calculation of the corresponding olive oil–water and hexadecane–water partition coefficients, J. Chem. Soc., Perkin Trans. 2 (1987) 797–803, https://doi.org/10.1039/P29870000797.

[17] P. Siriviboon, C. Tungkaburee, N. Weerawongphrom, C. Kulsing, Direct equations to retention time calculation and fast simulation approach for simultaneous material selection and experimental design in comprehensive two dimensional gas chromatography, J. Chromatogr. A 1602 (2019) 425–431, https://doi.org/10.1016/j.chroma.2019.05.059.

[18] C.F. Poole, Gas chromatography system constant database over an extended temperature range for nine open-tubular columns, J. Chromatogr. A 1590 (2019) 130–145, https://doi.org/10.1016/j.chroma.2019.01.028.

[19] C.F. Poole, Wayne State University experimental descriptor database for use with the solvation parameter model, J. Chromatogr. A 1617 (2020) 460841, https://doi.org/10.1016/j.chroma.2019.460841.

[20] C.F. Poole, Selection of calibration compounds for selectivity evaluation of wall-coated, open-tubular columns for gas chromatography by the solvation parameter model, J. Chromatogr. A 1629 (2020) 461500, https://doi.org/10.1016/j.chroma.2020.461500.

[21] L.M. Blumberg, Temperature-programmed gas chromatography, Wiley-VCH, Weinheim, 2010.

[22] J.G. Speight (Ed.), Reaction mechanisms in environmental engineering: Analysis and prediction, Butterworth-Heinemann an imprint of Elsevier, Kidlington, Oxford, United Kingdom, 2018.

9

[23] E.C.W. Clarke, D.N. Glew, Evaluation of thermodynamic functions from equilibrium constants, Transactions of the Faraday Society 62 (1966) 539, https://doi.org/10.1039/tf9666200539.

[24] M.H. Abraham, C.F. Poole, S.K. Poole, Classification of stationary phases and other materials by gas chromatography, J. Chromatogr. A 842 (1999) 79–114, https://doi.org/10.1016/S0021-9673(98)00930-3.

[25] C.F. Poole, T.O. Kollie, Interpretation of the influence of temperature on the solvation properties of gas chromatographic stationary phases using Abraham's solvation parameter model, Anal. Chim. Acta 282 (1993) 1–17, https://doi.org/10.1016/0003-2670(93)80347-N.

[26] H.C. Tülp, K.-U. Goss, R.P. Schwarzenbach, K. Fenner, Experimental determination of LSER parameters for a set of 76 diverse pesticides and pharmaceuticals, Environ. Sci. Technol. 42 (2008) 2034–2040, https://doi.org/10.1021/es702473f.

[27] A.B. Strobel, T. Egert, P. Langguth, Predicting Leachables Solubilization in Polysorbate 80 Solutions by a Linear Solvation Energy Relationship (LSER), Pharm. Res. 38 (2021) 1549–1561, https://doi.org/10.1007/s11095-021-03096-8.

[28] C.F. Poole, S.N. Atapattu, S.K. Poole, A.K. Bell, Determination of solute descriptors by chromatographic methods, Anal. Chim. Acta 652 (2009) 32–53, https://doi.org/10.1016/j.aca.2009.04.038.

[29] M.H. Abraham, A. Ibrahim, A.M. Zissimos, Determination of sets of solute descriptors from chromatographic measurements, J. Chromatogr. A 1037 (2004) 29–47, https://doi.org/10.1016/j.chroma.2003.12.004.

[30] C.F. Poole, T.C. Ariyasena, N. Lenca, Estimation of the environmental properties of compounds from chromatographic measurements and the solvation parameter model, J. Chromatogr. A 1317 (2013) 85–104, https://doi.org/10.1016/j.chroma.2013.05.045.

[31] F. van der Plas, M. Dral, P. Berg, Π. Γεωργακόπουλος, R. Huijzer, N. Bochenski, A. Mengali, B. Lungwitz, C. Burns, H. Priyashan, J. Ling, E. Zhang, F.S.S. Schneider, I. Weaver, S.Kadowaki Rogerluo, Z. Wu, J. Gerritsen, R. Novosel, Z.Moon Supanat, M.Abbott luis-mueller, N. Bauer, P. Bouffard, S. Terasaki, S. Polasa, TheCedarPrince, Pluto.jl (2022), https://doi.org/10.5281/zenodo.7226553.

[32] J. Bezanson, A. Edelman, S. Karpinski, V.B. Shah, Julia: A Fresh Approach to Numerical Computing, SIAM Review 59 (2017) 65–98, https://doi.org/10.1137/141000671.

[33] J.M. White, P.K. Mogensen, B. Johnson, J. Li, C. McBride, M. Lubin, J. Weidner, Y. Yu, B. Arthur, A. Arslan, M. Zaffalon, I. Dunning, R. Arutjunjan, T. Holy, A. Noack, G. Datseris, A. Sakai, B. Legat, T. Sampson, A. Singhvi, T. Lienart, C. Rackauckas, Q. Zhang, Jérémy Affan, K. Thelate, T. Kelman, J. Omotani, J. Assländer, F. Zierler, N. Ignatiadis, V. Martinek, A. Sengupta, I. Butterworth, LsqFit.jl, 2012. https://github.com/JuliaNLSolvers/LsqFit.jl. accessed 22 January 2024.

[34] D.W. Marquardt, An Algorithm for Least-Squares Estimation of Nonlinear Parameters, Journal of the Society for Industrial and Applied Mathematics 11 (1963) 431–441, https://doi.org/10.1137/0111030.

[35] K. Levenberg, A Method for the Solution of Certain Non-Linear Problems in Least Squares, Quarterly of Applied Mathematics 2 (1944) 164–168.

[36] D. Bates, A. Noack, S. Kornblith, M. Bouchet-Valat, M.K. Borregaard, A. Arslan, J. M. White, D. Kleinschmidt, P. Alday, G. Lynch, I. Dunning, P.K. Mogensen, S. Lendle, D. Aluthge, pdeffebach, J.B.S. Calderón, A. Patnaik, B. Born, B. Setzler, C. DuBois, J. Quinn, M. Dutta, O. Slámečka, P. Bastide, V.B. Shah, A. Blaom, B. König, B. Kamiński, GLM. jl, 2023. https://doi.org/10.5281/Zenodo.7734970.

[37] P.K. Mogensen, A.N Riseth, Optim: A mathematical optimization package for Julia, Journal of Open Source Software 3 (2018) 615, https://doi.org/10.21105/joss.00615.

[38] C. Rackauckas, Q. Nie, DifferentialEquations.jl – A Performant and Feature-Rich Ecosystem for Solving Differential Equations in Julia, JORS 5 (2017) 15, https://doi.org/10.5334/jors.151.

[39] J. Leppert, L.M. Blumberg, M. Wüst, P. Boeker, Simulation of the effects of negative thermal gradients on separation performance of gas chromatography, J. Chromatogr. A (2021) 461943, https://doi.org/10.1016/j.chroma.2021.461943.

[40] C.F. Poole, Gas chromatography system constant database for 52 wall-coated, open-tubular columns covering the temperature range 60-140 °C, J. Chromatogr. A 1604 (2019) 460482, https://doi.org/10.1016/j.chroma.2019.460482.

[41] S.D. Martin, C.F. Poole, M.H. Abraham, Synthesis and gas chromatographic evaluation of a high-temperature hydrogen-bond acid stationary phase, J. Chromatogr. A 805 (1998) 217–235, https://doi.org/10.1016/S0021-9673(98)00007-7.

[42] T.M. McGinitie, B.R. Karolat, C. Whale, J.J. Harynuk, Influence of carrier gas on the prediction of gas chromatographic retention times based on thermodynamic parameters, J. Chromatogr. A 1218 (2011) 3241–3246, https://doi.org/10.1016/j.chroma.2010.09.068.

[43] P. Kakanopas, P. Janta, S. Vimolmangkang, F. Hermatasia, C. Kulsing, Retention index based approach for simulation of results and application for validation of compound identification in comprehensive two-dimensional gas chromatography, J. Chromatogr. A 1679 (2022) 463394, https://doi.org/10.1016/j.chroma.2022.463394.

[44] J. Boelrijk, B. Ensing, P. Forré, B.W.J. Pirok, Closed-loop automatic gradient design for liquid chromatography using Bayesian optimization, Anal. Chim. Acta 1242 (2023) 340789, https://doi.org/10.1016/j.aca.2023.340789.

[45] J. Boelrijk, B. Pirok, B. Ensing, P. Forré, Bayesian optimization of comprehensive two-dimensional liquid chromatography separations, J. Chromatogr. A 1659 (2021) 462628, https://doi.org/10.1016/j.chroma.2021.462628.

D. List of abbreviations

^1D	first dimension, first column in GC×GC
^2D	second dimension, second column in GC×GC
ABC model	thermodynamic three-parameter-model of Clark and Glew
AI	artificial intelligent
BETX	standard mixture containing benzene, ethylbenzene, toluene, *o*-xylene, *m*-xylene , *p*-xylene
DFG	German Research Foundation
DOE	design of experiment
EI	electron ionisation
FAME	fatty acid methyl ester
FFTGGC	flow field thermal gradient gas chromatography
FID	flame ionisation detectors
GC	gas chromatography
GC×GC	comprehensive two dimmensionalgas chromatography
GC-ToF-MS	gas chromatography coupled with time of flight mass spectrometry
GLC	gas-liquid-chromatography
HETP	height equivalent to a theoretical plate
HPLC	high performance liquid chromatography
K-centric model	distributive centric three-parameter model, Blumberg's model
LC	liquid chromatography
LES	linear elution strength
LSER	linear solvation energy relationship, Abraham's model
LSERD	LSER database of UFZ
MDGC	multidimensional gas chromatography
ML	machine learning
MS	mass spectrometry
NIST	National Institute of Standards and Technology
ODE	ordinary differential equation
PAH	polyaromatic hydrocarbon
PCA	principal compound analysis
PCB	polychlorinated biphenyl
PLSDA	partial least square discriminant analysis
RF	random Forest
RI	retention index
rmse	root mean square error
SVM	support vector machines
ToF-MS	time of flight mass spectrometry
UFZ	Helmholtz Centre for Environmental Research
VOC	volatile organic compound
WCOT	wall-coated-open-tubular
WSU	Wayne State University

E. List of symbols

chromatographic quantities

t_R	retention time
t_M	void time
L	column length
d	inner diameter
p_i, p_o	inlet and outlet pressure
η	viscosity of the carrier gar
F	volume flow

R_T	heating rate
r_T	dimensionless heating rate
$R_{T,0}, r_{T,0}$	heating rate where $T_{elu}=T_{char}$
$t_{M,ref}$	reference void time
θ_{ref}	average thermal constant
T_{init}	initial temperature
T_{elu}	elution temperature

V_m, V_s	volume of the mobile phase and the stationary phase
d_f, d_c	film thickness and column diameter
β	phase ratio
k	retention factor
K	distribution coefficient
RI	retention index
m/z	mass-to-charge-ratio

Van Deemter equation

$\bar{H}$	height of a theoretical plate
N	number of theoretical plates
$\bar{A}$	Eddy-diffusion term
$\bar{B}$	longitudinal diffusion term
$\bar{C}$	mass transfer term
$\bar{u}$	average mobile phase velocity

Simulation

x	Position
σ	spatial band width

τ_R	peak width
H	local plate height
u_m	velocity of the mobile phase
u	analyte velocity

thermodynamic quantities

T	temperature
ΔG	Gibbs free energy
ΔH	enthalpy
ΔS	entropy

R	molar gas constant
ΔC_p	change of the isobaric molar heat capacity

T_{ref}	reference temperature
$\Delta H_{ref}, \Delta S_{ref}$	enthalpy, entropy at $T = T_{ref}$

T_{char}	characteristic temperature
θ_{char}	characteristic thermal constant
$\Delta H_{char}, \Delta S_{char}$	enthalpy, entropy at $T = T_{char}$

A, B, C	empirical retention parameters for Clark and Glew retention model (ABC-model)

LSER quantities

E, S, A, B, L	solute descriptors
e, s, a, b, l, c	system constants
I_R	refractive index
V	characteristic volume

F. List of figures

G. List of tables

H. List of equations

Acknowledgements

Zusammenfassung

Flüchtige chemische Verbindungen sind in unserem Alltag allgegenwertig. Ein Teil von ihnen ist z.B. für den wahrnehmbaren Geruchseindruck der Lebensmittel und deren Authentizität verantwortlich, andere spielen bei der Entstehung gesundheitlicher Risiken eine Rolle. Eine Technik zur Untersuchung und Bestimmung flüchtiger Verbindungen ist die Gaschromatographie (GC). Mit steigendem Schutzniveau im Umwelt-, Gesundheits- und Verbraucherschutz wächst der Bedarf an Untersuchungsmethoden flüchtiger Verbindungen. Die Entwicklung neuer Messmethoden ist oftmals ressourcen-, zeit- und kostenintensiv. Eine geeignete Computersimulation kann die Entwicklung neuer Messmethoden optimieren. Für eine solche Simulation sind Rechenmodelle notwendig, die einerseits die Wechselwirkung der flüchtigen Verbindungen beschreiben sowie das gaschromatographische System abbilden.

Die Vorliegende Arbeit gibt zunächst eine Einführung in das Messprinzip und den Aufbau eines Gaschromatographen und eine Übersicht über die notwendigen Modelle zur Beschreibung der Wechselwirkung der Analyten und zur Vorhersage gaschromatographischer Trennungen. Da für das Simulationsmodell entsprechende Daten zur Beschreibung bzw. Bestimmung der Retention benötigt werden, beschäftigen sich die drei vorgestellten Untersuchungen mit der Bestimmung und Abschätzung dieser Retentionsdaten.

Im Rahmen der ersten Studie wurde eine umfangreiche Datenbank mit thermodynamischen Retentionsparametern für eine Vielzahl von flüchtigen Verbindungen aufgebaut (u.a. für FAMEs, Triglyceride, PAHs, PCBs und allergene Duftstoffe). Für 900 Kombinationen von rund 320 Subtanzen auf insgesamt 20 verschiedenen stationären Phasen wurden Retentionsfaktoren aus isothermen Messungen bestimmt und die Parameter für die bekannten Retentionsmodelle (ABC-Modell, K-zentrisches Modell, thermodynamisches Modell) bestimmt. Neben eigens bestimmten Daten wurden auch verfügbare Daten aus der Literatur eingepflegt. Dabei wurde ein standardisiertes Vorgehen zur Bestimmung der Parameter präsentiert und Qualitätskriterien für geeignete Retentionsparameter festgelegt. Der Simulation gaschromatographischer Trennungen unter Verwendung der Retentionsparameter der Datenbank wurden reale temperaturprogrammierte Messungen gegenübergestellt. Die relative Abweichung der Simulation betrug dabei größtenteils <1 %.

In der zweiten Studie wurde der Zusammenhang zwischen der messbaren Elutionstemperatur und der charakteristischen Temperatur untersucht. Die charakteristische Temperatur ist der wichtigste Retentionsparameter im „verteilungszentrischen Retentionsmodell" (K-zentrisches Modell) nach Blumberg. Einflüsse des Temperaturprogramms durch die Starttemperatur und die Heizrate wurden untersucht. Mithilfe des Datensatzes konnte ein Rechenmodell aufgestellt werden, welches eine Abschätzung der charakteristischen Temperatur aus einfachen temperaturprogrammierten Messungen ermöglicht. Dies erweitert insbesondere für leichtflüchtige Verbindungen wie z.B. BETX-Verbindungen oder Aldehyde und Ketone den Vorhersagebereich verglichen mit bisherigen Schätzmodellen. Die Vorhersage von Retentionszeiten basierend auf dem Regressionsmodell konnte am Beispiel von Alkoholen und Phenonen demonstriert werden.

In der dritten Studie wurde der Ansatz des „Linear Solvation Energy Relationship"-Modells (LSER) genutzt, um für die Simulationssoftware nutzbare „K-zentrische" Retentionsparameter aus LSER-Stoffdaten abzuschätzen. Zwei stationäre Phasen konnten mittels LSER charakterisiert werden. Für ca. 300 Verbindungen konnten K-zentrische Retentionsparameter geschätzt werden und die Daten mit den Parametern aus isothermen Messungen verglichen werden. Simulationen temperaturprogrammierter GC Trennungen unter Verwendung der mittels LSER ermittelten Retentionsparameter wurden mit isothermen Retentionsparametern verglichen und realen Messungen gegenübergestellt. Die Simulation mit isothermen Parametern stimmte dabei >95 % mit realen Messungen überein. Die Übereinstimmung der Simulation basierend auf LSER-Daten betrug >90 %.

Die vorliegende Arbeit ebnet somit den Weg für die Entwicklung einer Simulation komplexer GC-Systeme, insbesondere der umfassenden GC (GC×GC) oder neuartiger Techniken wie der Gaschromatographie mit räumlichen Temperaturgradienten. Die Bestimmung der Retentionsparameter aus temperaturprogrammierten Messungen können in Verbindung mit dem Simulationspaket für die Entwicklung eines selbstoptimierenden GC Gerätes dienlich sein.